THE PROCEEDINGS OF
THE PHYSICAL SOCIETY
Section B

VOL. 65, PART 3 1 March 1952 No. 387 B

Characteristics of Radio Echoes from Meteor Trails : III
The Behaviour of the Electron Trails after Formation

BY J. S. GREENHOW
Jodrell Bank Experimental Station, University of Manchester

Communicated by A. C. B. Lovell; MS. received 14th September 1951

ABSTRACT. This paper deals with the durations and amplitudes of the radio echoes reflected from meteor trails. For wavelengths of 4·2 and 8·4 m the durations of most echoes are shown to be very nearly proportional to the square of the wavelength, as predicted by simple diffusion theory. It is suggested that long duration meteor echoes are due to total reflection from trails of very high electron density, and it is shown that the amplitudes of these echoes would only be of the same order as the amplitudes of the short duration echoes from trails of low electron density discussed in an earlier paper. Further evidence is given to show that the amplitude fluctuations in the radio echoes are caused by distortion of the column of ionization, relative motion of several reflecting centres due to wind turbulence producing changing interference conditions. Turbulent winds of the order of 20 m/sec are inferred at altitudes of 80 to 100 km.

§ 1. INTRODUCTION

In the first part of this series of papers (Lovell and Clegg 1948, to be referred to as I) the problem of the scattering of radio waves from the ionization produced by meteors was considered. Formulae were derived for the intensity of the scattered radio wave at the instant of formation of the electron trail, but its subsequent behaviour was not considered. From early observations of durations and amplitude it did not seem possible to explain the subsequent conditions in the electron trail in any simple manner (see for example Lovell 1950). In the present paper recent work on the problem of the durations and amplitude fluctuations will be discussed in relation to the condition of the ionized trail in the period following its formation.

The amplitude fluctuations in the radio echoes from meteor trails have been described by Greenhow (1950). Instead of the regular decay in amplitude to be expected from the diffusion of a uniform column of electrons, the amplitudes of all long duration echoes show fluctuations of the type illustrated in Plates II (*a*) and (*b*). The period of fluctuation is proportional to the radio wavelength, and at $\lambda = 8{\cdot}4$ m varies between 0·04 and 0·4 sec. It was suggested that these fluctuations were due to the distortion of the trail by turbulent winds, but neither the size or shape of the reflecting centres, nor the reason for the maintenance of the long duration echoes was discussed. These problems are dealt with in the present paper.

§ 2. TECHNIQUE

The technique and apparatus used in this work have been described previously (Davies and Ellyett 1949, Greenhow 1950). Two identical transmitting and receiving systems operating at wavelengths of 4·2 and 8·4 m were used. The transmitters were pulsed and the peak powers adjusted so that echoes appearing simultaneously on the two wavelengths had the same amplitudes. The normal pulse repetition frequency was 150 c/s, but this was automatically increased to 750 c/s for the first half second of every echo, in order to resolve the initial diffraction pattern which occurs as the meteor passes through successive Fresnel zones[*] (Davies and Ellyett 1949). The receiver outputs were fed on to the vertical deflection plates of two cathode-ray tubes. On the arrival of a meteor echo the tubes were photographed by a camera through which the film moved continuously at right angles to the direction of the receiver deflections, with a speed sufficient to separate individual echo pulses. In the original apparatus (Greenhow 1950) the first 0·1 sec of the echoes was lost, as the camera motor required this time to accelerate from rest to its operating speed. This dead time was eliminated in later experiments by triggering a single-sweep time-base with a duration of 0·1 sec from the first echo pulse to be received. This time-base was applied to the horizontal plates of the cathode-ray tubes, in order to spread out the first few echo pulses along the slowly moving film.

§ 3. ECHO DURATIONS AND THEIR VARIATION WITH WAVELENGTH: THE AMPLITUDES OF LONG DURATION METEOR ECHOES

(i) *Low Electron Densities and Short Durations*

The amplitude of the radio echo reflected from a meteor trail has been calculated in I on the assumptions that the electron density in the trail is low, and the diameter of the trail is small compared with a wavelength. The incident wave therefore penetrates to all the electrons, which scatter freely and in phase over any cross section. The following expression was obtained for the received power:

$$\epsilon = \frac{PG^2N^2\lambda^3}{12\pi^2R^3}\left(\frac{\mathbf{e}^2}{\mathbf{m}\mathbf{c}^2}\right)^2 \text{ watts}^{\dagger}, \qquad \ldots\ldots(1)$$

where N is the number of electrons per cm in the trail, P the transmitter power, G the aerial gain, λ the wavelength, R the range and $\mathbf{e}^2/\mathbf{m}\mathbf{c}^2$ the classical electron radius. An electron trail in the high atmosphere will immediately diffuse and hence the echo amplitude from such a trail would be expected to decay exponentially due to destructive interference.

The amplitude A at any time should be related to the initial amplitude A_0 by the expression

$$A = A_0 \exp(-16\pi^2 Dt/\lambda^2), \qquad \ldots\ldots(2)$$

where D is the diffusion coefficient (Herlofson 1947). The form of this equation has been verified with respect to the variation with λ for wavelengths of 4·2 and 8·4 metres. 134 echoes which occur simultaneously on both wavelengths and which decay exponentially to zero have been obtained; an example is shown in

[*] The amplitude changes due to diffraction which occur during the formation of the ionized column will be referred to in this paper as Fresnel oscillations.

[†] This differs from eqn. (1) of I by a factor of 2. This error arose because of the use of $G\lambda^2/8\pi$ as the power available in a matched load connected to the aerial instead of $G\lambda^2/4\pi$.

Plate I (*a*). Both echoes show Fresnel oscillations and the echo at 4·2 m decays much more rapidly than at 8·4 m. Assuming the decay times T_1 and T_2 to be related to the wavelength λ_1 and λ_2 by a power law of exponent n then $T_1/T_2=(\lambda_1/\lambda_2)^n$.

Values of the exponent n have been determined for the 134 echo pairs and the distribution is shown in fig. 1. The most probable value of n is 2 as predicted theoretically, although the spread in the distribution is greater than that introduced experimentally, a significant number of high values being observed. These high values may be due to the cooling of the trail which is initially at a temperature greater than that of the atmosphere, so producing a diffusion coefficient which is a decreasing function of time. A small number of very low values of n are also observed, and these may be due to echoes observed at very low heights where the loss of electrons by attachment becomes significant. This effect would tend to make the echo duration independent of wavelength.

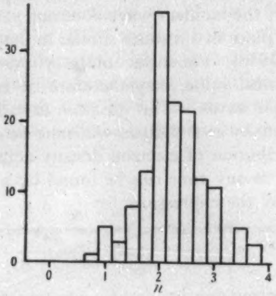

Fig. 1. Distribution of exponent n for 134 short duration echo pairs. n is calculated from $T_1/T_2=(\lambda_1/\lambda_2)^n$. T_1 and T_2 are the decay times to half the maximum echo amplitudes at wavelengths of λ_1 and λ_2.

These 134 echo pairs were obtained during the 1950 Perseid meteor shower, for which the mean height of ionization is approximately 95 km (Manning, Villard and Peterson 1949, Millman and McKinley 1949). Equation (2) can thus be used to obtain an estimate of the diffusion coefficient D at an altitude of 95 km. Substitution for A, A_0 and t for each meteor echo in eqn. (2) gives the most probable value of D as 4×10^4 cm²/sec. This is in reasonable agreement with the value determined from the measured values of the atmospheric temperature and density for a height of 95 km * (Whipple 1939). The radio echoes from Perseid meteor trails should therefore decay to $1/e$ of their initial amplitudes in approximately 0·1 sec at 8·4 m. An inspection of all the records obtained during the Perseid meteor shower showed that 60 % had durations of this order. These echoes therefore appear to be of the type which would obey the Lovell–Clegg formula. If values for the equipment parameters are substituted in eqn. (1), it is found that a meteor trail with 10^{12} electrons per cm should give an echo amplitude of ten times the receiver noise level and so be easily detectable.

The remaining 40 % of the echoes, although having amplitudes of the same order as the other 60 %, had much longer durations (in some cases up to 100 sec)

---

* Other experiments by Davidson and Hazzaa in which D has been measured at lower altitudes do not show such good agreement with accepted values. Possible deviations from the simple decay curve predicted by (2) are discussed by them.

.B
5
2

and it is obvious that the simple behaviour is not followed by these trails. A possible explanation of these long duration echoes will now be discussed.

(ii) *High Electron Densities and Long Durations*

(*a*) *Theoretical considerations of the amplitudes.* In order to account for long duration meteor echoes it has been suggested that the electron density in the trails is greater than the critical density for the wavelengths employed (Millman and McKinley 1949, Lovell 1950).

If the electron density is very high, the Lovell–Clegg formula will not be valid as all the electrons in the column will not scatter independently. In the case of a trail of large diameter, the incident wave does not penetrate to the centre, and total reflection will take place in a manner similar to that occurring in reflection at the ionosphere (Pierce 1938). The surface of the cylinder inside which the electron density exceeds the critical value, may therefore be considered to be effective for the reflection of radio waves. The variation in radius of this cylinder for a trail of high electron density as it diffuses will now be considered.*

For a gaussian distribution of electron density across the trail, the electron density n_r at a radius r at any time can be found by a solution of the diffusion equation, and is given by the expression

$$n_r = \frac{N}{4\pi D(t+k)} \exp\left\{\frac{-r^2}{4D(t+k)}\right\} \qquad \ldots\ldots(3)$$

where N is the linear electron density, and k a constant depending upon the initial conditions in the trail. If the distribution across the trail, when it is first formed, is assumed to be gaussian with a standard deviation equal to r_0, the initial trail radius, then $k = r_0^2/4D$. r_0 will be of the order of a few mean free paths, and so the constant k is negligible except for very small values of t.

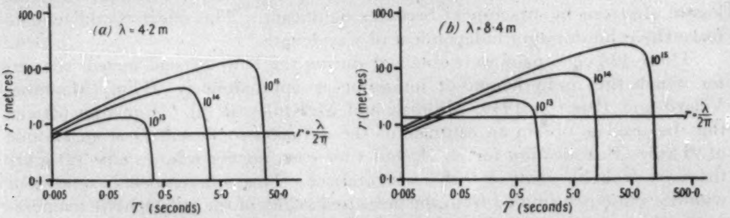

Fig. 2. Theoretical variation in radius of the critical density contour for a meteor trail of high electron density. T is the time from the formation of the trail. Curves are drawn for trails with 10^{13} to 10^{15} electrons per cm and $D = 4 \times 10^4$ cm^2/sec.

The variation in radius with time of the critical density contour is obtained by equating n_r to N_c, the critical density, in eqn. (3). Curves for wavelengths of 4·2 and 8·4 m are shown in fig. 2 for trails with line densities between 10^{13} and 10^{15} electrons per cm. In all cases the radius of the cylinder grows very rapidly after the formation of the trail. It then remains almost constant for some time, and eventually falls rapidly to zero.

---

* A detailed investigation of the reflection of radio waves from ionized columns for various electron distributions and for a wide range of electron densities has recently been made by Kaiser and Closs (1952). Their results for trails of high electron density reduce to those described in this paper when the diameter of the trail becomes comparable with the wavelength.

The variation in amplitude of the echo reflected from a trail of high electron density can now be calculated approximately by assuming that the cylinder inside which the electron density exceeds the critical value behaves as a metallic reflector. For an incident spherical wave, an approximate expression for the backward scattering area ρ of a metallic cylinder, of radius r greater than $\lambda/2\pi$, can be obtained using a standard method (Taylor and Westcott 1948). ρ is given by $\rho = 2\pi Rr$, where R is the range and r the radius of the reflecting cylinder. The variation of r for a high electron density meteor trail has been determined from eqn. (3), so the variation in the scattering area of the trail may be found throughout its life.

The echo amplitude is proportional to $\rho^{1/2}$ and values of this expression normalized through division by $(R\lambda)^{1/2}$ are shown in fig. 3 for trails of 10^{13} to 10^{15} electrons per cm. The echo duration T is also normalized through multiplication by D/λ^2. From fig. 3 it can be seen that the amplitude of an echo from a very dense meteor trail should only vary by a small amount during most of its life, rising and falling very rapidly near the beginning and end of the echo.

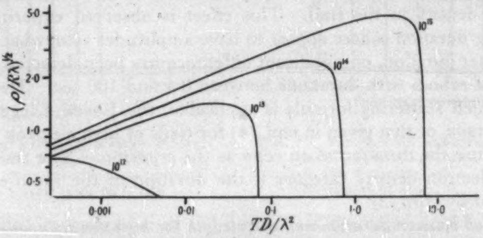

Fig. 3. Variation with time of the echo amplitudes from meteor trails of high electron density. Ordinate : square root of the backward scattering area ρ normalized through division by $(R\lambda)^{1/2}$. Abscissa : time from the formation of the trail normalized through multiplication by D/λ^2.

The initial backward scattering area for a trail of less than 10^{12} electrons per cm can be easily derived from the Lovell–Clegg formula and it is found to be $\rho = 2\pi N^2(e^2/mc^2)^2\,\lambda R$. The variation of $(\rho/R\lambda)^{1/2}$ for a trail with a line density of 10^{12} electrons/cm is also shown in fig. 3 for comparison with the values for trails of large electron density. The decay of the curve was calculated from eqn. (2). It can be seen that the maximum amplitude of the echo from a trail of 10^{14} electrons per cm is only 3·5 times greater than the echo from a trail with 10^{12} electrons per cm. If the Lovell–Clegg formula remained valid the ratio in amplitudes would be 100.

An approximate scattering formula for such high density trails can be derived as follows : The maximum echo amplitude is obtained when the radius r_{m} of the reflecting cylinder is a maximum. This maximum radius obtained by differentiating eqn. (3) is given by $r_{\mathrm{m}}^2 = N/2{\cdot}7\pi N_{\mathrm{c}}$. The maximum scattering area is therefore $\rho_{\mathrm{m}} = 2\pi R r_{\mathrm{m}} = 1{\cdot}2RN^{1/2}\lambda(e^2/mc^2)^{1/2}$. If P is the transmitter power, and G the aerial gain, the power ϵ delivered into a matched load at the receiver can be obtained in a manner similar to that adopted by Lovell and Clegg for trails of low electron density. We obtain for ϵ

$$\epsilon = \frac{PG^2N^{1/2}\lambda^3}{20\pi^3R^3}\left(\frac{e^2}{mc^2}\right)^{1/2} \qquad \text{......(4)}$$

This expression resembles the Lovell–Clegg formula in the variation with λ, R, P and G, but the echo amplitude increases only as the fourth root of the line density instead of linearly.

(*b*) *Relation of echo amplitude to duration.* From fig. 3 it can be seen that, owing to the rapid rise and fall of r, the echo duration is given to within a very close approximation by the time for which the radius of critical density is greater than zero.

When the electron density becomes high, therefore, the primary effect is to lengthen the duration of the echo, rather than to increase its amplitude. An echo from a trail with less than 10^{12} electrons per cm decays to $1/e$ of its initial value in approximately 0·1 sec at 8·4 m, this decay time being independent of the actual line density. For higher density trails, however, the echo duration is proportional to the line density, and fig. 3 shows that a trail of 10^{14} electrons/cm should give an echo duration of more than 12 sec for $D = 4 \times 10^4 \text{ cm}^2/\text{sec}$, the amplitude increasing by only a factor of 3·5. With the equipment sensitivity used, on which electron trails with line densities of much less than 10^{12} are not measurable, we have the condition that the echo amplitude should be almost independent of the electron density in the trail. This effect is observed experimentally and although long duration echoes appear to have amplitudes somewhat greater than those of shorter duration, no significant difference has been detected in the mean amplitudes of echoes with durations between 0·1 and 100 sec. Hence in order to decide which scattering formula is applicable, the Lovell–Clegg formula for low density trails, or that given in eqn. (4) for trails of high electron density, it is necessary to use the duration of an echo as the criterion. The trail comes into the 'high' electron density category if the duration of the radio echo exceeds that predicted by eqn. (2).

(*c*) *Relation between duration and wavelength for high density trails.* For trails of high electron density an expression for the echo duration T can be obtained by writing $r = 0$, and $n = N_c$ in eqn. (3); then

$$T = \frac{N}{4\pi D N_c} - \frac{r_0^2}{4D}. \qquad \ldots\ldots(5)$$

The second term in this expression is negligible, so that

$$T \propto N\lambda^2/D. \qquad \ldots\ldots(6)$$

In order to test this predicted variation with λ, echoes occurring simultaneously at 4·2 and 8·4 metres, with similar signal to noise ratios, were selected for measurement. The times taken for the echoes to decay into the receiver noise levels were used as measures of the durations, and the distribution of values of the exponent n is shown in fig. 4. The distribution has a cut off above $n = 2$, and most of the values are less than this figure. The variation in the ratio of the durations on the two wavelengths with duration is shown in fig. 5. Here the lifetimes for the 4·2 m components of the echoes are used as standards of comparison. Initially a λ^2 law is followed, but as the echo lifetime increases the mean value of n decreases, showing that the duration becomes less dependent upon wavelength.

Since diffusion alone should give a λ^2 variation it appears that for very dense meteor trails other processes must be occurring which affect the duration of the echo. Possible causes of this effect will now be discussed.

(d) Loss of electrons by recombination. The effect of recombination has been discussed briefly by Lovell (1950) who showed that it is of negligible importance for a trail with a line density of 10^{10} electrons per cm. On the other hand if his criteria are applied to meteor trails with line densities greater than 10^{13} electrons per cm, the effect of recombination becomes considerable. The recombination coefficient assumed by Lovell was 10^{-8} cm^3/sec, the effective value for the E region. This figure, however, is probably several orders of magnitude too large even for very dense meteor trails during the times in which a detectable echo is obtained; a more detailed investigation of the problem is discussed below. Apart from diffusion, electrons in a meteor trail could be lost by recombination with positive ions N^+, and attachment to neutral particles n_0.

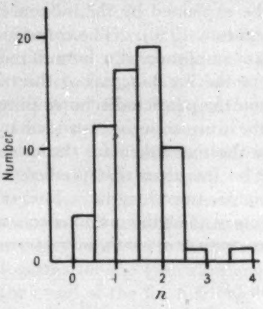

Fig 4. Exponent n for long duration echoes, calculated from $T_1/T_2=(\lambda_1/\lambda_2)^n$. T_1 and T_2 are the times for the disappearance of the echo wavelengths of λ_1 and λ_2.

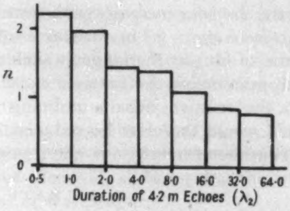

Fig. 5. Variation of exponent n, calculated from $T_1/T_2=(\lambda_1/\lambda_2)^n$, with T_2. T_1 and T_2 are the durations of a meteor echo at wavelengths of λ_1 and λ_2.

The rate of fall of electron density from these causes will be given by

$$dN_e/dt = -\alpha N_e N^+ - \beta N_e n_0, \qquad \ldots\ldots (7)$$

where α is the recombination coefficient for electrons and positive ions, and β the attachment coefficient for electrons with neutral particles. In the meteor region the atmosphere consists almost entirely of molecular oxygen and nitrogen, and so we are chiefly concerned with the recombination of electrons with positive N_2 and O_2 ions, for which $\alpha = 10^{-12}$ cm^3/sec (Bates, Buckingham, Massey and Unwin 1939), and the attachment of electrons to neutral O_2 molecules, for which $\beta = 10^{-16}$ cm^3/sec (Bates and Massey 1943).

Unless $n_0 > 10^4 N_e$ the first term in (7) is predominant. It will be shown later that this condition never applies during the lifetime of the echo from a high density meteor trail, and so the effect of attachment may be neglected. Thus for meteor trails we have, approximately,

$$dN_e/dt = -\alpha N_e^2 \quad \text{or} \quad N_e = N_0/(1+\alpha N_0 t), \qquad \ldots\ldots (8)$$

where N_0 is the initial electron density.

A trail with a line density of 10^{15} electrons per cm may be considered as a specific example. For an initial trail radius of 10 cm the electron density at the centre is approximately 3×10^{12} electrons per cm^3. According to (5) diffusion alone would reduce this to $1{\cdot}3 \times 10^7$ electrons per cm^3, the critical density at

8·4 m, in approximately 100 seconds. Equation (8) shows that recombination alone would only reduce the electron density to 10^{10} electrons per cm^3 in this time and so its effect is several orders of magnitude less than that of diffusion.

At a height of 95 km n_0 is approximately 10^{14} particles per cm^3 and so the attachment term in (7) only becomes comparable with the recombination term after 100 seconds. The additional decrease in electron density due to attachment is therefore small.

(*e*) ***Effect of turbulence on echo duration.*** The considerations in § 3 (*d*) show that recombination effects are unlikely to influence the departure from a λ^2 law in long duration echoes. The departures can be explained by the influence of atmospheric turbulence on the meteor trail (Greenhow 1950). The consequent distortions would progressively reduce the mean amplitude of a long duration echo below that predicted theoretically owing to the breaking up of the trail. As the disorder increases with time, its effect upon the predicted echo amplitude is greater at $\lambda = 8{\cdot}4$ m than at $\lambda = 4{\cdot}2$ m since the time scale is expanded by a factor of four at the longer wavelength. Hence the time taken for the echo to disappear below the receiver noise level would be less than that predicted by (5), the relative departure being greater at longer wavelengths. The ratio T_1/T_2 would therefore be reduced. Some aspects of these distortion effects will be considered below.

§ 4. RATE OF DISTORTION

An estimate of the rate of distortion of meteor trails due to turbulence can be arrived at in the following manner. The majority of the ionized trails produced by meteors are markedly aspect sensitive, and a radio echo is only obtained when the trail is at right angles to the observer. In fig. 6 (*a*) a meteor is travelling in the direction AC. No echo will be received until the meteor approaches the foot of the perpendicular from the observing station O to the trail at S; the amplitude

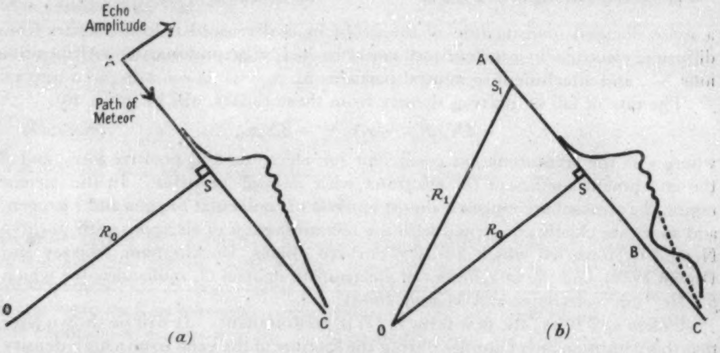

Fig. 6.

(*a*) Formation of Fresnel oscillations as the meteor crosses the foot of the perpendicular to the trail, and then passes through successive Fresnel zones, followed by a simple decay in echo amplitude as the trail diffuses.

(*b*) Distortion of the trail producing fluctuations in amplitude by interference between the off-perpendicular reflection from S_1 and the main right-angle reflection.

then rises rapidly to a maximum as the meteor crosses this point, and executes small oscillations as successive Fresnel zones are traversed. This phenomenon has been observed experimentally, and it is used to determine meteor velocities (Davies and Ellyett 1949). In the absence of any other effect the echo amplitude would then decay uniformly (Plate I (*a*)); as discussed previously, however, this uniform decay will be influenced by atmospheric turbulence (Plate I (*b*), (i)). If, when the meteor reaches the point B (fig. 6 (*b*)) the column of ionization has become distorted so that an appreciable echo is received from another section of the trail in addition to the main right-angle reflection, then the echo amplitude will be modified.

The time between the formation of the first maximum of the Fresnel pattern and the onset of the amplitude fluctuations is variable, and gives a measure of the rate of distortion of the trail. Considering now only those echoes of the Fresnel type[*] figs. 7 (*a*) and (*b*) are histograms showing the percentage of echoes in various duration groups in which the zones are followed by large amplitude fluctuations (only echoes with amplitudes greater than four times the receiver noise have been considered). Over 97% of the echoes with durations less than 0·2 sec decay to zero without fluctuating but almost all those with durations greater than 1·6 sec show fluctuations in amplitude; these limits give the probable time taken for a trail to distort sufficiently to give a non-specular reflection. The histograms for the two wavelengths are almost identical, showing that the time of the onset of the fluctuations is independent of wavelength.

.B
5
2

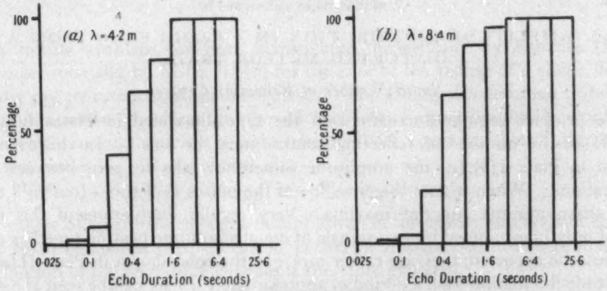

Fig. 7. Percentage of Fresnel type echoes which show large amplitude fluctuations after the formation of the zones.

The time taken for sufficient trail distortion to occur, in order that echoes are obtained from points other than the R_0 point, varies between 0·2 sec and 1·6 sec. It should therefore be possible for meteor trails with durations greater than these values, but which do not initially show suitable right-angle points, to deform subsequently so as to give an echo at a later time. Such an echo would not show Fresnel zones at the beginning.

[*] Although the zone formation is only sufficiently well defined in a small percentage of all echoes to enable the velocity of the meteor to be accurately determined, in many echoes the rapid rise in amplitude is present, followed by one or two maxima and indications of other distorted zones. In these cases it is obvious that the main echo has been obtained by right-angle reflection, but for some minor reason, such as small turbulent effects or receiver noise fluctuations, the Fresnel oscillations are not clear.

Fig. 8 shows the results of an analysis of 620 measurable meteor echoes obtained during the 1950 Perseid stream. The percentage of the echoes in various duration groups which are of the Fresnel type are shown. At 4·2 m almost 100% of the echoes with durations less than 0·2 sec are of the Fresnel type, but only 9% of those lasting more than 1·6 sec show Fresnel oscillations. The remaining 91% have therefore been seen after distortion.

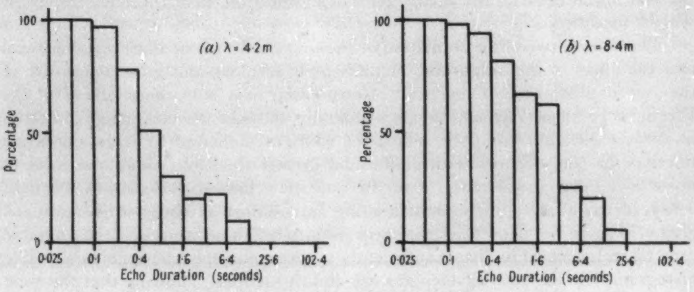

Fig. 8. Percentage of echoes which are of the Fresnel type.

§ 5. AMPLITUDE DISTRIBUTION IN A RADIO ECHO FROM A DISTORTED METEOR TRAIL

(i) *Small Number of Reflecting Centres*

To produce regular fluctuations of the type illustrated in Plates I (*b*), (ii) and II (*a*) the number of reflecting centres must be small. In the example shown in Plate I (*b*), (ii) the amplitude sometimes falls to zero between the fluctuations. When it does the envelope of the pulses is of the $+(\cos^2\theta)^{1/2}$ type with sharp minima and flat maxima. Very regular fluctuations of this type would only be produced by two signals of equal amplitude beating together and, as would be expected, they are rather rare. In the echo shown in Plate II (*a*) an amplitude fluctuation with a period of approximately 0·1 sec can be seen at 8·4 m. The fluctuations are not very regular, and it is probable that small reflections are being obtained from other parts of the trail in addition to two main centres. This fluctuation corresponds to a relative line of sight velocity of the centres of approximately 40 m/sec. The equivalent fluctuation with a period of 0·05 sec is present at 4·2 m, but the echo at this frequency differs from the 8·4 m echo in that the amplitude of the oscillation disappears 5·5 sec from the beginning of the echo. The probable explanation is that the diffusion coefficient varies with height, and so reflecting centres at different heights diffuse at varying rates. As the duration increases the disorder along the trail will increase, and so the fluctuations will become correspondingly more confused. This is found experimentally, and regular fluctuations usually occur only within the first few seconds of an echo. An example of the confused fluctuations normally occurring in a long duration echo is shown in Plate II (*b*).

(ii) *Large Number of Reflecting Centres*

If the received signal is made up of a large number of wavelets scattered from reflecting centres moving with random motion, then the resultant echo amplitude should follow a Rayleigh distribution of the form

$$P(R)\,dR = \frac{R}{\psi}\exp\left(\frac{-R^2}{2\psi}\right)dR \qquad \ldots\ldots(9)$$

where $P(R)$ is the probability of the amplitude lying between R and $R+dR$. The amplitudes of several very long duration echoes have been measured pulse by pulse. Log$[M(R)/R]$ has been plotted against R^2 for each wavelength, and the curves for one echo of duration 35 sec at 4·2 m and 57 sec at 8·4 m are shown in fig. 9 (M is the frequency of occurrence of amplitude R). The points lie approximately on straight lines in agreement with (9).

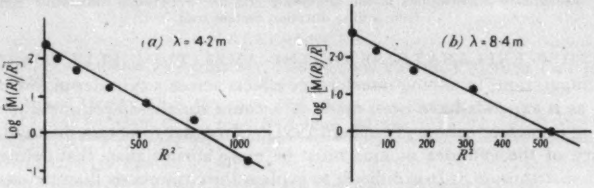

Fig. 9. Rayleigh distribution of amplitudes in a long duration meteor echo. *M* is the frequency of occurrence of amplitude *R*.

A similar problem has been investigated theoretically by Ratcliffe (1948) and experimentally by Mitra (1949) for the case of the fading of a single down-coming ray reflected from the ionosphere. The fading was assumed to be due to the interaction of a large number of wavelets of equal amplitude, scattered from centres moving with line of sight velocities with a gaussian distribution about an r.m.s. value V_0. It was shown that

$$p(\nu_\tau)\,d\nu_\tau = c\exp\left[-\{\nu_\tau/2\pi\sigma\tau(2\psi)^{1/2}\}^2\right]d\nu_\tau \qquad \ldots\ldots(10)$$

The values of ν_τ are the changes in amplitude in successive intervals of time τ (τ is small compared with the mean period of fluctuation). The probability distribution of the amplitude changes is therefore gaussian.

In addition, the r.m.s. line of sight velocity is given by

$$|\nu_\tau|/\overline{R}\tau = 8V_0/\lambda, \qquad \ldots\ldots(11)$$

where λ is the wavelength. In the meteor echoes which have been analysed τ was taken as the interval between successive echo pulses. The units of amplitude were arbitrary. The probability distributions of the amplitude changes between successive pulses are shown in fig. 10, together with the gaussian curves giving the best fits. There is reasonable agreement between the theoretical and experimental distributions.

Substitution of experimental values in eqn. (11) enabled the r.m.s. line of sight velocity of a single centre to be determined. The values obtained were 14·7 m/sec from the 4·2 m echo, and 15·0 m/sec from the equivalent echo at 8·4 m, confirming the predicted variation of the amplitude distribution with wavelength. This value of V_0 also compares favourably with the relative line of sight velocity of two centres determined from the simple fluctuations (Greenhow 1950). The above results show that for a very long duration meteor echo, the number of scattering centres causing the amplitude fluctuations may become large, through an increase in the disorder along the trail due to turbulence.

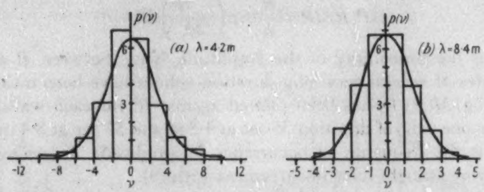

Fig. 10. Probability distributions of the amplitude changes ν between successive echo pulses from a long duration meteor trail.

§6. OTHER EXPLANATIONS OF THE AMPLITUDE FLUCTUATIONS

(i) Suggestions involving interference effects across a cylinder of low electron density as it expands have been made to account for the amplitude fluctuations occurring in meteor echoes (Feinstein 1951). In order to obtain fluctuations the boundary of the cylinder of ions must be more abrupt than that defined by a gaussian distribution. It is difficult to explain the continuous fluctuations which occur throughout echoes lasting up to a minute or so by mechanisms of this type. Expansions of hundreds of wavelengths would be required in some cases, the rate of expansion varying between 4 and 40 m/sec for different echoes. Nor can the constancy in amplitude of the long duration echoes be explained, as the initial echo decay would be very rapid for an expanding trail, and the echo would decay into the receiver noise level after only one or two fluctuations.

(ii) In order to account for the phenomenon observed in long duration meteor echoes McKinley and Millman (1949) have postulated the presence of discrete regions in the upper atmosphere where meteor ionization is maintained and enhanced. Initially a very dense trail of small diameter is formed, and after delays of up to several seconds clouds of ions with diameters of many wavelengths grow in the special regions, and from these detectable meteor echoes are obtained. Elsewhere they assume that the ions rapidly diffuse and do not produce a detectable echo. Interference may take place between the waves reflected from different clouds, or between different parts of the same cloud, so producing amplitude fluctuations. It has been shown, however, that a trail which is formed with a density exceeding the critical value can remain overdense for many seconds while undergoing the normal process of diffusion, and it is unnecessary to postulate additional effects to hold the trail together or enhance the ionization. In addition, a trail can reach a diameter sufficient to give a detectable echo within 0·05 sec of its formation. The discrete echoes obtained from single long duration meteor trails by Millman and McKinley and the delay in appearance of these echoes, are more easily explained by the progressive distortion of parts of the trail at increasing distances from the R_0 point so as to give echoes differing in range by an amount greater than half the transmitter pulse width. A further argument in favour of trail distortion is that, in general, long duration echoes appear at the same instant on different wavelengths.

If the theory of McKinley and Millman is correct, echoes should appear earlier at $\lambda = 4$ m than at $\lambda = 8$ m, as the clouds of electrons would reach detectable size sooner on the shorter wavelength, but no instances of this occurrence have been observed. A number of long duration echoes are observed at $\lambda = 8$ m which do not appear at all on 4 m and this behaviour can be explained if the trail has diffused to below critical density at $\lambda = 4$ m before distorting sufficiently to give a detectable echo.

ACKNOWLEDGMENTS

The author is indebted to Dr. A. C. B. Lovell, the Director of the Jodrell Bank Experimental Station, for his interest and advice. He also wishes to thank Dr. T. R. Kaiser for several useful suggestions, and Mrs. J. Haselgrove, who assisted in the film analysis. The work was made possible through financial assistance from the Department of Scientific and Industrial Research.

REFERENCES

BATES, D. R., BUCKINGHAM, R. A., MASSEY, H. S. W., and UNWIN, J. J., 1939, *Proc. Roy. Soc.* A, **170,** 322.
BATES, D. R., and MASSEY, H. S. W., 1943, *Phil. Trans. Roy. Soc.* A, **170,** 322.
DAVIES, J. G., and ELLYETT, C. D., 1949, *Phil. Mag.*, **40,** 614.
FEINSTEIN, J., 1951, *J. Geophys. Res.*, **56,** 37.
GREENHOW, J. S., 1950, *Phil. Mag.*, **41,** 682.
HERLOFSON, N., 1947, *Rep. Prog. Phys.*, **11,** 444 (London: Physical Society).
KAISER, T. R., and CLOSS, R. L., 1952, *Phil. Mag.*, **43,** 1.
LOVELL, A. C. B., 1950, *Sci. Progr.*, **38,** 22.
LOVELL, A. C. B., and CLEGG, J. A., 1948, *Proc. Phys. Soc.*, **60,** 491.
MANNING, L. A., VILLARD, O. G., and PETERSON, A. M., 1949, *J. Appl. Phys.*, **20,** 475.
MILLMAN, P. M., and MCKINLEY, D. W. R., 1949, *Sky and Telescope*, **8,** 114.
MCKINLEY, D. W. R., and MILLMAN, P. M., 1949, *Proc. Inst. Radio Engrs., N.Y.*, **37,** 364.
MITRA, S. N., 1949, *Proc. Instn. Elect. Engrs.*, Pt. III, **96,** 505.
PIERCE, J. A., 1938, *Proc. Inst. Radio Engrs., N.Y.*, **26,** 892.
RATCLIFFE, J. A., 1948, *Nature, Lond.*, **162,** 9.
TAYLOR, D., and WESTCOTT, C. H., 1948, *Principles of Radar* (Cambridge: University Press).
WHIPPLE, F. L., 1939, *Popular Astronomy*, Vol. 47, No. 8.

The Propagation of Sound through Gases contained in Narrow Tubes

BY L. E. LAWLEY
King's College, Newcastle-upon-Tyne

Communicated by E. G. Richardson; MS. received 25th October 1951

ABSTRACT. A comprehensive investigation is made into the validity of the Helmholtz–Kirchhoff equations for the absorption and velocity of sound in a gas contained in a narrow tube. Results are given for air, oxygen, nitrogen and hydrogen contained in tubes of radii between 0·15 mm and 1·17 mm at frequencies between 60 and 150 kc/s. The form of both the velocity and absorption equations is confirmed, but the viscosity–thermal conductivity constant is found experimentally to be about 5% above the theoretical value. A method is outlined in which the free space absorption can be calculated from measurements in a tube at varying pressures, and results are given in the case of oxygen.

§ 1. INTRODUCTION

WHEN a plane sound wave is propagated in a tube of radius r at a frequency f, the amplitude absorption coefficient per cm is given by

$$\alpha_{\mathrm{T}}=[(\pi f)^{1/2}/rV_0]C \qquad \ldots\ldots(1)$$

and the free space velocity of sound in the gas V_0 is reduced to V, where

$$(V_0-V)/V_0=C/2r(\pi f)^{1/2}. \qquad \ldots\ldots(2)$$

C is a constant of the gas given by

$$C=[\eta^{1/2}+(\gamma-1)(K/C_p)^{1/2}]/\rho^{1/2} \qquad \ldots\ldots(3)$$

where η is the viscosity and K the thermal conductivity. The above equations derived by Helmholtz and Kirchhoff are applicable to the case where the layer of gas immediately affected by the walls is small compared with r.

Many experimental investigations have been carried out, but the theory has never been verified completely and several workers have reported complete disagreement with the above equations. The work of Kaye and Sherratt (1933) and Norton (1935) verified the form of the velocity equation in several gases up to frequencies of 50 kc/s and in tubes down to 5 mm diameter, but the value obtained for the constant C was about 10% below the theoretically calculated value. In narrow tubes of 1 mm diameter at frequencies up to 200 kc/s Vance (1932) reported that the velocity of sound in air fell to 160 m/sec. The results of the experimental work on absorption are less conclusive. In the case of tubes down to 6 mm diameter at low frequencies in air, Waetzmann and Wenke (1939) found the absorption to be 10–15% above the theoretical values. Under similar conditions Fay (1940) suggested a second-order term involving frequency. For narrow tubes down to 0·6 mm diameter at frequencies up to 115 kc/s May (1938) found the absorption in air to be at least 50% higher than that calculated theoretically.

The object of the present investigation is to provide a comprehensive experimental test of the validity of the Helmholtz–Kirchhoff absorption equation over a wide range of f, r and C. Experimental values of velocity have also been obtained and are compared with the theoretical equation.

§ 2. APPARATUS

The apparatus was similar in principle to that used by both Norton and May. An interferometer system was set up inside the tube and the propagation constants of the gas were derived from observations of the reaction on the oscillator circuit as the reflector was moved along the tube.

A number of magnetostrictive transducers were made from 2 mm diameter monel rod so as to cover the frequency range from 60 to 150 kc/s. The required transducer was fixed in a small exciter coil which was inductively coupled to a conventional Hartley oscillator. A steady polarizing field for the monel rod was provided by a small permanent magnet. Variations in the anode current of the oscillator valve were observed with a galvanometer, the steady current being backed off with a 4-volt accumulator.

The tubes used in this work were Hysil 'Veridia' precision glass tubes, 4 inches long, having internal radii between 0·15 mm and 1·17 mm and wall thickness about 2 mm. To each of these 'working tubes' was joined a 3 mm diameter tube 3 inches long, and the two tubes were accurately aligned.

A transducer could then be pushed along the 3 mm diameter tube until it nearly touched the working tube and completely covered its mouth (fig. 1).

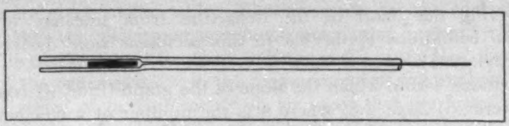

Fig. 1. Typical tube, source and reflector.

This system enabled any transducer to be used with any tube. The monel rod was fixed firmly in the tube by a cork mounting glued to it at the nodal point and the exciter coil fitted round the outside of the tube. A reflector of metal or glass rod was clamped in a reflector head which moved along an accurate screw thread.

The whole interferometer system fitted into a gas-tight cylindrical chamber which could be evacuated and filled with the gas to be investigated. A mercury thermometer was arranged to be in good thermal contact with the glass working tube but was not in direct contact with the gas in the chamber. A heater winding round the outside of the chamber and a thermostat enabled the temperature to be kept near 27° C. During the course of an experiment, manual control of temperature was maintained by means of external resistances. A thermistor placed near the transducer and connected in a bridge circuit was used to observe slight temperature variations with very little time lag.

§ 3. METHOD OF MEASUREMENT

In order to measure absorption, the oscillator was tuned near to the resonant frequency of the transducer until the latter took control of the frequency of oscillations. The reflector was then moved slowly away from the source while maximum and minimum galvanometer readings were taken through as many wavelengths as possible. The natural logarithms of the differences between successive maximum and minimum readings $\delta\theta$ were plotted against the number of half wavelengths. The intensity absorption per wavelength $\mu = 2\alpha\lambda$ is given by the slope of the resulting graph. The half wavelength was obtained from the distance moved by the reflector between successive maxima. The frequency was measured with an accurate crystal check wavemeter, and hence the velocity could be calculated.

When taking readings it was necessary to keep the temperature steady so that it did not vary by more than about 0·02° C per minute. A slight temperature drift causes the resonant frequency of the rod to vary, and this causes the operating point to move up or down the crevasse. This not only causes a drift of the galvanometer spot but also alters the sensitivity of the system and hence gives rise to an error in the measured value of α. Such an effect can be detected and eliminated by taking a set of readings as the reflector moves away from the source and then, immediately afterwards, another set as it returns towards the source.

The slope of the graph ($\ln \delta\theta$, λ) is only equal to the absorption coefficient μ under certain conditions. The limits are set by two factors: (*a*) when the reflector is too near the source Hubbard's function P_0 (Hubbard 1931) is not logarithmic; (*b*) when the variations in the steady anode current I_a become too large δI_a is no longer proportional to δR, the change in acoustic radiation resistance.

By observing the onset of the departure from linearity of the graph $(\ln \delta\theta, \lambda)$, two conditions applicable to this oscillator were derived similar to those of Hardy (1943).

The conditions within which the slope of the graph $(\ln \delta\theta, \lambda)$ could be taken to equal μ were: (i) $2\mu n > 2{\cdot}5$, where n is the number of wavelengths between source and reflector, (ii) $\delta I_a/I_a < 0{\cdot}01$. By working well within the limits set by these conditions no tendency to depart from linearity was observed.

When $\lambda > 3{\cdot}4 \times$ tube radius, no transverse vibrations can be propagated in the gas, and the wave front is plane. Since the Helmholtz–Kirchhoff theory applies only to plane waves, this condition was observed throughout the work.

§4. DISCUSSION OF RESULTS

The aim of the work was to test eqns. (1) and (2) under the following conditions: (*a*) vary r only, (*b*) vary f only, (*c*) vary both V_0 and C—this was done by using several gases, (*d*) vary C without varying V_0—this was done by varying the gas pressure since $C \propto 1/p^{1/2}$.

The work may conveniently be divided into two sections—that corresponding to conditions (*a*), (*b*) and (*c*), in which the gas pressure remained constant, and that corresponding to (*d*), where the pressure was varied. The results in the two sections will be discussed separately.

(i) *Classical Gases at Normal Pressure*

The first series of experiments was carried out on dry air at atmospheric pressure. Measurements were made on five tubes having radii between 0·15 mm and 1·17 mm at 60, 80, 100, 120 kc/s. This was done to enable the effect of tube radius and frequency to be examined independently if necessary. After a small correction had been made for the free gas absorption ($\alpha_G = 0{\cdot}001$ at 100 kc/s), the tube absorption α_T was found to be proportional to $f^{1/2}/r$ for all tubes and frequencies used. The results are shown in fig. 2 together with the best straight line through the points as calculated by the method of least squares. The theoretical absorption is also shown as calculated from eqn. (1), the values for the viscosity, etc., being taken from the *International Critical Tables*. It may be seen that the experimental results can be represented

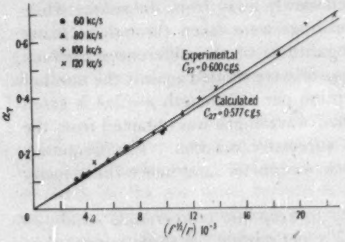

Fig. 2. Air. Absorption.

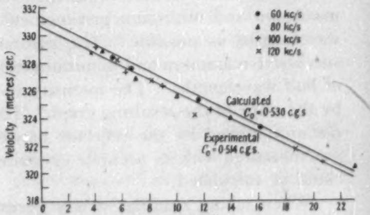

Fig. 3. Air. Velocity.

by eqn. (1) provided a slightly higher value is assumed for the viscosity–thermal conductivity constant C. The value of the constant C at 27° c calculated from eqn. (3) and the experimental value deduced from the slope of the graph of α_T against $f^{1/2}/r$ are given in the table. Similar results for the constant C at 0° c are obtained when the velocity measurements are plotted against $1/rf^{1/2}$, as shown in fig. 3. The extrapolated free space velocity is 0·7 m/sec low, probably owing to an error of the order of 0·2% in the measurement of the pitch of the reflector screw. The series of measurements on air show that the forms of the terms involving f and r in eqns. (1) and (2) are correct.

Similar measurements were then made on oxygen and nitrogen at a pressure of 76 cm Hg within the same range of radius and frequency. The results are of the same form as those for air and show much less scatter owing to the fact that the pressure was kept constant instead of being subjected to atmospheric variations. Finally, measurements were made on hydrogen since it has properties very different from those of the gases previously investigated. Only a few measurements were taken at 120 and 150 kc/s, and their accuracy was not high owing to the experimental difficulties of measurement in this gas. However, the results plotted in fig. 4 are sufficient to show that large discrepancies do not occur in gases having low density. The velocity readings in this case were used only as a check on the gas purity. The results for all the gases are summarized in the table.

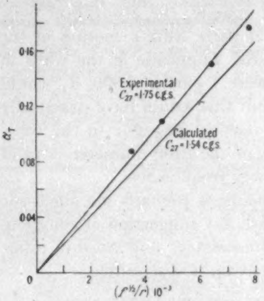

Fig. 4. Hydrogen. Absorption.

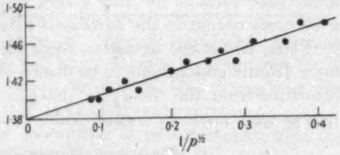

Fig. 5. Oxygen. Pressure variation.

Gas	Air	Oxygen	Nitrogen	Hydrogen
Calculated C_{27}	0·577	0·582	0·580	1·54
Experimental C_{27} (from absorption readings)	0·600	0·604	0·624	1·75
$(C_{27})_{\text{exp}} - (C_{27})_{\text{calc}}$ (%)	+4	+4	+8	+14
Calculated C_0	0·530	0·535	0·533	1·42
Experimental C_0 (from velocity readings)	0·514	0·590	0·571	—
$(C_0)_{\text{exp}} - (C_0)_{\text{calc}}$ (%)	−3	+10	+7	—

This shows that the absorption readings are all a few per cent higher than the theoretically calculated values, and there is the possibility of an increase in the lighter gases. Taking the nitrogen results as typical, the average deviation from the mean of C_{27} is 2·4%, giving a probable error of 0·6% for the mean value of C_{27}. Thus the increase in the experimental value of C_{27} is considered to be significant. The values of C_0 from the velocity measurements show a similar increase, but the accuracy of these figures is not high since the subtraction of two large numbers of almost equal magnitude is involved.

Henry (1931) has estimated the corrections applicable to the velocity equation in a practical case where the assumptions made in the derivation of the theory do not hold completely. Some of the possible causes of deviation from the simple theory are as follows:

(1) Yielding of the tube walls, (2) slip between the gas and the tube walls, (3) motion of the gas normal to the walls, (4) temperature jump at the walls and the existence of rapidly damped temperature waves in the walls, (5) irregular motion of the gas produced by tube irregularities or waviness, (6) vibration of the reflector, (7) variations in tube diameter, (8) acoustic coupling of the gas behind the reflector to the column in front. The absence of any large discrepancy in the results as the tubes or transducers are changed eliminates many of these factors as the cause of the increased absorption. Henry's work indicates that only irregular motion of the gas and motion normal to the walls are likely to produce any appreciable effect. In the smooth glass tubes used, irregularities in the walls were considered to have a negligible effect since, when a tube was roughened with carborundum until it was quite opaque, the absorption only increased by 7%. Henry's equations show that if there were a motion of the gas normal to the walls such that the ratio of radial amplitude at the walls to longitudinal amplitude at the centre of the tube were 1 part in 1000, α_T would be increased by 0·02 in a tube 1 mm in diameter, but this would have practically no effect on velocity. The assumption that the viscous drag due to the walls of the tube extends for only a very small fraction of the tube diameter is valid in all cases except in the narrowest tube at the lower frequencies.

Thus, whilst the deviation from the simple theory is perhaps too small for more definite conclusions to be drawn as to its cause, any suggestion of complete departure from the theory in the case of high frequencies and narrow tubes such as were made by Vance, May, Fay and others can be discounted.

(ii) *Absorption Measurements with Varying Pressure*

Finally, in a further series of measurements, the gas pressure was varied, and since $C \propto 1/p^{1/2}$ it was possible to check the theoretical absorption eqn. (1), as C only was varied. As the pressure is reduced, however, the free gas absorption α_G in the absence of a tube becomes appreciable. In order to find the form of the absorption equation under these conditions, the Helmholtz–Kirchhoff theory was taken to a further degree of approximation. The final equation showed that the total absorption could, in this case, be represented by the sum of the simple tube absorption and the free gas absorption, the product terms in the equation being negligible. Thus

$$\alpha = [(\pi f)^{1/2}/rV_0]C + [2\pi^2 f^2/V_0^3]\sigma, \qquad \ldots\ldots(4)$$

where $\sigma = [\frac{4}{3}\eta + (\gamma - 1)K/C_p]/\rho$. Hence, if the gas pressure alone is varied, we may write for the total absorption

$$\alpha = K_T/p^{1/2} + K_G/p, \qquad \ldots\ldots(5)$$

where p is the gas pressure and K_T and K^G are constants from which the simple tube absorption and the free gas absorption can be calculated. Multiplying by $p^{1/2}$ we have $\alpha p^{1/2} = K_T + K_G/p^{1/2}$. Hence by measuring α as p is varied, K_T and K_G can be obtained from a graph of $\alpha p^{1/2}$ against $1/p^{1/2}$.

Absorption measurements were made on oxygen at 120 kc/s in a 1·5 mm diameter tube throughout the pressure range 130 to 5 cm Hg. Fig. 5 shows the linear relationship between $\alpha p^{1/2}$ and $1/p^{1/2}$, thus giving confirmation of the form of eqn. (5). It also indicates that, apart from free gas absorption, the Helmholtz–Kirchhoff equation is valid in this case when the constant C is within the range 0·45 to 2·25. The slope and intercept of the line give $K_T = 1{\cdot}38$ and $K_G = 0{\cdot}246$, whereas by calculation from the theoretical equation (4) we obtain $K_T = 1{\cdot}25$, $K_G = 0{\cdot}180$. The value of the tube absorption given by K_T agrees with the results obtained for the tube effect at atmospheric pressure. The value of K_G indicates that the free gas absorption is 37% higher than that calculated theoretically.

It will be seen that this is a possible method of measuring free gas absorption. No assumptions are made about the tube absorption except that it follows the $1/p^{1/2}$ law and that the tube and free gas absorption are simply additive. The advantage of the method is that, provided the tube radius is too small for radial resonance to occur at the frequency used, only plane waves may be propagated through the tube. The free gas absorption can therefore be measured under plane wave conditions as required by the theory. This is most important, as it has been shown that the presence of transverse modes of vibration in normal interferometers could be responsible for many of the reports of abnormally high absorption in classical gases (Bell 1950). Unfortunately, however, at normal pressures and in the widest tube which will permit plane wave propagation at a given frequency, the ratio of classical gas absorption to tube absorption is negligibly small. Since free gas absorption depends on $1/p$ and tube absorption on $1/p^{1/2}$, this ratio increases as the pressure is reduced, but even at a pressure of 5 cm Hg it is only 0·06 at 120 kc/s. As may be seen from fig. 5, this implies that unless α can be measured to within 1% throughout the pressure range the results are useless in this method of interpretation.

The value obtained for the free gas absorption is in agreement with the more recent results of other workers. Sivian (1947) found that in both oxygen and nitrogen the absorption was about 50% higher than that calculated from the theoretical equation. However, since the theoretical basis of the equations for viscous absorption due to the tube and to the free gas is the same, one would not expect the latter to be more than about 10% above the calculated value, as was the case with tube absorption only. Work now being carried out on carbon dioxide contained in tubes shows that although molecular absorption is present as in the free gas, it does not contribute appreciably to the tube absorption. Much of the increase in free gas absorption in the case of oxygen may therefore be attributed to molecular absorption.

Similar results were obtained for nitrogen by Zmuda (1951) who showed that the free gas absorption at atmospheric pressure is 32% above the classical value, due to the slow exchange of energy between the translational and rotational degrees of freedom.

§ 5. CONCLUSION

The results of this work show that over a wide range of frequency and tube radius the Helmholtz–Kirchhoff equations are of the right form, but the viscosity–thermal conductivity term as measured in these experiments is about 5% higher than that calculated theoretically. The variation of absorption with pressure shows that over a considerable range of pressures the total absorption is the sum of that due to the tube and to the free gas.

ACKNOWLEDGMENTS

The author wishes to thank Professor W. E. Curtis for providing the facilities for carrying out this research and Dr. E. G. Richardson for his supervision of the work. He is also grateful to Dr. J. F. W. Bell for helpful suggestions and to Mr. J. Atkinson of the Gateshead Instrument Co. for construction of the interferometer chamber.

REFERENCES

Bell, J. F. W., 1950, *Proc. Phys. Soc.* B, **63,** 958.
Fay, R. D., 1940, *J. Acoust. Soc. Amer.*, **12,** 62.
Hardy, H. C., 1943, *J. Acoust. Soc. Amer.*, **15,** 91.
Henry, P. S. H., 1931, *Proc. Phys. Soc.*, **43,** 340.
Hubbard, J. C., 1931, *Phys. Rev.*, **38,** 1011.
Kaye, G. W. C., and Sherratt, G. G., 1933, *Proc. Roy. Soc.* A, **141,** 123.
May, J., 1938, *Proc. Phys. Soc.*, **50,** 553.
Norton, G. A., 1935, *J. Acoust. Soc. Amer.*, **7,** 16.
Sivian, L. J., 1947, *J. Acoust. Soc. Amer.*, **19,** 914.
Vance, C. B., 1932, *Phys. Rev.*, **39,** 737.
Waetzmann, E., and Wenke, W., 1939, *Akust. Z.*, **4,** 1.
Zmuda, A. J., 1951, *J. Acoust. Soc. Amer.*, **23,** 472.

The Magnetic Electron Microscope Objective Lens of Lowest Chromatic Aberration

By G. LIEBMANN

Research Laboratory, Associated Electrical Industries Ltd., Aldermaston, Berks.

MS. received 25th September 1951

ABSTRACT. The shortest focal length f and smallest chromatic aberration constant C_c of an objective lens is directly proportional to the square root of the (corrected) accelerating voltage V_r and inversely proportional to the maximum magnetic field strength H_p in the parallel part of the pole piece gap. For given values of V_r and H_p, both f and C_c fall monotonically with the relative pole-piece separation S/D, although the reduction is insignificant for $S/D > 2$. For each lens geometry there exists an optimum set of lens dimensions.

§ 1. INTRODUCTION

Fluctuations of the accelerating voltage, or of the exciting lens current, and the velocity spread of the electrons emitted by the cathode, as well as energy losses in the specimen, lead to a loss of resolution in the electron microscope. The radius δr of the disc of confusion, referred back to the object plane of an objective working with high magnification, is usually written in this form:

$$\delta r = \left(\frac{2\delta H}{H} - \frac{\delta V}{V}\right) C_c \alpha, \qquad \ldots\ldots(1)$$

where $\delta H/H$ and $\delta V/V$ are the relative changes of lens current or lens voltage, α is the semi-aperture angle at the object and C_c is the chromatic aberration constant. C_c is nearly equal to the focal length of the objective. It is obvious from eqn. (1) that the loss of resolution is less the smaller the chromatic aberration constant C_c. This led von Ardenne in 1940 to construct an objective of very short focal length ($f=0{\cdot}09$ cm at 70 kv); he found that the main limit for the shortest focal length obtainable was iron saturation.

In subsequent development of electron microscopes there was a tendency to use longer focal length objectives, but at the 1951 Electron Microscopy Conference in St. Andrews Le Poole and van Dorsten described an objective of 0·08 cm focal length. These authors presented an approximate theory of the shortest possible focal length, based on the focusing property of the uniform field between plane parallel pole pieces.*

In this paper the results of an earlier investigation on magnetic lenses (Liebmann and Grad 1951) will be applied to a more complete analysis of the problem of the magnetic lens of shortest focal length or lowest chromatic aberration.

§ 2. THE CONDITIONS FOR SHORTEST FOCAL LENGTH

In the earlier investigation the focal properties and aberrations of a series of symmetrical lenses of bore $2R=D$ and pole separation S were computed for several values of S/D as function of the lens excitation parameter

$$k^2=0{\cdot}022\,H_0^2R^2/V_r. \qquad \ldots\ldots(2)$$

In a subsequent paper, discussing the magnetic objective lens of smallest spherical aberration (Liebmann 1951), the effect of changing the lens radius R, for fixed H_0 and V_r, was investigated for several values of S/D. It was found there that for each lens geometry S/D there is an optimum value of k^2, with a corresponding value of R.

The same method, of studying the effect of a change in R, can be applied to see whether there is a value of $k^2=k^2_{\min}$ which makes the focal length f of the objective, or its chromatic aberration constant C_c, a smallest value (in absolute units). It is found that there are such values $k^2_{\min}$ for each lens geometry S/D,† one value of $k^2_{\min}$ for the smallest focal length, and another, somewhat larger, value for the smallest value of C_c. These values of $k^2_{\min}$ are plotted as functions of S/D in fig. 1.

As H_0 and V_r had been assumed fixed, eqn. (2) determines a unique value R_0 for each lens geometry S/D, for which f becomes a minimum; similarly for C_c. Moreover, from eqn. (2) follows

$$R_0 \propto V_r^{1/2}H_0^{-1} \qquad \ldots\ldots(3)$$

for $f_{\min}$ as well as for $(C_c)_{\min}$; the constant of proportionality is a function of S/D. It is more convenient to replace H_0, the maximum field strength along the axis, by H_p, the field strength between the parallel iron surfaces of the pole-piece tips, as in the discussion on the objective lens of lowest spherical aberration, because the maximum obtainable value of H_p is known for each kind of iron used. One can then write

$$R_0=BV_r^{1/2}H_p^{-1}\,(\text{cm}), \qquad \ldots\ldots(4)$$

---

* See also Lenz (1950, eqn. (12)).

† Earlier results, for $0{\cdot}2\leqslant S/D\leqslant 2$, were extended to $S/D=4$.

where the geometrical constant B is only a function of the relative pole-piece separation S/D:

$$B=(k^2_{\min}/0{\cdot}022)^{1/2}(H_0/H_p)^{-1}. \qquad \ldots\ldots(5)$$

As f/R and C_c/R had previously been shown to be functions of k^2, different for each value S/D, one has obviously

$$f_{\min}=(f/R)_m R_0 \text{ (cm)} \quad \ldots\ldots(6) \quad \text{and} \quad (C_c)_{\min}=(f/R)_m R_0 \text{ (cm)}, \quad \ldots\ldots(7)$$

where $(f/R)_m$ is the value of f/R at $k^2_{\min}$.

Equations (4), (6) and (7) show that $f_{\min}$ and $(C_c)_{\min}$ are directly proportional to the square root of the (corrected) accelerating voltage $V_r[V_r=V(1+10^{-6}V)]$ and inversely proportional to the field strength H_p.

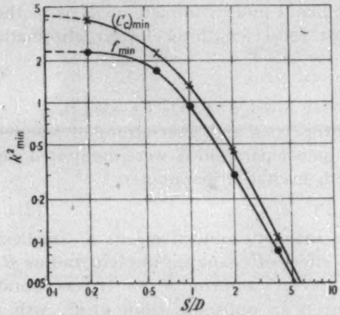

Fig. 1. $k^2_{\min}$ as function of S/D for shortest focal length $f_{\min}$ and smallest chromatic aberration constant $(C_c)_{\min}$.

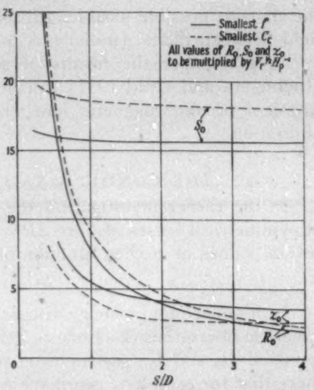

Fig. 2. Optimum values of lens radius R_0, pole separation S_0 and specimen distance z_0 from centre plane for lens of smallest f or smallest C_c as functions of S/D.

§ 3. VARIATION OF LENS CONSTANTS WITH S/D

It is interesting to compare the shortest focal length and smallest chromatic aberration constant of lenses of different gap width. By insertion of the values of $k^2_{\min}$ from fig. 1 into eqn. (5), the values of the optimum lens radii R_0 for each pole separation S/D are found from eqn. (4), one value of R_0 yielding the lens of shortest focal length, the other one the lens of smallest chromatic aberration constant. The corresponding values of f and C_c are then found from eqns. (6) and (7). The result is plotted in figs. 2 and 3, the full lines referring to the lenses of shortest focal lengths, the dashed lines referring to the lenses of smallest chromatic aberration constants. It is seen that all parameters R_0, f and C_c fall monotonically with an increase in S/D, but for $S/D \geqslant 2$ the further decrease in f and C_c is small. The limiting values for $S/D \to \infty$ are: $f_{\min} \to 6{\cdot}75\ V_r^{1/2}H_p^{-1}$ cm and $(C_c)_{\min} \to 5{\cdot}31\ V_r^{1/2}H_p^{-1}$ cm, which are nearly reached for $S/D \simeq 4$.

For a more complete appraisal of a lens as an electron microscope objective one requires a knowledge of the specimen position z_0 (with reference to the centre plane of the lens), and of its spherical aberration constant C_s. These were therefore determined for the relevant values of $k^2_{\min}$, and are also shown in figs. 2 and 3. z_0 is so large at very small values of S/D that the specimen lies just outside the field. For increasing values of S/D the specimen position moves into the gap between the pole pieces, approaching a distance of approximately $0{\cdot}23S$ from the centre plane for lenses of shortest focal length, and of approximately $0{\cdot}14S$ for lenses of smallest chromatic aberration constant. The spherical aberration constant C_s shows a minimum for $S/D \simeq 1{\cdot}2$ and rises approximately linearly for large values of S/D. However, over the likely range of S/D used in practice, C_s is quite small, of the order of the best values used in present-day instruments.

Two further sets of curves in figs. 2 and 3 represent the pole-piece separation S_0 for smallest f or smallest C_c, and the lens excitation parameter $NIV_r^{-1/2}$. Both these functions show only very small variation with S/D.

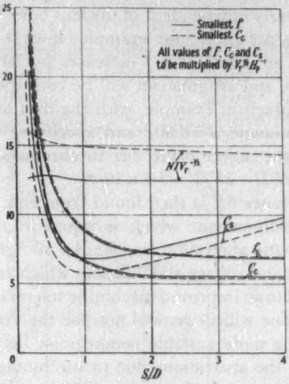

Fig. 3. $f_{\min}$, $(C_c)_{\min}$, C_s and $NIV_r^{-1/2}$ as functions of S/D.

The values of R_0, S_0, f, C_c, C_s and z_0 plotted in figs. 2 and 3 are obtained in cm if the values read off the curves are multiplied by the factor $V_r^{1/2}H_p^{-1}$, where V (and V_r) is measured in volts and H_p in gauss. For the usual range of voltages and magnetic materials met in present-day electron microscopy this factor $V_r^{1/2}H_p^{-1}$ lies between 0·01 and 0·05, and mostly between 0·01 and 0·02. Hence, f, C_c and C_s are all of the order of 0·1 cm, if the objective is designed for minimum f or minimum C_c, whereas S_0 will mostly lie between 0·02 and 0·03 cm.

As a more detailed example, the data of Le Poole and van Dorsten's lens, as given in their lecture, will be compared in the table with the data derived from fig. 2, the same values of S/D, V_r and H_p being chosen ($V = 80$ kv, $V_r = 86{\cdot}5$ kv, $H_p = 24\,000$ gauss).

Lens type	R_0 (cm)	S_0 (cm)	S/D	$f_{\min}$ (cm)	$(C_c)_{\min}$ (cm)	C_s (cm)	z_0 (cm)	NI
Le P. & v. D. (exp)	0·025	0·20	4	0·085	—	—	—	*c.* 4000
Shortest *f* (calc.)	0·024	0·19	4	0·083$_5$	0·066$_7$	0·120	0·043	3680*
Smallest C_c (calc.)	0·027	0·22	4	0·084$_5$	0·066$_4$	0·115	0·032	4210*

* Nominal values (to be increased by about 5% to 10% for loss in iron circuit).

The calculated data are seen to be in very good agreement with the experimental values.

§4. ASTIGMATISM IN A SHORTEST FOCAL LENGTH OBJECTIVE

Figures 2 and 3 would indicate that, for given pole-piece gap S_0, a slight advantage could be obtained regarding the smallest values of f or C_c by decreasing the lens bore $D=2R_0$, keeping S_0 nearly constant. However, this will be offset by increased astigmatism. The astigmatic difference Δ of the foci of an elliptically distorted lens is approximately (Hillier and Ramberg 1947, Sturrock 1951)

$$\Delta/f \propto 4\delta R/R, \qquad \ldots\ldots(8)$$

where δR is the difference of the radii of the largest and smallest bore of the distorted lens. It is known from practical experience that the absolute values of the machining tolerances of such small bores as are used in the lenses here under discussion are nearly independent of the lens bore.* Assuming, therefore, $\delta R=$ constant, one has $\Delta/f \propto 1/R$; for example, if S/D is decreased from the value $S/D=4$ to such an extent that f increases by 10% ($S/D \simeq 1{\cdot}5$), R_0 will increase by a factor 2·6, and astigmatism will be correspondingly diminished.

Applying this to a practical example, with the data of the table as a starting point, assuming a semi-angle $\alpha=0{\cdot}002$ and specifying a disc of confusion of 100 Å ($\delta r=5\times10^{-7}$) in the object plane due to chromatic aberration alone, one finds from eqn. (1) $2\delta H/H-\delta V/V=3{\cdot}8\times10^{-3}$.

The machining tolerance δR is then found from eqn. (8), for a smallest disc of confusion due to astigmatism which is equal in diameter to the disc of confusion due to chromatic aberration, as $\delta R \simeq 4\times10^{-5}$ cm. The slightly higher requirement for current and voltage stabilization, which an increase of C_c by 10% would mean, would lead to an improved machining tolerance of $\delta R \simeq 1{\cdot}2\times10^{-4}$ cm. In practice, therefore, one will in general not use the very shortest focal length possible, but will seek a more suitable compromise between lowest geometric optical aberrations and the aberrations due to machining defects.

ACKNOWLEDGMENT

The writer wishes to thank Dr. T. E. Allibone for permission to publish this paper.

REFERENCES

von Ardenne, M., 1940, *Z. Phys.*, **115**, 339.
Hillier, J., and Ramberg, E. G., 1947, *J. Appl. Phys.*, **18**, 48.
Lenz, F., 1950, *Z. angew. Phys.*, **2**, 448.
Le Poole, J. B., and van Dorsten, A. C., 1951, Electron Microscopy Conference, St. Andrews, 19th–20th June.
Liebmann, G., 1951, *Proc. Phys. Soc.* B, **64**, 972.
Liebmann, G., and Grad, M.E., 1951, *Proc. Phys. Soc.* B, **64**, 956.
Sturrock, P. A., 1951, *Phil. Trans. Roy. Soc.* A, **243**, 387.

---

* For very small bores, corresponding to $S/D \geqslant 4$, they may even be greater for smaller bores than for somewhat larger bores. This compensates for the fact that for large S/D values the influence of the elliptically distorted hole on the focal length becomes reduced and the astigmatism of the whole lens is less.

Effect of Strain Ageing upon the Distribution of Glide Bands in Cadmium Crystals

By D. F. GIBBONS*

Department of Metallurgy, University of Birmingham

Communicated by A. H. Cottrell; MS. received 2nd November 1951

ABSTRACT. It is shown that there is a marked difference in the distribution of visible glide bands, after plastic deformation, between cadmium crystals containing small amounts of nitrogen and those relatively free from nitrogen. The distribution of glide bands in the crystals containing nitrogen is compared with Lüders bands in strain-aged mild steel.

§ 1. INTRODUCTION

It has been demonstrated previously (Cottrell and Gibbons 1948) that an effect of a small amount of nitrogen in solution in cadmium crystals is to induce the phenomenon called 'strain ageing' or 'thermal hardening', which gives rise to a discontinuous stress–strain curve, fig. 1, curve (*a*). If such a crystal is re-tested immediately it gives a smooth curve, fig. 1, curve (*b*), in which it can be seen that the critical shear stress is lowered. However, the original discontinuous type of curve may be regained by annealing at room temperature, fig. 1, curve (*c*). By analogy with the discontinuous stress–strain curve obtained with strain-aged mild steel specimens, the stress at which plastic deformation first occurs will be called the 'upper yield stress' and the stress at which plastic deformation continues the 'lower yield stress'.

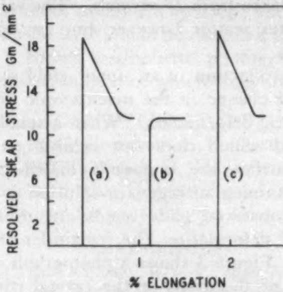

Fig. 1. Shear stress–strain curves for a cadmium crystal containing nitrogen. (*a*) Crystal in annealed state, (*b*) immediate re-test, (*c*) after further anneal at 24° c for 2 hrs.

This phenomenon in single crystals was first observed by Orowan (1934) using zinc crystals; nitrogen in solution has since been shown to be the cause (Wain and Cottrell 1950). Orowan called the phenomenon 'thermal hardening' because of the increase in critical shear stress caused by annealing. This phenomenon should not be confused with the 'hardening', i.e. increase in critical shear stress, caused by developing an oxide or surface layer on a crystal

---

* Now Research Fellow at Institute for the Study of Metals, University of Chicago, U.S.A.

(Andrade and Randall 1948, Harper and Cottrell 1950). 'Hardening' by a surface layer does not produce an 'upper yield stress' and, furthermore, if such a crystal is immediately re-tested it has the same critical shear stress, provided there has been negligible work hardening, and not a lowered critical shear stress as would be the case if the crystal strain-aged.

§2. MATERIAL AND EXPERIMENTAL RESULTS

The cadmium used was supplied by the Imperial Smelting Corporation Ltd. and was of high purity (99·999%); the only metal impurities which could be detected spectrographically were lead, copper and iron. This cadmium was further distilled three times under a vacuum of 10^{-6} cm Hg in order to remove any gaseous impurities. The crystals used during the investigation were grown in a modified type of Andrade travelling furnace (Andrade and Roscoe 1937). All crystals which are free from nitrogen show no strain aging and have a critical shear stress of $7{\cdot}0 \pm 1$ g/mm^2 when strained at a rate of about 10^{-5} sec^{-1}. This figure is an average taken from 20 crystals. This extremely low value for the critical shear stress also gives an indication of the high purity of the crystals, since it is the lowest reported value for the critical shear stress of cadmium crystals of which the writer is aware. Crystals containing nitrogen and exhibiting strain ageing have a value for the lower yield stress of $11{\cdot}5 \pm 2$ g/mm^2. This figure is an average taken from 17 crystals. The values for the upper yield stress show a much greater scatter however, but are on average 70% greater than the lower yield stress.

Coincident with the production of an upper yield stress in these cadmium crystals there is a marked change in the macroscopic distribution of the glide bands formed during plastic deformation. When a small (e.g. 1%) shear strain has occurred in a crystal which does not exhibit strain ageing, the glide bands observed on its surface are uniformly distributed (see fig. 2, Plate). However, in crystals containing nitrogen in solution it is found that, after a similar shear strain, the observed glide bands are grouped into one or more localized regions of heavy deformation, the remainder of the crystal being free from visible glide bands. Figure 3 shows a photograph of such a region. This region started from one of the grips of the crystal (this grip is just off the photograph) and extended for about one-sixth of the length of the specimen. The shear strain in this region is about 10%. Photographs of parts of this band at higher magnification are shown in figs. 4 and 5. Figure 4 shows the centre of the region where the glide bands are densely packed, and fig. 5 shows the end of the region where there is a gradual decrease in density of the glide bands. When the shear strain in the region is greatly increased, to about 150%, the end of the band becomes much more sharply pronounced, revealing a sharp change from the region of densely packed glide bands to the part of the crystal where none are visible.

§3. DISCUSSION

This region of heavy glide must not be confused with the phenomenon of geometric softening or 'stove piping' as described by Andrade and Roscoe (1932). In the case of geometric softening the localized band of heavy glide is caused by the rotation of the slip direction and slip plane towards the axis of tension during plastic deformation, so increasing the resolved shear stress on the plane and causing apparent softening. Geometric softening is only noticeable when χ (the angle between the slip plane and the axis of tension) is greater than about 45°. However, in the present investigation, regions of localized glide were observed in all crystals which showed strain ageing, even where χ was as low as 9°: for example, figs. 3–5 are from a crystal for which $\chi = 11°$. Furthermore, in the crystal of fig. 2, which did not show strain ageing, $\chi = 52°$, which is in the region where geometric softening might occur, but in spite of this the glide bands were uniformly distributed.

It has already been stated (Cottrell and Gibbons 1948) that there is a similarity between the strain ageing of cadmium crystals and the yield phenomenon of mild steel. This investigation has now shown another similarity, since these localized regions of glide may be compared with the Lüders bands which occur in mild steel, these bands being localized regions of the specimen which have deformed plastically while the rest of the specimen remains undeformed. However, the regions of heavy glide in cadmium differ markedly from Lüders bands in one respect. A Lüders band in steel is first formed at the onset of the yield point elongation and then spreads along the specimen until, at the end of the yield point elongation, it has covered the whole of the gauge length. In the case of cadmium, however, the rate of work hardening within the region of heavy glide is very low indeed, since cadmium recovers rapidly at room temperature. Therefore, instead of spreading along the whole length of the specimen, the region continues to deform by itself; very large local deformations (for example, shear strains of 270%) can be obtained in this way in the localized region of glide. Fig. 6 shows a silhouette photograph of a specimen which contained two of the regions, in each of which large strains have occurred.

ACKNOWLEDGMENTS

The author wishes to thank Professor A. H. Cottrell for his encouragement and helpful discussions, and Professor D. Hanson, in whose laboratories the investigation was made, and the Department of Scientific and Industrial Research for their interest and for providing facilities for this investigation.

REFERENCES

Andrade, E. N. da C., and Randall, R. F. Y., 1948, *Nature, Lond.*, **162**, 890.
Andrade, E. N. da C., and Roscoe, R., 1937, *Proc. Phys. Soc.*, **49**, 152.
Cottrell, A. H., and Gibbons, D. F., 1948, *Nature, Lond.*, **162**, 488.
Harper, S., and Cottrell, A. H., 1950, *Proc. Phys. Soc.* B, **63**, 331.
Orowan, E., 1934, *Z. Phys.*, **89**, 605, 614, 634.
Wain, H. L., and Cottrell, A. H., 1950, *Proc. Phys. Soc.* B, **63**, 339.

Single Contact Lead Telluride Photocells

By A. F. GIBSON
Physics Department, Telecommunications Research Establishment, Great Malvern, Worcs.

Communicated by R. A. Smith; MS. received 11*th September* 1951, *and in amended form* 21*st November* 1951

ABSTRACT. In a recent paper the photoconductivity of lead sulphide films was discussed in terms of a barrier mechanism. Large single crystals of lead telluride have now been grown and, with these, single barrier photocells can be prepared. The simplest barrier is formed at a metal–semiconductor contact. Such barriers, as exhibited in rectifiers, have been mainly studied. It is found that the photosensitivity and time constant of such cells is determined by the total current at the contact point, as expected from barrier theory. The variation in barrier height with temperature and time has also been determined.

---

§ 1. GENERAL INTRODUCTION

It is well known that an evaporated or chemically deposited film of PbS consists of a large number of microcrystals separated by potential barriers. These barriers are believed to be the chief cause of the high resistance of such films (Chasmar 1948, Sosnowski, Starkiewicz and Simpson 1947, etc.). Clearly, therefore, if the layer resistance is to change appreciably on illumination the change must occur at the high resistance barriers, any change in the resistance of individual crystals being unimportant. On this basis a theory of photoconductivity has been devised (Gibson 1951) which assumes that on the free surface of each microcrystal there are surface states of the type envisaged by Bardeen (1947). The surface states carry a net positive or negative charge depending on whether the crystal is of p or n type, and a Schottky type barrier is formed. On illumination by light of suitable wavelength electrons and positive holes are produced within the space charge region of the barrier. For n-type crystals the free holes are drawn to the surface by the intense local electric field and for p-type crystals electrons move to the surface. In either case the net surface charge, which determines the barrier height, is reduced and conduction is facilitated. This action is illustrated in fig. 1.

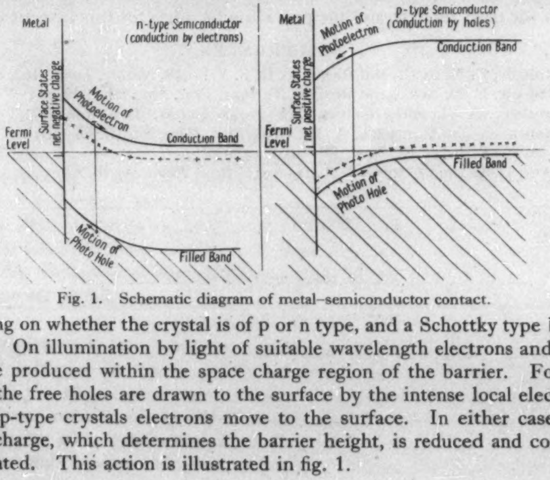
Metal
n-type Semiconductor
(conduction by electrons)
Surface States
net negative charge
Motion of Photoelectron
Fermi Level
Conduction Band
Motion of Photo Hole
Filled Band
Metal
p-type Semiconductor
(conduction by holes)
Motion of Photoelectron
Conduction Band
Surface States
net positive charge
Fermi Level
Filled Band
Motion of Photo Hole

Fig. 1. Schematic diagram of metal–semiconductor contact.

Calculations of the sensitivity and time constant of PbS photoconductive layers on this theory leads to fair and sometimes good agreement with experiment (Gibson 1951). An evaporated layer, however, consists of many millions of barriers and it is clearly desirable to study single-barrier photocells. Large single crystals of PbTe are now available in this laboratory (Lawson 1951) and have been used to make such photocells. The simplest possible system consists of a single Schottky barrier in the semiconductor and a metal contact. This constitutes a rectifier and hence the standard theory of crystal rectification is applicable.

§ 2. THEORETICAL INTRODUCTION

In view of the high mobility of electrons and holes in PbTe the diode theory of rectification is appropriate (Torrey and Whitmer 1948). The current at any applied voltage is determined by the *difference* in the number of current carriers flowing in each direction across the barrier and is given by

$$i=i_0 \exp(-\mathbf{e}\phi/\mathbf{k}T)\{1-\exp(-\mathbf{e}V/\mathbf{k}T)\}, \qquad \ldots\ldots(1)$$

where V is the applied voltage, ϕ the barrier height relative to the Fermi level and $\mathbf{e}$ the electronic charge. By convention V and i_0 are counted positive when the rectifier is biased in the high resistance direction (metal positive for a p-type crystal). The constant i_0 is determined by the number and mobility of the current carriers in the semiconductor.

The diode formula fails in all practical rectifiers in two main respects and PbTe rectifiers are no exception to this rule. These failures are :

(i) No point-contact rectifier is known to give the correct value of the constant $\mathbf{e}/\mathbf{k}T$. It is common to include a constant β in the quantity $\mathbf{e}/\mathbf{k}T$ where β is always less than unity. This procedure is quite empirical but facilitates the description of experimental results.

(ii) At high voltages in the blocking direction eqn. (1) fails completely to describe the observed current which increases with voltage more rapidly than expected. Various theoretical explanations have been given to account for the failures of the diode theory (e.g. Torrey and Whitmer 1948) but these are of no importance in the present context. There is some theoretical justification for assuming that ϕ is a function of voltage in the blocking direction. This arises as follows: As the barrier viewed from the semiconductor gets higher and steeper in the blocking direction it becomes thinner at the top. Tunnelling is then possible, which reduces the effective barrier height as viewed from the metal. In the simplest case of a triangular barrier ϕ is given by

$$\phi=\phi_0-CV, \qquad \ldots\ldots(2)$$

where C is a dimensionless constant which can be enumerated theoretically if sufficient approximations are made. Alternatively, the reduction in barrier height with voltage may be due to an image force effect. For the present purpose, however, eqn. (2) can be considered as empirical and the physical cause of barrier height reduction is immaterial. It will be shown later that for voltages greater than about 1 volt eqn. (2) is a reasonable description of the experimental results.

In addition to the variation in carrier current with applied field we shall require the variation of photoconductive sensitivity with voltage. Using the symbols employed in the previous paper (Gibson 1951) the photoconductive sensitivity is defined as $S=d(\Delta\sigma/\sigma)/dI$, where $\Delta\sigma$ is the incremental change in conductivity σ produced by illumination of intensity I. The sensitivity is then given by the relation

$$S=\tau/N\boldsymbol{k}T \quad \text{where} \quad N=(KM/2\boldsymbol{e}^2\phi)^{1/2} \qquad \ldots\ldots(3)$$

(Gibson 1951). In eqn. (3) τ is the time constant of the barrier, K the dielectric constant and M the density of impurities in the semiconductor, all in rationalized m.k.s. units. The general nature of eqn. (3) is stressed in the previous paper. The equation is of the same form in any theory relying upon a decrease in barrier height on illumination, independent of the type of barrier envisaged.

As the experiments to be described were carried out at a constant temperature the quantity $N\boldsymbol{k}T$ can be considered constant and only the variation in τ with voltage is required. The time constant of the barrier is simply derived as it is the lifetime of the electrons or holes injected into the surface states on illumination and as such is inversely proportional to the number of carriers of opposite sign available for recombination. This is the total number of carriers at the surface of the crystal and, as the direction of motion is immaterial, is given by the *sum* of the number of carriers flowing both ways across the barrier. Hence

$$\frac{1}{S} \propto \frac{1}{\tau} \alpha n = n_0 \exp\left(-\frac{\boldsymbol{e}\phi}{\boldsymbol{k}T}\right)\left\{1+\exp\left(-\frac{\boldsymbol{e}V}{\boldsymbol{k}T}\right)\right\}, \qquad \ldots\ldots(4)$$

where n is the total number of carriers at the surface when a potential V is applied. This equation is identical with eqn. (1) with the appropriate sign changed. Naturally the variation in ϕ with voltage given by eqn. (2) and the inclusion of an arbitrary constant β are equally applicable here. To conclude therefore, the full current and sensitivity equations of a rectifier photocell may be written:

In the blocking direction

$$i=i_0 \exp\left\{-\beta\boldsymbol{e}\frac{(\phi_0-CV)}{\boldsymbol{k}T}\right\}\left\{1-\exp\left(-\frac{\beta\boldsymbol{e}V}{\boldsymbol{k}T}\right)\right\}, \qquad \ldots\ldots(5)$$

and

$$\frac{1}{S}=\frac{1}{S_0}\exp\left\{-\beta\boldsymbol{e}\frac{(\phi_0-CV)}{\boldsymbol{k}T}\right\}\left\{1+\exp\left(-\frac{\beta\boldsymbol{e}V}{\boldsymbol{k}T}\right)\right\}. \qquad \ldots\ldots(6)$$

In the easy flow direction

$$i=i_0 \exp\left\{-\frac{\beta\boldsymbol{e}\phi}{\boldsymbol{k}T}\right\}\left\{\exp\left(\frac{\beta\boldsymbol{e}V}{\boldsymbol{k}T}\right)-1\right\}, \qquad \ldots\ldots(7)$$

and

$$\frac{1}{S}=\frac{1}{S_0}\exp\left\{-\frac{\beta\boldsymbol{e}\phi}{\boldsymbol{k}T}\right\}\left\{\exp\left(\frac{\beta\boldsymbol{e}V}{\boldsymbol{k}T}\right)+1\right\}. \qquad \ldots\ldots(8)$$

§ 3. EXPERIMENTAL METHODS

Single crystals of PbTe cleaved from samples prepared by W. D. Lawson of this laboratory were mounted on the ground end of a Dewar type cell blank. Fine nickel wires were soldered on to the two extreme ends of the crystal and a tungsten cats-whisker was pressed on to the crystal. The use of three contacts allows the resistance of the soldered junctions to be estimated if required but in general their resistance was quite negligible compared with that of the cats-whisker. The cats-whisker was made of 0·005 inch diameter tungsten wire electrolytically pointed unless otherwise stated. No 'forming' processes were used. Each cell was provided with a sapphire window and evacuated. As expected from experience with PbTe photoconductive films, there was little or no rectification or photosensitivity at room temperature, but on cooling to, say, 90° K the contact resistance increased markedly, rectification occurred and photosensitivity appeared at all contacts, including soldered junctions. The source of illumination was a monochromator fitted with two LiF prisms. The radiation was interrupted at 800 c/s and the resulting signal amplified at this frequency.

It was soon noticed that only p-type crystals of PbTe produced good rectifiers and marked photo-effects. This is analogous to the well-known result that only n-type germaniun and p-type silicon produce good rectifiers. This feature of PbTe was not unexpected as it is known that only p-type PbS gives good rectification and transistor action (Legrand 1948, Gebbie, Banbury and Hogarth 1950). The experiments to be described are, therefore, on cooled p-type specimens of PbTe unless otherwise stated. The density of current carriers and the sign of their charge was determined from Hall constant data obtained by Dr. E. H. Putley of this laboratory.

The time constant τ of a metal–PbTe photocell is very short and of the order of 1 μsec or less. This is similar to that of germanium rectifier photocells. In view of the very short time constant the voltage dependence of τ could not readily be measured directly and hence only the observed photosensitivity could be compared with the theoretical equations already given. The sensitivity of these cells is considerably less than that of evaporated layers.

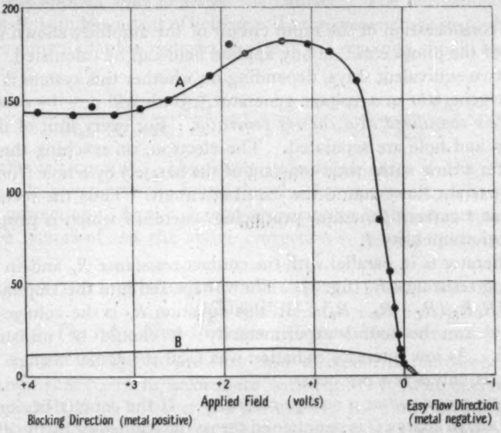

Fig. 2. Variation in signal from p-type PbTe photodiode with bias voltage.
Curve A. Observed signal in arbitrary units.
Curve B. Calculated photovoltage.

§ 4. THE INTERPRETATION OF RESULTS

In order to decrease the height of a space-charge barrier in a p-type crystal electrons must be captured in the surface states. This involves the motion of charged particles produced by the primary illumination, as illustrated in fig. 1. An e.m.f. is therefore developed even at zero applied field. As will be shown the photo e.m.f. developed in the cell is itself voltage-dependent and hence the magnitude of the contribution from the photo e.m.f. and photoconductivity at any applied field must be carefully distinguished. This will now be discussed.

Consider the results given in fig. 2. The curve A represents the signal actually observed at the output of an amplifier following the illuminated cell to which a steady bias voltage is applied. The signal is made up of two parts for all applied voltages, except zero where only the photo e.m.f. contributes. It will be appreciated that the photo e.m.f. is of fixed polarity (such that the metal becomes negative) whereas the photocurrent reverses on reversal of the applied voltage. Clearly the photo e.m.f. and photoconductive signal are additive in the blocking direction and subtract from one another in the forward direction.

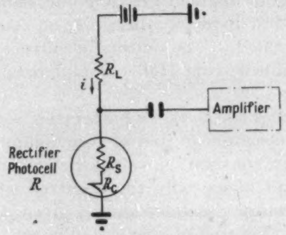

Fig. 3. Input circuit arrangement.

From a consideration of the input circuit of the amplifier shown in fig. 3 the magnitude of the photo e.m.f. at any applied field can be calculated. This may be done in two equivalent ways, depending on whether this system is considered as a current generator or a voltage generator. Both will now be described.

(*a*) *System considered as a current generator.* For every unit of illumination one electron and hole are separated. The electron, on reaching the surface, is captured after a time τ (the time constant of the barrier) by a hole from the metal and a unit current flows round the external circuit. Thus the rectifier can be considered as a current generator producing current i which is proportional to the illumination intensity I.

This generator is in parallel with the contact resistance R_C and in series with the spreading resistance R_S (fig. 3). The voltage fed into the amplifier is therefore $\Delta V \propto IR_C R_L/(R_L+R_C+R_S)$. In this equation R_C is the voltage-dependent quantity and can be found experimentally; it should be measured under illumination. As low intensity radiation was used the actual change in R_C with illumination is only a few per cent.

(*b*) *System considered as a voltage generator.* If the contact be considered as a capacity C, and a charge Q is maintained across the condenser by the illumination the resulting voltage is Q/C. The charge Q is related to the illumination intensity by the relation

$$Q = I\tau = ICR_e = IC\,\frac{R_C(R_L+R_S)}{R_C+R_L+R_S},$$

where R_e is the effective shunt resistance across the contact capacitor C. The voltage fed into the amplifier from this generator is then given by

$$\Delta V \propto IR_C R_L/(R_L+R_C+R_S),$$

which is the result already obtained.

This expression allows the photo e.m.f. at any applied voltage to be computed since R_C, R_L and R_S can be measured and the magnitude of the photo e.m.f. at one voltage (i.e. $V=0$) is known. In order to simplify the above expression the spreading resistance R_S can be neglected compared with the load resistance R_L.

The theoretical photo e.m.f. given by the above formula is plotted in fig. 2 (curve B) using the measured values of R_C, R_L and R_S. It will be seen that the photo e.m.f. is largely independent of voltage in the blocking direction and the magnitude of the photocurrent, represented by the difference between curves A and B, largely independent of small variations in the photo e.m.f. It is found in practice sufficiently accurate to assume the photo e.m.f. to be independent of voltage in this direction. In the easy flow direction however the two contributions to the resulting signal are of comparable magnitude and both approach zero as the field becomes sufficient to remove the barrier entirely, as would be expected. An enlarged diagram of this portion of the curve is given later (fig. 6).

When the photoconductive signal has been obtained, the cell sensitivity defined as above may be derived from it. This is done by consideration of the input circuit (fig. 3). It can readily be shown by differentiation that for small signals ($\Delta\sigma \ll \sigma$)

$$\frac{\Delta\sigma}{\sigma} = \frac{\Delta R_C}{R_C} = \frac{\text{Signal}}{V}\,\frac{R_L + R_C + R_S}{R_L}, \qquad \ldots\ldots(9)$$

where V is the applied voltage across the contact. The derivation of eqn. (9) assumes that R_C is independent of voltage. In the present case this is not justified and it can be shown that the right-hand side of the equation should be multiplied by the quantity

$$1 + \frac{i}{R_L + R_C + R_S}\,\frac{\partial R_C}{\partial i} = 1 - \frac{V R_L}{R_C(R_L + R_C + R_S)}\,\frac{\partial R_C}{\partial V},$$

where i is the cell current. The factor reduces to unity if $\partial R_C/\partial i$ or $\partial R_C/\partial V$ equals zero. In practice it was found that this factor never leads to more than a 25 per cent correction. As the change in sensitivity with voltage usually covers two or three factors of ten the above correction is usually quite unimportant.

§ 5. THE VOLTAGE CHARACTERISTICS OF PbTe RECTIFIER PHOTOCELLS

(i) *The Easy Flow Direction: Current Measurements*

As the applied voltage in the easy flow direction is increased the barrier resistance approaches zero in accordance with eqn. (7). The current does not become indefinitely large, however, but is limited by the finite spreading resistance of the crystal at the contact point. When the spreading resistance becomes the controlling factor, the current is given by

$$V - \phi = iR_S, \qquad \ldots\ldots(10)$$

from which the barrier height ϕ may be determined. The current–voltage relation of a typical contact in the low resistance direction is given in fig. 4 (*a*), the intercept on the voltage axis indicating the value of ϕ in volts. Unfortunately it is always possible to draw a straight line through the last few points of any curve of this type and hence this method of obtaining ϕ is of doubtful accuracy. The accuracy may be improved by the following procedure. As the current–voltage relation is drawn on a large scale a number of high-voltage points are not included in the diagram but these points may be used in a plot of $V-\phi$ against current i using logarithmic coordinates. This is shown in fig. 4 (*b*). For this curve the value of ϕ determined as above is used. A 45° line is now drawn through the available points: this indicates whether or not an ohmic region has been reached and eqn. (10) is valid. The spreading resistance is determined from this curve and ϕ re-determined. The second value is likely to be more accurate than the first.

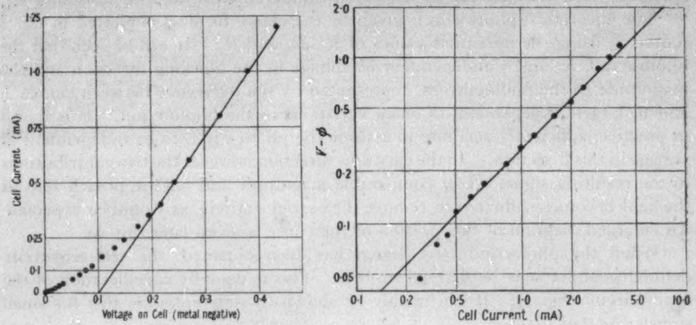

(*a*) (*b*)

Fig. 4. Forward characteristic of p-type PbTe rectifier at 90° K. (*a*) low voltages, (*b*) high voltages.

The spreading resistance of most cells, like that shown in fig. 4, was about 300 ohms. As the specific resistance of p-type PbTe crystals at 90° K is about 1 ohm cm the theoretical spreading resistance would be about 40 ohms if the contact area were equal to the tungsten wire diameter (Benzer 1949). In fact the contact area was probably less than this, as inferred from the high value of R_S obtained. PbTe is unlike Ge in this respect as the spreading resistance in Ge diodes is usually less than the theoretical value. In addition, the spreading resistance in Ge is rarely accurately ohmic (Benzer 1949).

When the spreading resistance has been determined, the voltage iR_S is subtracted from the measured voltage across the cell to obtain the barrier voltage drop.

The latter should be used in eqns. (5), (6), (7) and (8). The validity of eqn. (7) can now be checked. The equation may be written in the form

$$(i+i_0')/i_0' = \exp(\beta \boldsymbol{e} V/\boldsymbol{k}T), \quad \text{where} \quad i_0' = i_0 \exp(\beta \boldsymbol{e}\phi/\boldsymbol{k}T).$$

The graph of $\log(i+i_0')$ against V should be a straight line and a value of i_0' must be obtained by trial and error to achieve this. This procedure, which is quite common, is more reasonable than might at first be expected, as the value of i_0' chosen only affects the low voltage points. It is found that i_0' increases as the temperature increases (as expected from eqn. (7)) and hence the trial and error method becomes more difficult.

The slope of the resulting straight line, as shown in fig. 3, should be $\beta \boldsymbol{e}/\boldsymbol{k}T$, and hence a value of β can be obtained. Values of β obtained in this way are given in the table.

(ii) *The Easy Flow Direction*: *Photosensitivity Measurements*

To analyse the photo response in the easy flow direction the observed signal is plotted against the voltage drop across the barrier (the spreading resistance having been taken into account) and the theoretical photo e.m.f. plotted on the same diagram. This is shown in fig. 6. Both curves should meet the voltage axis at $V = \phi$ and an extrapolation of the experimental curve to this point seems reasonable. This implies agreement between theory and observation but it is clearly impossible to observe zero sensitivity directly as the signal disappears into the background noise before this condition is achieved.

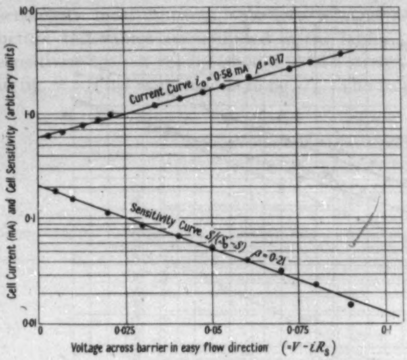

Fig. 5. Curves illustrating determination of constant β from conductivity and photosensitivity measurements.

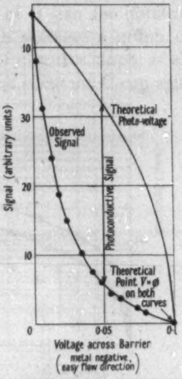

Fig. 6. Variation in signal from p-type PbTe photodiode with bias voltage (easy flow direction only).

As the photoconductivity and photo e.m.f. are 180° out of phase in this bias direction the theoretical photo e.m.f. is greater than the observed signal at all voltages and the photoconductive signal is given by the difference between the two curves. From this the photoconductive sensitivity, defined as above, is derived. Re-writing eqn. (8), the sensitivity should be given by

$$\frac{S}{S_0' - S} = \exp\left(-\frac{\beta e V}{\boldsymbol{k}T}\right) \quad \text{where} \quad \frac{1}{S_0'} = \frac{1}{S_0}\exp\left(-\frac{\beta e \phi}{\boldsymbol{k}T}\right).$$

A suitable value of S_0' to produce a linear relation between $\log\{S/(S_0' - S)\}$ and V is obtained by trial, as done in fig. 5, and the value of β can again be obtained. The value of S_0 is not critical and often $S_0' \gg S$ is quite adequate. The values of β obtained by this method are included in the table.

(iii) *The Blocking Direction*: *Current Measurements*

The current in the blocking direction should be given by eqn. (5) as already described. There are three voltage regions over which this equation may be examined. These are as follows.

(*a*) *Low voltages* such that $CV \ll \phi_0$ and $\exp(-\beta e V/\boldsymbol{k}T)$ is comparable with unity: in this region the theoretical equation can in principle be checked by finding a value of i_0' and obtaining a value of β in the usual way. In practice however the voltage range over which the above conditions hold is too narrow and the value of i_0 too critical for an accurate determination of β. Nevertheless values of β obtained in this way are included in the table.

(*b*) *High voltages* such that $\exp(-\beta eV/kT) \ll 1$: in this region the current is determined entirely by the variation in effective barrier height with voltage. A graph of $\log i$ against V should be a straight line at high voltages, the slope of the line giving the constant C. That a straight line is obtained is indicated in fig. 7 for a typical cell at two temperatures. Values of C obtained by this method are given in the table.

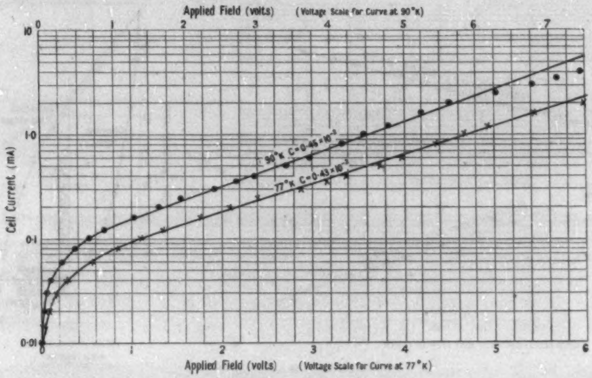

Fig. 7. Back characteristic of p-type PbTe rectifier at 90° K and 77° K (metal positive, blocking direction).

(*c*) *Intermediate voltages*: it can readily be shown by differentiation of eqn. (5) that the current voltage curve passes through an inflection and hence the quantity di/dV has a minimum. This minimum should occur at a voltage given by

$$\beta eV_{\min} = 2kT \log(1/C). \qquad \ldots\ldots(11)$$

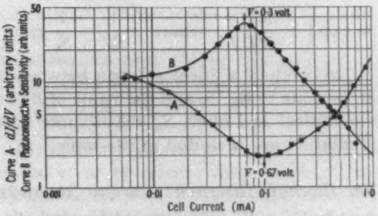

Fig. 8. Metal positive, blocking direction, cell current 90° K.
Curve A indicates minimum in di/dV.
Curve B indicates maximum in photoconductive sensitivity.

That di/dV does in fact have a minimum is shown by curve A of fig. 8 for a typical cell. It is, however, a shallow minimum for all cells examined and the voltage at which the minimum occurs is not easily determined. From the value of $V_{\min}$ either the constant β or the constant C may be determined if the other is assumed known. In view, however, of the large error that can occur in the determination of $V_{\min}$, together with the fact that C appears within a logarithmic term, it is advisable to use the equation to obtain β, not C. Values obtained in this way are included in the table.

(iv) *The Blocking Direction: Photosensitivity Measurements*

A similar set of three important voltage regions hold for photoconductive sensitivity measurements. At low voltages a value of β can be obtained as before and values are included in the table. At high voltages a graph of log sensitivity against voltage should yield a straight line of negative slope, as shown in fig. 9. This is analogous to fig. 7. The value of the constant C can again be obtained and is given for a number of cells in the table.

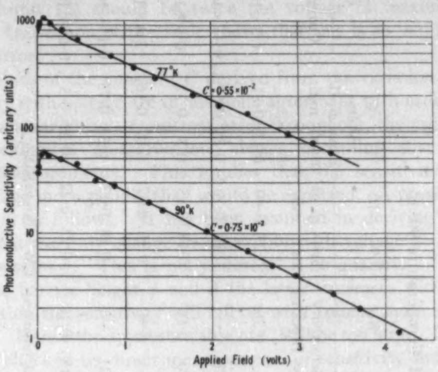

Fig. 9. Variation in photoconductive sensitivity of p-type PbTe photodiode at 90° K and 77° K (metal positive, blocking direction).

At intermediate voltages it can be shown that the sensitivity passes through a maximum (corresponding to the inflection in the current–voltage relation) at a voltage given by the relation

$$\beta \boldsymbol{e} V_{\max} = \boldsymbol{k} T \log(1/C). \qquad \ldots\ldots(12)$$

It will be noticed that eqns. (11) and (12) differ only by a factor two and hence it is to be expected that the minimum in di/dV will occur at twice the voltage of the sensitivity maximum.

A typical sensitivity curve indicating the maximum in sensitivity is given in fig. 8, curve B. This curve also shows directly that the sensitivity is almost inversely proportional to the cell current at high voltages. This arises because the quantity $\exp(-\beta \boldsymbol{e} V/\boldsymbol{k} T)$ becomes very small at high voltages and eqns. (5) and (6) tend to become identical. In other words the current in the field direction becomes very much larger than the current against the field and approximately equal to the sum of the two currents.

(v) *Discussion of Results given in the Table*

(*a*) The resistance of soldered junctions to PbTe does not usually exceed 5 ohms but occasionally a soldered contact with p-type material can have a resistance of about 100 ohms at 90° K. The rectification and photoconductivity

Cell Temperature 90° K

1	2	3	4	5	6	7	8	9	10	11	12	13	14	15
Cell No.	Contact Type	holes/cm³	ϕ (volts)	β						Volts		Constant C		$R_C(\Omega)$ at zero volt
				Current		Sensitivity		Sens. di/dV		Sens. di/dV		Current	Sens.	
				Easy	Blocking	Easy	Blocking	max.	min.	max.	min.			
1	SJ	5×10^{16}	—	—	0·33	—	0·36	0·37	0·40	0·11	0·21	$1{\cdot}3\times10^{-2}$	$1{\cdot}7\times10^{-2}$	125
3	CW	10^{18}	0·10	0·17	0·19	0·21	—	0·20	0·16	0·26	0·67	$0{\cdot}45\times10^{-2}$	$0{\cdot}75\times10^{-2}$	2000
8	CW	10^{18}	0·085	0·16	0·18	0·20	0·16	0·18	0·15	0·3	0·72	$0{\cdot}4\times10^{-2}$	$0{\cdot}5\times10^{-2}$	2000
8A	SJ	10^{18}	—	0·38	0·33	—	0·40	0·46	0·37	0·07	0·16	$2{\cdot}4\times10^{-2}$	—	27
15	CW	5×10^{16}	0·125	0·18	0·18	0·21	—	0·18	0·17	0·34	0·75	$0{\cdot}15\times10^{-2}$	$0{\cdot}145\times10^{-2}$	5000
19	CW	10^{18}	0·09	0·22	0·12	0·18	0·12	0·23	0·22	0·22	0·5	$0{\cdot}65\times10^{-2}$	$0{\cdot}78\times10^{-2}$	1500

SJ = Soldered junction; CW = Cats-whisker of such contacts is large enough for measurements to be made. Figures for two soldered contacts are included in the table. The value of ϕ cannot be obtained for these junctions from the easy flow current curves as the resistance of the other contact becomes important.

(*b*) The agreement between the values of β (columns 5, 6, 7, 8, 9 and 10) obtained by different methods is within the limits of experimental error, thus indicating the validity of eqns. (5), (6), (7) and (8). It will be noticed that the value of β is greater for soldered junctions than for cats-whisker contacts. This agrees with the general experience that good large area contacts yield values of $\boldsymbol{e}/\boldsymbol{k}T$ nearer to the theoretical value. The fact that β is not equal to unity does not invalidate the main purpose of the experiments which is to relate the total current and photosensitivity. As the current is an observable quantity any semi-empirical formula would suffice.

(*c*) According to the theory already given the voltage at which di/dV is a minimum (column 12) should be twice the voltage of maximum sensitivity (column 11). Inspection of the table shows that this is so within the limits of experimental error.

(*d*) The values of the constant C derived from the variation of current and photosensitivity with voltage are in adequate agreement with each other. There does however appear to be a consistent error throughout, the value of C derived from photoconductive measurements always exceeding that derived from conductivity measurements. This implies that the sensitivity falls off with increasing voltage more rapidly than would be expected. A possible explanation of this effect is as follows. It has been assumed in deriving the theoretical equation (6) that the only change in sensitivity with voltage is due to variation in the time constant τ. This is not justified. The quantity N in eqn. (3) is a function of the barrier height ϕ and if the latter decreases with voltage in the blocking direction the sensitivity will fall off with voltage more rapidly than the time constant. Hence the apparent value of C will be too large. This hypothesis could only be checked by direct measurements of sensitivity and time constant.

§ 6. THE HEIGHT OF THE SCHOTTKY BARRIER AT PbTe SURFACES

It is apparent from the table that at 90° K the height ϕ of the barrier is about 0·1 volt. This is obtained from the easy flow bias direction as already described.

(i) *The Variation in ϕ with Temperature*

The current–voltage relations of four cells have been measured at various temperatures. From these curves the barrier height ϕ and the value of the constant β can be obtained. In all cases ϕ decreases with increasing temperature. Due to the poor accuracy of this experiment it is not possible to be certain of the exact form of the variation but in all cases it has been possible to draw a straight line through the available points. The results for one cell are given in fig. 10 (*a*). The slope $d\phi/dT$ for this cell was rather less than that of the others examined, thus allowing a wider temperature range to be covered. Adequate rectification at room temperature is unusual. Values of $d\phi/dT$ obtained were as follows:

$d\phi/dT$ (v/°K)	4×10^{-4}	7×10^{-4}	8×10^{-4}	8×10^{-4}
ϕ at 90° K (v)	0·13	0·11	0·12	0·125

In addition to the variation in ϕ with temperature it was found that β was also temperature dependent, increasing to a maximum at about 200° K and subsequently falling again slowly. At no temperature did β reach unity, though a maximum of about 0·5 was not uncommon.

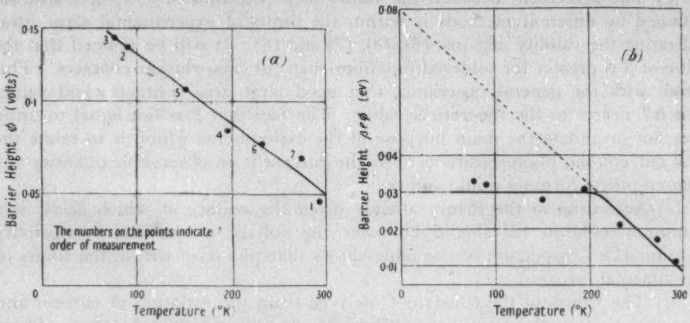

Fig. 10. (*a*) Variation in barrier height ϕ with temperature. (*b*) Variation in barrier height $\beta e\phi$ with temperature.

There is, in principle, a second method of obtaining ϕ. It can be obtained from the variation in contact resistance with temperature at $V=0$. From eqn. (5) it is clear that, if $eV<kT$, then $i=i_0\{\exp(-\beta e\phi/kT)\}(eV/kT)$ or

$$\log\left(\frac{\text{Resistance}}{\text{Temperature}}\right)=\frac{\beta e\phi}{kT}+\text{constant}. \qquad \ldots\ldots(13)$$

Hence a plot of $\log(R/T)$ measured at low voltages against the reciprocal of the absolute temperature should have a slope $\beta e\phi/k$. It was found that the inclusion of the temperature in the log term was quite unimportant and did not materially affect the shape of the curve obtained but it is nevertheless included in the curve given in fig. 11. This figure refers to the cell described in fig. 10 (*a*). In all, six cells have been examined in this respect. The similarity to the resistance temperature relation of normal evaporated or chemical cells (e.g. Gibson 1951) is quite apparent.

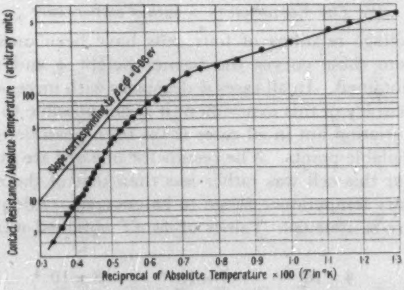

Fig. 11. Variation in contact resistance of p-type PbTe rectifier with temperature.

As ϕ and $\beta e\phi$ are both functions of temperature any correlation between figs. 10(*a*) and 11 is complicated. A rough correlation can be obtained in the following rather crude manner.

From the measured values of ϕ and β the variation of $\beta e\phi$ with temperature can be obtained, as shown in fig. 10(*b*). Errors, of course, increase as the error in β is now included. The resulting curve (fig. 10(*b*)) appears to be horizontal below 200° K and hence the resistance temperature curve (fig. 11) is a straight line in this region. The values of $\beta e\phi$ are 0·03 ev (fig. 10(*b*)) and 0·022 ev (fig. 11).

At temperatures above 200° K the quantity $\beta e\phi$ falls off and is given approximately by the relation $\beta e\phi = A - BT$ (fig. 10(*b*)) where A and B are constants. Substituting this relation into eqn. (13) shows that the slope of the resistance–temperature curve should now increase suddenly to the value $A/\boldsymbol{k}$. From fig. 10(*b*) the value of A can be deduced to be about 0·08 ev and a line corresponding to this energy has been drawn in fig. 11. It should be parallel to the experimental curve. As before, the agreement is only approximate. It is, however, difficult to see any other way in which these two experiments can be correlated.

Finally it should be added that a decrease in ϕ with increasing temperature is not unreasonable theoretically. The density of surface states is fixed but their occupation density decreases with temperature in accordance with standard Fermi statistics, thus decreasing ϕ. The exact variation in ϕ with temperature depends upon the numerical constants of the model envisaged.

(ii) *The Variation of ϕ with Time*

Early in this work it was noticed that the contact resistance of a cats-whisker contact increased steadily with time of exposure to the air. This effect does not appear to occur at soldered junctions to any appreciable extent.

Experiments on this effect were first carried out by Mr. F. Goode of Cambridge University working as a Vacation Student in this laboratory. Further measurements were carried out by the writer. The results may be summarized as follows.

(*a*) The contact resistance at $V=0$ of a freshly cleaved crystal increases steadily for the first few days after exposure. The resistance measurement is carried out at 90° K, the crystal being allowed to warm up to room temperature between measurements. The best empirical formula to fit the results was $\log R = \text{constant} \times (\text{time})^{1/2}$ where $\log R$ is presumably proportional to the barrier height ϕ.

(*b*) The slope of the resistance–temperature relation at low temperatures increases with time approximately as $(\text{time})^{1/2}$.

(*c*) The barrier height ϕ obtained by the back projection of easy flow current curves increases with time in a similar manner. It was not possible to confirm that ϕ was accurately proportional to $(\text{time})^{1/2}$ because of considerable scatter on the experimental points.

(*d*) If, after a few days exposure, the crystal surface was carefully scraped with a razor blade the contact resistance could be decreased appreciably, subsequent exposure causing it to rise steadily again. With careful scraping, the contact resistance could be reduced in two or three 'steps'. This experiment was thought to indicate that the surface film was not of negligible thickness. In view of the above it would appear likely that the surface states are levels within an oxide film formed on the crystal surface. Such a film should cease to grow after a few days but in fact it was found that further exposure of the contact (up to about three months) caused a deterioration in its quality as a rectifier and as a photocell, partly due to an increase in the spreading resistance.

(iii) *The Variation of ϕ with Contact Metal*

According to the theory of Bardeen (1947) the barrier height should be largely independent of the metal used to make a contact. A number of metals have been tried, covering a range in work function from about three volts (Al and Mo) to six volts (Pt) but no significant change in ϕ was observed. The metals of low work function did not appear to give accurately ohmic spreading resistances but this feature was not studied in detail.

An attempt was made to see if there was any correlation between the nature of the metal and the magnitude of the photo e.m.f. obtained. However it was found that, even with any one metal, a variation of up to 100:1 in the magnitude of the photo e.m.f. could be obtained across any one crystal surface. The absolute magnitude of the photo e.m.f. or photoconductive sensitivity is a complex function of contact area, contact pressure, cleanliness, crystal impurity concentration, surface state density, optical absorption coefficient and other parameters. No significant variation between metals could be observed.

If, as the above experiments suggest, the Schottky barrier exists on the crystal surface when the metal is not in contact with the surface it should be possible to obtain a photo e.m.f. without a metal connection. A sheet of mica was therefore placed between the crystal surface and a wire gauze, through which the crystal could be illuminated. The resulting condenser had an impedance of about 100 megohms at 800 c/s (the light interruption frequency) and hence a high impedance input stage was used before the main amplifier. A small but significant signal was obtained on illumination of the cell. This experiment, together with the above, appears to demonstrate the existence of surface states on PbTe crystals.

§ 7. THE SPECTRAL RESPONSE OF PbTe RECTIFIER PHOTOCELLS

The spectral response of a typical cell is given in fig. 12. The spectral distribution of sensitivity is probably the most constant feature of all the cells examined, the shape indicated by fig. 12 being quite typical. This curve should be compared with that given by Moss (1948) for the spectral response of a PbTe evaporated layer. The fall in sensitivity at or about 5 μ is characteristic of PbTe at 90° K and the slow rise at shorter wavelengths suggests an approximately constant quantum efficiency.

It will be noticed that the spectral responses at zero volts (photo e.m.f.) and when a field is applied (photoconductivity) are not exactly the same. According to the theory they should be identical.

The spectral limits of a number of cells at 90° K are given in the following table, the value in each case being that at which the sensitivity is half maximum.

Type of Contact	CW	CW	CW	CW	CW	SJ	SJ	SJ
Wavelength (μ)	4·9	5·2	4·8	4·9	5·3	4·8	5·2	5·5

CW = cats-whisker; SJ = soldered junction.

Following the measurements made by Moss (1948) on photoconductive layers of PbTe attempts have been made to measure the shift of the spectral limit with temperature. This has been severely hampered by the fact that most cells have very little sensitivity at solid CO_2 temperature (195° K) and hence the only temperatures at which measurements could be made were 90° K and 77° K. The small temperature range implies large errors. The following table indicates the magnitude of the shift.

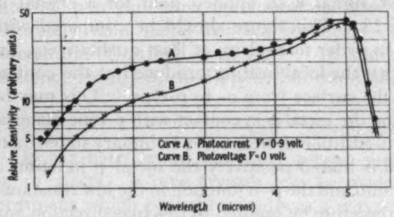

Fig. 12. Variation of photoconductive and photovoltaic signal with incident wavelength. Cell temperature 90° K. Relative magnitudes of curves adjusted for comparison.

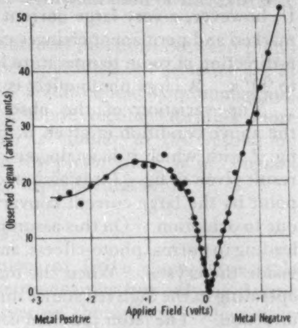

Fig. 13. Variation in signal with bias voltage from n-type PbTe with p-type surface. Cell temperature 90° K.

Type of contact	CW	CW	SJ	SJ
Density of holes/cm³ of crystal	5×10^{16}	10^{18}	5×10^{16}	5×10^{16}
Spectral shift (ev/° K × 10^4)	4·0 ± 0·5	5·3 ± 1·0	5·0 ± 1·0	5·8 ± 1·0

The observed shift is of the same magnitude as observed in evaporated layers of PbTe and is in the same direction.

There is little or no shift in the spectral limit with applied field though some cells showed a slight shift to longer wavelengths when a field of two or three volts was applied in the blocking direction. The effect, if any, was too small for adequate measurement.

§ 8. THE PHOTOSENSITIVITY OF n-TYPE PbTe CRYSTALS

It has already been stated that n-type crystals show poor rectification and negligible photo effects. This statement must now be qualified and the conditions under which photosensitivity can be achieved discussed.

With a freshly cleaved surface of n-type material the resistance in the two bias directions may differ by a factor of two or three. The direction of rectification is, of course, characteristic of an n-type semiconductor. The contact resistance is largely independent of temperature and increases only by a factor of two or three on cooling with liquid oxygen.

In the above condition the cell will show a very small photo e.m.f., considerably less than that obtained from p-type crystal. The magnitude of the photo e.m.f. does not increase appreciably on cooling. On passing a current through the contact in either direction the photo e.m.f. soon disappears into the current noise so generated. There is, therefore, no appreciable photo-conductivity sensitivity.

The above conditions do not represent rectification as normally understood. If, however, a very large current is passed for a short time through the contact, marked and permanent changes can occur. The crystal which still rectifies in the n-direction at room temperature becomes a rather poor p-type rectifier on cooling to 90° K. A large photo-effect is now observed at this temperature.

The variation of the observed signal with applied field for a crystal in the above condition is given in fig. 13. This figure should be compared with fig. 2 with which it is analogous. In order to explain, at least qualitatively, the result given in fig. 13 it is assumed that the local heating produced at the contact point by the large current converts the surface from n- to p-type. This may be due to oxidation. On this assumption the metal is in contact with p-type material leading to normal photo-effects, and in addition there is a p–n boundary somewhere inside the crystal. When the metal is biased positively the metal–p junction is operating in the high resistance direction and the p–n junction in the low resistance direction. The latter junction can therefore be ignored in this bias direction and hence the resulting signal will be characteristic of a metal–p junction. Comparison of figs. 13 and 2 shows that this is so. In the other bias direction, with the metal negative, the metal–p junction continues to be important at low voltages and the signal falls to zero in the usual way. In this bias direction the p–n junction is operating in the high resistance direction and soon becomes the main source of contact resistance. A signal appears which increases steadily (apparently linearly) with increasing voltage. The phase of this signal corresponds to a photo e.m.f. against the applied field, which is the expected direction for this type of barrier.

One interesting feature of these metal–p–n cells in the metal negative direction is the spectral response, which rises to a very high and narrow peak at long wavelengths (about 5 μ), the peak being relatively much greater than that in conventional p-crystal cells. It should be remarked, however, that metal–p–n cells have not been examined very fully and require further study.

The above effects, characterized by a fall and subsequent rise in photosensitivity when the metal is biased negatively, has also been observed in one nominally p-type crystal. Fortunately the actual crystal had been examined previously as regards Hall constant by Dr. E. H. Putley who stated that it was 'somewhat inhomogeneous'.

§ 9. LEAD TELLURIDE CRYSTAL–CRYSTAL CONTACTS

The characteristics of small area contacts between p-type crystals of similar impurity concentration have been measured. With these contacts it is not possible to obtain a simple quantitative theory of the variation in conductivity of photosensitivity with voltage and hence they have not received much attention. A qualitative theory of p–p contacts (two Schottky barriers back to back) suggests that the contact resistance at high voltages should decrease with voltage in both directions. A resistance fall occurs at silicon carbide contacts and the same model has been evoked to explain the results (Mitchell and Sillars 1949). It is found that the resistance of PbTe contacts falls by about 10 times when 1 volt is applied in either direction. No contact measured has ever been accurately symmetrical however. Similar statements apply to photosensitivity measurements, the lack of symmetry being even more pronounced. A symmetrical p–p junction should produce no photo e.m.f. if the contact is symmetrically illuminated but in practice this condition was never achieved and a photo e.m.f. was always observed. This experiment does however represent another demonstration of the existence of Schottky barriers on free crystal surfaces.

Contacts between p and n crystals and also internal junctions between p and n portions of the same single crystal are now being studied. The latter are of considerable interest and will be the subject of a subsequent communication. Internal p–n junctions are found to obey the diode rectifier formula more accurately than metal contact rectifiers. This is similar to the results on germanium (Goucher *et al.* 1951). In addition the photo e.m.f. is of constant efficiency from $1{\cdot}0\,\mu$ to $5{\cdot}0\,\mu$ within the limits of experimental error.

§ 10. CONCLUSIONS

It has been found that only p-type specimens of PbTe show appreciable photo effects. N-type crystals may be made photosensitive but only by drastic treatment which probably produces a p-type layer on the surface. The reason for this difference between p- and n-type samples is not known but is likely to be determined by the nature of the oxide film on the semiconductor surface.

The voltage dependence of the photosensitivity indicates that the time constant and sensitivity are determined by the total number of holes available for recombination with electrons injected into the surface states. This result, which supports the general barrier theory of photoconductivity, is not invalidated by the failure of the diode formula for crystal rectifiers as the conductivity of the contact is an observable quantity.

It is of interest to note that V. Roberts of this laboratory has observed large peaks of photosensitivity at the silver electrodes of chemically deposited PbS layers. The peak always occurs at the positive electrode, moving to the other electrode if the field is reversed. This implies photoconductivity at the metal–semiconductor contact and comparison with the polarity indicated in fig. 2 shows immediately that these layers must contain at least some p-type crystals.

It has been found that the height of the Schottky barrier decreases with increasing temperature. As already explained there is some doubt about the validity of the method of obtaining the barrier height but it is unlikely that the temperature dependence is seriously in error. The decrease in ϕ with temperature immediately offers an explanation of a discrepancy between theory and experiment described in a previous paper (Gibson 1951). It was then found that the equation $S=\tau/N\mathbf{k}T$ where $N=(KM/2\mathbf{e}^2\phi)^{1/2}$ was not in perfect agreement with experiments on PbS layers. It was there stated that the value of S increased on cooling from room temperature to 90° K by a factor of about 1·4 more than theory would demand. Now, however, it is known that ϕ for PbS increases on cooling by a factor of two in this temperature range and hence N decreases by $\sqrt{2}$ or S increases by a factor of about 1·4, as required.

ACKNOWLEDGMENTS

The author is indebted to his colleagues at Telecommunications Research Establishment for much help and advice, and particularly to those to whom reference is made in the text. He is indebted to the Chief Scientist, Ministry of Supply, and to the Controller, H.M. Stationery Office, for permission to publish this work.

REFERENCES

BARDEEN, J., 1947, *Phys. Rev.*, **71**, 717.
BENZER, S., 1949, *J. Appl. Phys.*, **20**, 804.
CHASMAR, R. P., 1948, *Nature, Lond.*, **161**, 281.
GEBBIE, H. A., BANBURY, P. C., and HOGARTH, C. A., 1950, *Proc. Phys. Soc.* B, **63**, 371.
GIBSON, A. F., 1951, *Proc. Phys. Soc.* B, **64**, 603.
GOUCHER, F. S., PEARSON, G. L., SPARKS, M., TEAL, G. K., and SHOCKLEY, W., 1951, *Phys. Rev.*, **81**, 637.
LAWSON, W. D., 1951, *J. Appl. Phys.*, in the press.
LEGRAND, K., 1948, *Z. Phys.*, **124**, 219.
MITCHELL, E. W. J., and SILLARS, R. W., 1949, *Proc. Phys. Soc.* B, **62**, 509.
MOSS, T. S., 1948, *Nature, Lond.*, **161**, 776.
SOSNOWSKI, L., STARKIEWICZ, J., and SIMPSON, O., 1947, *Nature, Lond.*, **159**, 818.
TORREY, H. C., and WHITMER, C. A., 1948, *Crystal Rectifiers* (New York : McGraw-Hill Inc.).

Lead Sulphide Rectifier Photocells

BY A. F. GIBSON
Physics Department, Telecommunications Research Establishment,
Great Malvern, Worcs.

Communicated by R. A. Smith ; *MS. received* 11*th September* 1951, *and in amended form* 21*st November* 1951

ABSTRACT. Following the study of lead telluride rectifier photocells described in a contemporary paper, similar properties have been found for lead sulphide.

§ 1. INTRODUCTION

LARGE single crystals of PbS of relatively high purity ($\sim 5 \times 10^{16}$ carriers/cm^3) are available naturally from Sardinia and in addition single crystals with carrier concentrations of the order of 5×10^{18} per cm^3 have been grown synthetically in this laboratory. In common with PbTe only p-type specimens show marked rectification and photo-effects. Familiarity with the previous paper on PbTe will be assumed.

§ 2. THE VOLTAGE CHARACTERISTICS OF PbS RECTIFIER PHOTOCELLS

The variation of contact current and photosensitivity with voltage of PbS rectifiers is very similar to that of PbTe and can be described by the same equations. As might be expected from experience with PbS films photosensitivity at room temperature occurs, presumably because the barrier height ϕ is still appreciable at this temperature (usually about 0·1 volt). The barrier height increases with decreasing temperature in a manner similar to that in PbTe.

The occurrence of sensitivity and rectification at room temperature increased the temperature range over which the voltage parameters could be measured.

In particular the constant C (eqn. (2) of the preceding paper (Gibson 1952, to be referred to as I)) could be determined over a range of temperatures. This experiment seemed to justify a theoretical calculation of C for comparison with the results. This was carried out by Mr. D. Hum of the Mathematics Division, Telecommunications Research Establishment, for a particular crystal assuming that the barrier was triangular in shape, and that the density of impurities in the semiconductor was 2×10^{17} per cm^3. In addition, the experimentally obtained values of ϕ were used. The results obtained are illustrated in the table.

Temperature (°K)	290	195	90
ϕ (V) from forward characteristic	0·08	0·13	0·20
C_{exp} from photosensitivity measurements	$6{\cdot}4 \times 10^{-2}$	$4{\cdot}8 \times 10^{-2}$	$1{\cdot}6 \times 10^{-2}$
C_{exp} from current measurements	$5{\cdot}4 \times 10^{-2}$	$3{\cdot}1 \times 10^{-2}$	$1{\cdot}6 \times 10^{-2}$
C_{theor}	$7{\cdot}0 \times 10^{-2}$	$4{\cdot}2 \times 10^{-2}$	$1{\cdot}9 \times 10^{-2}$

The value of C at 90° K is comparable with the values given for PbTe in I (see table). As before, the value of C from photosensitivity measurements is generally larger than that obtained from current measurements.

It is found that PbS contacts differ from PbTe in one major respect, namely the occurrence of a marked forward signal similar to that obtained in n-type PbTe (fig. 13 of I). At first this was dismissed as due to inhomogeneity in the crystals but in fact this additional signal is observed in all specimens provided a sufficiently great contact pressure is applied. Unlike that obtained in n-type PbTe the forward signal in p-type PbS saturates at high voltages. In addition the spectral response of the contact is the same in this voltage region as in the back direction. There is some evidence that this signal is 'intrinsic' in the sense that it is due solely to an increase in the number of carriers within the body of the semiconductor and is not a barrier phenomenon.

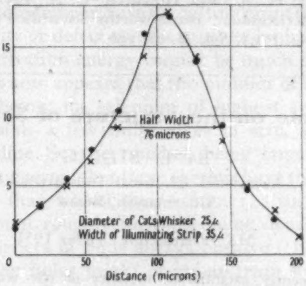

Variation of signal strength with position of light beam.

§ 3. THE DISTRIBUTION OF SENSITIVITY ABOUT A CONTACT POINT

The use of a PbS crystal at room temperature allows the cell window to be removed and the sensitivity measured with a small spot of light from a short focal length objective. In fact a fine line of light was used, traversed in a direction at right angles to the line. The variation of signal strength with position is given in the figure. To obtain the sensitivity distribution a correction must be applied for the finite size of the source. If the distribution in intensity across the slit of light is square-topped the correction can be shown to be quite trivial. Assuming this to be so, the figure represents the distribution of sensitivity around the point. The half width obtained, namely 76μ, compares with about 200μ for a germanium photo diode.

Physically this experiment implies that an electron produced by the illumination a distance 38μ from the contact point has a probability of one half of reaching the contact to produce photoconductivity. This experiment is directly analogous to electron injection into p-type PbS transistors, the only difference being that here the electrons are produced optically within the material and do not enter from an emitter contact. According to Banbury, Gebbie and Hogarth (1951) the current gain in one of their PbS transistors fell to one-half the value at zero electrode separation when the electrodes were 37μ apart. The excellent agreement with the above figure must be in part fortuitous even though both crystals were from the same source and the same diameter of tungsten wire was used in both experiments.

An attempt was made to examine the sensitivity distribution at low temperatures but this was hampered by the necessity of using a window. It would appear that the width of the distribution increases by about three or four times on cooling to 90° K.

Finally it should be noted that the diffusion length for electrons in p-type PbS derived from the above experiment refers only to the surface regions and probably depends on surface treatment, hole density, etc. Combined with mobility measurements from Hall data the above experiment indicates that, in the sample used with 5×10^{16} holes per cm^3, the electron lifetime is about 0·5 microseconds.

REFERENCES

BANBURY, P. C., GEBBIE, H. A., and HOGARTH, C. A., 1951, *Semi-conducting Materials*, ed. H. K. Henisch (London : Butterworths Scientific Publications), p. 83.
GIBSON, A. F., 1952, *Proc. Phys. Soc.* B, **65**, 196.

A Note on the Structure of Selenium

BY E. BILLIG
Research Laboratory, Associated Electrical Industries Ltd., Aldermaston Court, Aldermaston, Berks.

MS. received 8*th October* 1951

ABSTRACT. The recently established identity of the width of the (optical) energy gap, 2·05 ev, for both amorphous and crystalline selenium, suggests that the chain structure of crystalline selenium is maintained also in the amorphous phase. The low electrical conductivity of amorphous selenium is ascribed to potential barriers existing between individual chains.

THE mechanism of the electrical conductivity of selenium has been in doubt for many years and this has been a handicap to the full understanding of the properties of Se barrier cells. It is the purpose of this note to review some recent work, mainly on single crystals, with a view to clarifying the situation.

Optical measurements (Dowd 1951) on some comparatively large single crystals of Se have definitely established the existence of a fundamental absorption band determined by the atomic lattice structure of crystalline Se. The absorption edge is more definite and much sharper than in polycrystalline Se and, at room temperature, lies at $\lambda_0 = 6\,120\,\text{Å}$, practically the same as in amorphous Se. In the past the peak in the photoconductivity curve of polycrystalline Se had to be used (von Hippel 1948) for the location of the energy gap of Se crystals; the shape of the photoconductivity curve, however, is not so directly related to the gap width as is the absorption edge, the former being dependent on such additional factors as density of traps, recombination rates, etc. The establishment of the sharp absorption edge now confirms the generally accepted view that the essential pattern, the long chains, are preserved in the amorphous state. From the close agreement of the wavelength at the absorption edge, that is of the width of the forbidden energy zone in the two cases ($\boldsymbol{hc}/\boldsymbol{e}\lambda_0 = 2{\cdot}05\,\text{ev}$), one may conclude that the spacing of the Se atoms along the chains is the same in the amorphous as in the crystalline material.

Regarding the nature of the electrical conductivity of Se, Plessner (1951) concluded from his experiments on single and polycrystals the following:

(*a*) The average mobility of the current carriers is much lower than in most other solids, being of the order of $0{\cdot}2\,\text{cm}^2/\text{v sec}$ in the single crystals and an order of magnitude lower for polycrystalline material at room temperature; it rises exponentially with the temperature, the 'activation energy' being 0·13 ev. Plessner ascribes this behaviour to the presence of potential barriers within the solid.

(*b*) Intrinsic conductivity in solid Se is negligible, the number of carriers that can be thermally excited across an energy gap of 2 ev being insignificant.

(*c*) The number of free current carriers, as determined from measurement of Hall effect and thermo-electric power, is almost independent of temperature over the range tested—room temperature to melting point (220° c)—which implies that practically all impurity or defect centres must be ionized at room temperature or even below; their activation energy cannot be much more than $\boldsymbol{k}T$.

On the other hand, it now appears that the number of carriers varies with the size of the crystallites, being, for selenium of highest available purity*, about $10^{14}/\text{cm}^3$ for single crystals a few millimetres in size, and between 10^{16} and $10^{17}/\text{cm}^3$ for polycrystalline Se, the number being larger the smaller the size of the crystallites. It is suggested that these carriers have their origin at the surface of the crystallites rather than within their volume: a surface density of 10^{12} to 10^{13} per cm^2 would account roughly for the volume densities quoted.

The charge of the carriers in Se is always positive ('holes'), but their origin is rather uncertain. The holes might originate from some acceptor impurity (having fairly high electron affinity) or, alternatively, from structural defects in the lattice. Such defects would act as effective traps for electrons from the valency band, thus creating a hole there which would be free to drift about the lattice. There is no direct evidence to decide between these two alternatives, but recent experience with germanium is rather suggestive. As has been shown by Scaff and Theuerer (1945), single crystals of very high purity n-type Ge can be converted into p-type by mere quenching. This suggests that acceptor centres are created (and frozen in) on the production of purely structural defects in an

---

* 'Spectroscopically standardized selenium shot' supplied by Johnson, Matthey & Co. Ltd.

.B
5
2

otherwise almost perfect crystal lattice of extremely high chemical purity. It is possible that the acceptor centres in Se arise similarly from structural defects of the crystallites. Plessner's observation that the number of carriers in Se decreased on annealing seems to confirm the view that the 'centres' are due to crystal defects rather than to impurities, and the fact mentioned above that the density of carriers is larger for smaller crystallites suggests that these centres or electron traps probably arise at their surface.

(*d*) The electrical conductivity of single crystals along the chains, i.e. along the hexagonal *c*-axis, is about 10 times greater than across them.

The fact that potential barriers seem to exist even for conduction parallel to the chains might be due to the relatively short length of individual chains, with the carriers subsequently having to cross to neighbouring chains. Within any individual chain an excess electron (or hole) moves in a perfectly periodic field due to regularly spaced Se atoms; it can be regarded as practically 'free' in the sense of a Bloch wave moving along a one-dimensional lattice. It is only at the ends of the chains that the electron wave encounters a potential barrier of finite height. On the other hand, it is known (Brill and Krebs 1945) that whilst the length of the unit cell along the hexagonal *c*-axis, i.e. the interatomic spacing along the chain, is quite definite, 2·30 Å, the axial ratio c/a and hence the spacing between neighbouring chains varies between certain limits depending on various factors during crystal growth and heat treatment. The periodicity of the interatomic potential in the *a*-direction, i.e. across the chains, is therefore less perfect and this, together with the considerably larger distance from any one atom to its nearest neighbour in another chain, 3·48 Å, is probably the cause of the much lower electrical conductivity across the chains.

The potential barriers observed in *polycrystalline* material are probably located in the grain boundaries. When amorphous Se is heated to a temperature between 80 and 210° c, crystallites start growing from various nuclei. With increasing time and temperature of the heat treatment given, these crystallites grow until they eventually come into contact, when further heating will have little effect. However, even when the crystallization has thus been completed, the individual grains having grown independently of each other will be orientated at random. They will remain separated from each other by a boundary region, a skin of more or less disorientated or amorphous material (Krebs 1951, Henisch and François 1951) which will present an effective barrier to the passage of the current carriers. The grain boundary region is rather sensitive to impurities. Again referring to Ge which crystallizes much more readily owing to its simple cubic structure, it has been shown (Hall 1950) that most impurities are much more soluble in the liquid than in the solid phase: the well-established technique of purification by controlled crystallization makes use of this fact by pushing these impurities ahead of the solidification front during crystal growth, leaving behind a crystal of high purity. A similar process will probably occur during the growth of Se crystals from the melt or from the amorphous solid. It is expected that impurities will be more soluble in the liquid or the amorphous phase which can accommodate foreign atoms of odd sizes and shapes much more readily than the, rather special, type of lattice of the Se crystals. The grain boundary material left at the end of the crystallization process will thus contain a comparatively large fraction of whatever impurities were present in the original melt. This is substantiated (Plessner 1951) by the fact that any iodine added to the melt does not change the number of current carriers within the crystallites: the observed reduction of resistivity with higher iodine content must be due to the effective bridging of the potential barriers in the grain boundaries.

The very much lower conductivity of *amorphous* selenium (of the order of 10^{-12}, compared with 10^{-5} (ohm cm)$^{-1}$ in crystalline Se) is probably due to the large number of barriers which a carrier has to traverse when travelling from chain to chain on its way from one electrode to the other. In the absence of Hall effect data for amorphous Se, only a very tentative suggestion can be made about the number of available current carriers by comparing the very low absorption ($\sim$1/cm) of long-wave, infra-red, radiation with the high absorption at the peak of the fundamental absorption band, $6{\cdot}5 \times 10^5$/cm for near ultra-violet, when presumably one electron per atom, i.e. $3{\cdot}7 \times 10^{22}$ per cm^3, can be excited into the conduction band. Disregarding any differences in the transition probabilities, one thus arrives at a value of $\sim 5 \times 10^{16}$ carriers/cm^3 which might be available for conduction in amorphous Se. This would then suggest that the low electrical conductivity of amorphous Se is not so much due to an excessively low number of available current carriers, but rather to their extremely low mobility caused by the high potential barriers between chains. This might also be the explanation for the very low photoconductivity, if any, in amorphous as compared with crystalline Se. (Some weak photoconductivity in thin amorphous Se films has recently been reported by Weimer (1950). However, in view of the many pitfalls associated with electrical measurements across thin films, it is rather difficult to assess critically the conclusions drawn from Weimer's experiments, as reported in his short letter.) Even after excitation into the conduction band by absorbing a photon, the electron, and the corresponding hole left in the valency band, will be free to move only along its own chain. In order to contribute to the photo-current it would still have to be lifted over the potential barriers, or to be lifted out of the 'traps', existing between individual chains. Such barriers are far fewer in the case of polycrystalline material, and are non-existent along the *c*-axis of perfect single crystals, hence their much higher photoconductivity.

A remark may be made about the nature (polarity) of the current carriers. Identity of polarity of the carriers for dark and photo-current would be expected for irradiation in the fundamental absorption band of intrinsic semiconductors, or for infra-red photoconductivity of impurity semiconductors. In the first case both the dark and the photo-current would be caused by the generation of electron-hole pairs on thermal or optical excitation, and in the latter case by the excitation of the donor or acceptor centres. For amorphous Se, Weimer reports holes to be the predominant carriers of the photo-current on irradiation in the fundamental absorption band.

Selenium, as the other elements in the sixth column of the periodic table, may be regarded as a molecular solid. With their two pronouncedly covalent bonds these elements readily form diatomic molecules in the vapour phase, and chain or ring structures in the liquid or solid phases; the chains remain more or less independent of each other owing to the comparatively large distance between them. Some correlation between the molecular spectrum and that of the condensed phases might thus be expected: for instance, the vibrational frequency of the diatomic molecule (391·77/cm or $11{\cdot}75 \times 10^{12}$/sec, from spectral analysis (Herzberg 1950)) should be approximately maintained in the chain molecule, at least to its order of magnitude. The usual selection rules restrict vibrational transitions in the molecule to the absorption of a single vibrational quantum, i.e. of wavelength $\lambda \simeq 25{\cdot}6\,\mu$ for Se. The high transparency of solid Se to infra-red radiation would then be the equivalent phenomenon in the solid. Here it is worth noting that other monatomic semiconductors such as diamond, Si, Ge, Te are similarly transparent to infra-red radiation.

The mechanism of long-wave absorption in Se is somewhat doubtful. Permanent dipoles such as give rise to the reststrahlen absorption in alkali halides and other polar compounds are non-existent in monatomic semiconductors, but the vibrations of the Se atoms against the bonding electrons might produce a dipolar moment sufficient for noticeable absorption. Extension into the far infra-red of the absorption measurements of Se should thus be interesting. Absorption with a well-defined peak in this region has recently been reported by Becker and Fan (1949) on Si at a wavelength of approximately $9\,\mu$. Such an absorption if found in Se might account for the disagreement of the values of dielectric constant and refractive index discussed by Dowd (1951).

A theoretical determination of the atomic band structure of the elements in the sixth group would be very valuable. One might expect a band structure with an energy gap decreasing with increasing atomic number similar to that in the fourth group (diamond, Si, Ge, Sn have gaps of ~7, 1·12, 0·76 and 0·1 ev respectively). For the elements in the sixth column where interaction between individual chain or ring-like molecules is much smaller than between neighbouring atoms within any one chain, the theoretical treatment might be considerably simplified by restricting it to a consideration of individual chains only, which would still reveal the more fundamental properties of the solid. A plane zigzag chain of infinite extension might suffice as a model in the first place. The actual structure of the chains in Se (as well as in Te) is not plane but spiralled, the bonding electrons of neighbouring atoms being $\ldots(p_x, -p_y), (p_y, -p_z), (p_z, -p_x), (p_x, -p_y)\ldots.$ Such an arrangement gives maximum overlap between electrons involved in the formation of a bond and minimum overlap between those not so involved. The plane zigzag arrangement, whilst still giving maximum overlap between the bonding p_x and p_y electrons, would produce a somewhat larger overlap between the neighbouring lone pairs, p_z^2, resulting in a fairly strong anti-bonding effect. The contribution to the bond of the $4s^2$ electrons as well as that of the lone electron pair, $4p_z^2$, from each Se atom might be neglected, leaving only two unpaired electrons, $4p_x$, $4p_y$, from each atom to form single ($p\sigma$) bonds at an angle of 90°* by combining with their opposite numbers from the nearest neighbours along the chain. When due allowance is made for hybridization of the 4s and 4p orbitals, it is feasible that an almost filled electron band will result which might be responsible for the positive polarity of the carriers, as observed. Conduction by holes rather than by electrons would generally be expected in solids of the sixth column of the periodic table as their electron bands originate from electronic levels of atoms which have an almost complete outer shell.

ACKNOWLEDGMENT

Thanks are due to Dr. T. E. Allibone for permission to publish this paper.

---

* The actual bond angle in the Se chain is 105°, due to hybridization of s- and p-electrons.

REFERENCES

BECKER, M., and FAN, H. Y., 1949, *Phys. Rev.*, **76**, 1531.
BRILL, R., and KREBS, H., 1945, *J.I.O.A. Report*, **56**, 10.
DOWD, J. J., 1951, *Proc. Phys. Soc.* B, **64**, 783.
HALL, R. N., 1950, *Phys. Rev.*, **78**, 645.
HENISCH, H. K., and FRANÇOIS, M., 1951, *Semi-Conducting Materials*, ed. H. K. Henisch (London : Butterworths Scientific Publications).
HERZBERG, G., 1950, *Molecular Spectrum and Molecular Structure I* (New York : von Nostrand).
HIPPEL, A. VON, 1948, *J. Chem. Phys.*, **16**, 372.
KREBS, H., 1951, *Semi-Conducting Materials*, ed. H. K. Henisch (London : Butterworths Scientific Publications).
PLESSNER, K. W., 1951, *Proc. Phys. Soc.* B, **64**, 671, 681.
SCAFF, J. H., and THEUERER, H. C., 1945, *N.D.R.C. Report*, 14–555.
WEIMER, P. K., 1950, *Phys. Rev.*, **79**, 171.

Electronic Structures and Physical Properties in the Alloy Systems Nickel–Copper and Palladium–Silver

BY B. R. COLES
Department of Physics, Imperial College, London

Communicated by M. Blackman ; MS. received 27th July 1951 *and in revised form 15th October* 1951

ABSTRACT. A comparison is made of the magnetic, electrical and thermo-electric properties of alloys in the two systems, and the lattice spacings, optical properties, electronic specific heat, and x-ray spectroscopy of the nickel–copper alloys are also considered. Palladium–silver alloys show the behaviour expected of them on the band theory of metals, but nickel–copper alloys show well-marked and consistent deviations. It is concluded that unoccupied d-electron levels exist in the copper-rich alloys, whereas such levels do not exist in the silver-rich palladium–silver alloys. From theoretical considerations it seems unlikely that the unoccupied levels form part of a collective d-band, and alternative models are discussed. That the two systems differ so markedly is surprising, but a tentative explanation of the differences is sought in the differing proportions of the atomic volume occupied by the ions in copper and in silver.

§1. INTRODUCTION

THE theoretical treatment of the transition metals and their alloys on the basis of the band theory of metals presents great difficulties, and only the end members of the transition groups have as yet received much attention. The model adopted has treated the overlapping s- and d-bands* in terms of a parabolic distribution of occupied states in the former—a long, low band—and a parabolic distribution of unoccupied states, or holes, in the latter—a high, narrow band (see fig. 7). Thus nickel is regarded as having 0·6 hole per atom in the 3d-band, and the same number of electrons in the 4s-band. This figure is the Bohr magneton number obtained from the absolute saturation moment. For this end member of a transition group it is probably

---

* For convenience these bands will be referred to throughout as the s- and d-bands, indicating the type of wave function which predominates, although each contains a certain admixture of other functions.

.B
5
2

justified to assume that one half band (containing all the d-electrons of one direction of spin) will be completely filled, no paired holes being present. On the addition of copper, possessing in the metallic state a full 3d-band and one electron per atom in the 4s-band, the Fermi surface will be raised in energy, and on the basis of a simple band model (Mott and Jones 1936) the number of d-band holes per atom should fall steadily, reaching zero at 60% copper. The observed fall of the mean saturation moment per atom and of the Curie point is in agreement with expectation.

A similar picture may be presented of the very closely related system palladium–silver: palladium is not ferromagnetic but an examination of its paramagnetic properties and of those of its alloys (Wohlfarth 1949 a) indicates that the number of unoccupied states per atom in the d-band (here the 4d-band) is of the same order as in nickel. The analogous alloy systems nickel–copper and palladium–silver show, however, marked differences in behaviour which cannot be accounted for in terms of any simple band theory. The present paper examines various physical properties in the two systems with special reference to these differences and their possible explanation. An experimental re-investigation of some properties is in progress, detailed results of which will be published later.

§ 2. PHASE EQUILIBRIA AND CRYSTAL STRUCTURES

The four metals nickel, copper, palladium, and silver all possess face-centred cubic structures at all temperatures below their melting points, and both the alloy systems under consideration show complete solid solubility. This makes it possible to examine properties over the whole range of composition without the intrusion of the complications attendant upon phase changes.

The variation with composition of the lattice spacings of these alloys is of interest, for the published data for nickel–copper show (Owen and Pickup 1934) a discontinuity in the slope of the curve at 60% copper*. This has been quoted as supporting the view that the d-band is completely full by this point. The preliminary results of a re-examination suggest, however, that no discontinuity in slope exists at that point, but that an appreciable change of slope of the lattice spacing curve occurs in the composition range where the Curie point is at, or near, room temperature (about 33% copper). The effect would therefore seem to be connected with the Curie point, and not with the filling of the d-band. Such behaviour is found in other alloy systems (Köster and Schmidt 1934), and the lattice spacing–temperature curve of body-centred iron shows a similar type of effect (Schmidt 1933).

Only scanty data (Stenzel and Weerts 1931) are available for the lattice spacings of the palladium–silver alloys, and a detailed investigation is therefore being undertaken. The results will be of great interest, for it will be seen in the following sections that filling of the d-band shows itself far more clearly in the physical properties of these alloys than it does in the nickel–copper system.

§ 3. MAGNETIC PROPERTIES

The behaviour of the ferromagnetic properties has provided the main ground for the belief that in nickel–copper alloys occupation of the 3d-band is complete with copper contents of more than about 60% copper. The work of Alder (1916) provided data (shown in fig. 1) for both saturation magnetic moments and Curie temperatures; the date of this work would seem to justify a re-investigation, but the Curie point results are confirmed by later workers (Krupkowski 1929, Marian 1937, Wheeler 1939). Saturation moment σ and Curie temperature θ fall linearly with copper content and extrapolate to zero at 60% copper; the alloy of highest copper content for which measurements were made contained 38% copper. These results, and those on other nickel alloys, have been interpreted by Mott and Jones (1936) on the assumption that the number of electrons per atom in the 4s-band remains constant at 0·6 per atom, all extra electrons (0·4 per substituted atom for copper) entering the 3d-band holes. Application by Wohlfarth (1949 b) of the collective electron treatment of ferromagnetism of Stoner (1939) suggests that the number of d-band holes does not become zero until a slightly greater copper content (about 65%) than that at which the saturation magnetization disappears.

---

* Compositions are expressed in atomic percentages throughout.

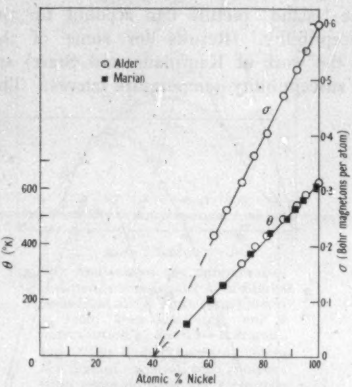

Fig. 1. Saturation magnetic moments σ and Curie temperatures θ of copper–nickel alloys.

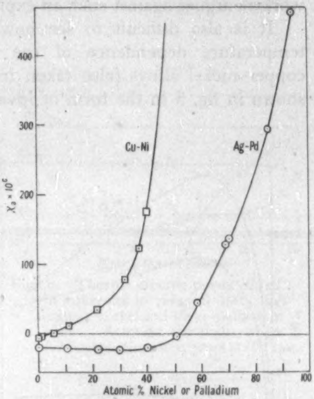

Fig. 2. Atomic susceptibility χ_a in c.g.s. units per gm atom for copper–nickel and silver–palladium alloys.

The paramagnetic properties of the copper-rich alloys are, however, inexplicable in terms of a simple collective electron model. The presence of d-band holes in non-ferromagnetic metals and alloys is indicated by high paramagnetic susceptibilities, approximately inversely proportional to the temperature at higher temperatures. When all d-band states are occupied diamagnetism is to be expected, as shown by copper and silver, the weak temperature-independent paramagnetism of the conduction electrons being insufficient to overcome the diamagnetism of the full inner shells. The room temperature atomic susceptibilities of the palladium–silver alloys (Svensson 1932), plotted in fig. 2, show exactly the behaviour to be expected if all the d-band holes have disappeared when a silver concentration of about 60% has been reached; even the slight increase in diamagnetism expected on adding palladium to silver (and reducing the number of electrons in the 5s-band) is found.

.B
5
2

The results plotted from the data of Kaufmann and Starr (1943) for nickel–copper non-ferromagnetic alloys are quite different. Quite small additions of nickel to copper (~5%) give rise to paramagnetism, the susceptibility increasing rapidly with the nickel content, and the conclusion that holes appear in the 3d-band at quite low nickel contents seems inevitable. Suggestions have been made that inhomogeneity in the alloys, with consequent formation of 'islands' of nickel-rich material in a matrix of nearly pure copper, might be the cause; but this is unlikely on general metallurgical grounds, and, as pointed out by Néel (1940), the agreement found between the results of various earlier workers argues against such an explanation.

It is also difficult to see how the 'island' picture can account for the temperature dependence of the susceptibility. Results for some of the copper–nickel alloys (also taken from the work of Kaufmann and Starr) are shown in fig. 3 in the form of inverse susceptibility–temperature curves. The copper-rich alloys give curves of unusual form but at no composition does any sharp change take place. The increase of susceptibility at higher temperatures can be explained, for alloys with low susceptibilities at such temperatures, in terms of temperature-induced transitions from the d-band to the s-band, but such behaviour could not be produced by the additive effects of a matrix of temperature-independent diamagnetism and islands of susceptibility similar to that of the 38% or 50% nickel alloys.

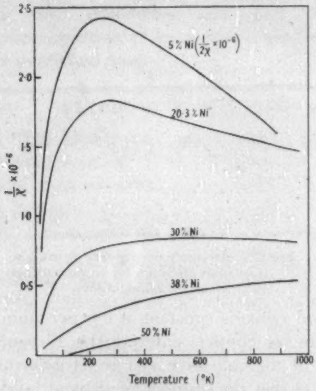

Fig. 3. Inverse susceptibility $1/\chi$ plotted against temperature for some copper–nickel alloys.

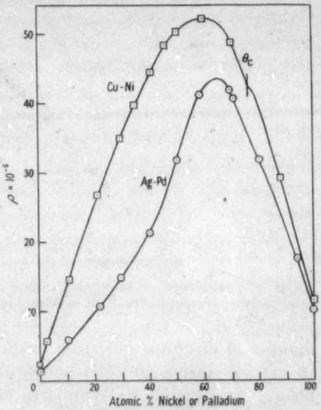

Fig. 4. Electrical resistance ρ in ohm cm^{-1} for copper–nickel and silver–palladium alloys. Results are for 0°c for silver–palladium and 100°c for copper–nickel. θ_C marks the point where ferromagnetism disappears at 100°c.

§ 4. ELECTRICAL RESISTANCE

The resistance–composition curves for the two systems are shown in fig. 4, the data being those of Giebel (1911) and Svensson (1932) for palladium–silver, and of Krupkowski (1929) for nickel–copper.

Mott (1935) has shown that the residual (temperature-independent) resistance of the palladium–silver alloys may be satisfactorily accounted for in terms of two contributions, one, ρ_s, for scattering processes involving s→s transitions, and one, ρ_d, from those involving s→d transitions. In fig. 5 is shown an analysis into two contributions of this sort of the experimental values for palladium–silver of the temperature-independent resistance ρ_0. It has been assumed that the ρ_d contribution only shows itself over the composition range suggested by the magnetic properties, and that the ρ_s contribution is slightly modified from the form ρ_s' both found and expected for alloy systems like silver–gold. This modification is due to the reduction of the 4s-electron density from 1·0 per atom in silver to 0·6 per atom in alloys containing more than 40% palladium. The ρ_d contribution so obtained behaves very much as might be expected, rising while initial additions of silver to palladium introduce a perturbing potential in the lattice field, and falling at higher concentrations as the d-band holes disappear.

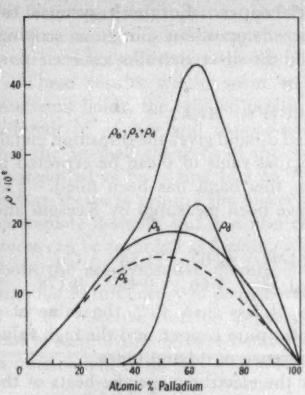

Fig. 5. Analysis of the temperature-independent resistance ρ_0 of silver–palladium alloys into a contribution ρ_s from s→s scattering, and a contribution ρ_d from s→d scattering. The dashed curve ρ_s' shows the type of variation with composition expected when the s-electron density is constant.

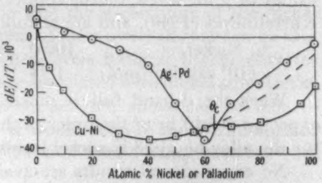

Fig. 6. Thermo-electric power dE/dT in millivolts in range 0–100°c for copper–nickel and silver–palladium alloys. θ_c marks the point where ferromagnetism disappears at 100°c.

For the resistance of the nickel–copper alloys, as can be seen from fig. 4, no such analysis is possible, and it would seem that some extra contribution to the resistance manifests itself over the whole composition range, and not only in alloys of more than 40% nickel. The resistance of copper-rich alloys is appreciably higher than that which would be given by a matrix of nearly pure copper with 'islands' of nickel-rich material.

§ 5. THERMO-ELECTRIC PROPERTIES

A detailed theoretical survey of the thermo-electric properties of nickel, palladium and their alloys is not yet available, although a qualitative explanation of the behaviour of some palladium-rich alloys has been given by Mott (1936a). Figure 6 shows the values of the thermo-electric power dE/dT plotted against atomic percentage of platinum for the two systems in the range 0–100° C. The data are those of Giebel (1911) for palladium–silver, and those calculated from the results of Chevenard (1926) for nickel–copper. For both systems the resemblance to the corresponding resistance–composition curves is striking, and the difference between the copper-rich and the silver-rich alloys is even more strongly marked.

§ 6. ELECTRONIC SPECIFIC HEAT

The high density of states in the partly filled d-band gives the transition metals a high electronic specific heat γT, and the actual value of γ can be expected to give information about the extent to which this band has been filled. The values of γ for a few nickel–copper alloys have been measured by Keesom and Kurrelmeyer (1940), and are as follows:

% Nickel	100·0	81·61	61·97	42·07	21·58	Cu
γ (10^3 cal/deg^2/mol)	1·74	1·58	1·52	1·66	0·457	0·178

Were the d-band full at nickel contents of less than 40% the value of γ expected would be of the order of that found for pure copper, and the high value for the alloy of 21·58% nickel implies the presence of d-band holes.

No experimental results are available for the electronic specific heats of the palladium–silver alloys.

§ 7. OPTICAL PROPERTIES

The optical properties of the nickel–copper alloys have been examined by Lowery, Bor and Wilkinson (1935) and by Bor, Hobson and Wood (1939). The results of the earlier investigation were discussed by Mott (1936b) in terms of the band model, but the later workers, in presenting further results, pointed out that the wavelength shift on alloying of an absorption band ascribed by Mott to 3d→4s transitions was far less than that implied by the theory.

§ 8. X-RAY SPECTROSCOPY

Farineau (1938) has examined the Lα emission bands of copper and nickel in their alloys with one another, these bands being provided by transitions from the 3d- and 4s- energy bands to the 2p level of the atom concerned. For pure nickel the nickel Lα band shows a sharp cut-off at high energy and the band is broadened by initial additions of copper; at higher copper contents it becomes appreciably narrower than in pure nickel. The copper band is complicated by the presence of high energy satellites but it is significant that it is completely unaffected by nickel additions of up to 40%. It would appear, therefore, that if d-band holes exist in the copper-rich alloys they are associated only with the nickel atoms, and that the anomalous properties are not caused by alterations in the band structure of copper.

Friedman and Beeman (1940) examined Kβ emission and absorption in these alloys, but results on such bands are not capable of straightforward interpretation. These workers considered their results consistent with those of Farineau.

§ 9. DISCUSSION

The above survey shows that, while a simple band model and a collective electron treatment are appropriate in the treatment of all available data on palladium–silver alloys, they fail entirely to account for the effects met with in the nickel–copper system when the copper content exceeds 60%. It should be emphasized that the situation is not that a few anomalous properties exist which are inexplicable by the treatment which seems so successful in dealing with the ferromagnetic properties: in fact all the physical properties are in agreement with one another in indicating the presence of d-band holes in copper-rich alloys, even at nickel contents as low as 5%.

These results would seem to imply either that the collective electron treatment holds, the relative positions of the 3d-band and 4s-band being rather different in copper and copper-rich alloys from those normally assumed, or that the 3d-shell electrons of the nickel atoms in the copper-rich alloys cannot be regarded as belonging to a collective d-band of the whole alloy. The latter picture seems to require the nickel atoms to be present in the form of ions with incomplete d-shells, but it is also conceivable that the d-electrons of the nickel atoms can be regarded as forming a band system of their own; all that can be said about the non-collective picture is that those d-levels lying at higher energies than the Fermi energy in copper-rich alloys are associated with nickel atoms only.

The collective electron approach for the copper-rich alloys can be seen to lead to improbable relative band positions. It would require the Fermi surface in pure copper to lie only a little way above the top of the 3d-band, as in fig. 7 (*c*) and, assuming that the effect of adding 5% nickel is to remove electrons from the region between the top of the d-band and the Fermi surface, the breadth of this region can have a value of only about 0·24 electron volt. This value, calculated assuming an approximately free-electron form for the 4s-band, is very much smaller than the value of 2·1 ev obtained from the optical properties referred to earlier, although the latter value is in good agreement with that obtained on the assumption that the two bands have similar relative positions in pure copper and pure nickel (see figs. 7 (*a*) and 7 (*b*)). The model of fig. 7 (*c*) implies that the d-band has moved to higher energies relative to the bottom of the s-band on going from nickel to copper, an improbable state of affairs in view

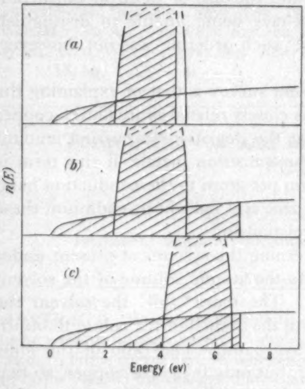

Fig. 7. Electron distribution curves. $n(E)$ = density of states. Shading indicates extent of occupation. (*a*) Normal picture of nickel. (*b*) Normal picture of copper (in agreement with optical properties). (*c*) Picture of copper required if 5% of nickel produces holes in copper 3d-band.

of the shift of the atomic 3d-states to lower energies relative to the 4s-state on going down the series Co→Ni→Cu→Zn.

If, however, the d-shell electrons of the nickel atoms do not form part of a collective d-band in the copper-rich alloys, as suggested by the x-ray spectroscopy of the alloys, the copper d-band may assume the position of fig. 7 (*b*), the holes being associated only with the nickel atoms. The presence of nickel ions of definite electronic configuration would explain such an effect, but it is not clear that these could give rise to a specific heat term linear with temperature, or to the observed temperature dependence of the susceptibility. Néel has attempted (1940) to describe the transition metals in general in terms of such ions 'bathing' in an atmosphere of s-band conduction electrons, but there has recently been experimental evidence that in an iron–cobalt alloy the non-integral magnetic moment is equally associated with the two kinds of atom (Shull 1951). The ion picture may, however, be appropriate for solid solutions of small amounts of a transition metal in a non-transition element.

An alternative which will account for the properties of the copper-rich nickel–copper alloys is a model in which the dissolved nickel atoms form a d-band of their own. This implies the presence of a nickel–nickel interaction at quite low nickel concentrations where like atoms are comparatively far apart, but the ferromagnetism of solid solutions of as little as 6% of iron in gold shows that such interactions can occur (Kaufmann, Pan and Clark 1945). The occupation of special lattice sites might be necessary, and the use of neutron diffraction techniques to examine such a possibility (x-rays being unable to distinguish copper and nickel) would be of great interest; such ordering was not, however, detected in the gold–iron alloys.

The main problem presented by the present survey is that of explaining the marked differences in behaviour of systems as closely related as are nickel–copper and palladium–silver. It is to be noted that the deviations occurring amount to differences in the effective valencies of the transition metals, if this term is taken as representing the electron contribution per atom to the conduction band of the alloy, and in alloy systems like nickel–zinc and palladium–cadmium these differences should be revealed in the phase relationships.

One suggestion that might be made concerning the systems at present under review is that the ratio of the ionic volume to the atomic volume of the solvent (copper or silver) might be of importance. The more 'full' the solvent the greater might be the tendency for overlap with the d-shell of the solute to occur, with the consequent formation of a collective band. The ratio of the ionic radius to the atomic radius is 0·875 for silver, but only 0·753 for copper, so that if this effect is of importance the tendency towards collective d-band formation would be greater in the palladium–silver system than in the nickel–copper system, at small concentrations of the transition metal. If such small differences can have such marked effects on the way in which the electron distribution of an alloy behaves, a very high degree of refinement will be required in theoretical treatments before confident predictions can be made of what will occur in a particular system.

ACKNOWLEDGMENT

The author's thanks are due to Dr. E. P. Wohlfarth for his helpful discussion of several points.

REFERENCES

Alder, M., 1916, *Thesis*, Zürich.
Bor, J., Hobson, A., and Wood, C., 1939, *Proc. Phys. Soc.*, **51**, 942.
Chevenard, P., 1926, *J. Inst. Met.*, **36**, 39.
Farineau, J., 1938, *J. Phys. Radium*, **9**, 447.
Friedman, H., and Beeman, W. W., 1940, *Phys. Rev.*, **58**, 400.
Giebel, W., 1911, *Z. anorg. Chem.*, **70**, 240.
Kaufmann, A. D., and Starr, C., 1943, *Phys. Rev.*, **63**, 445.
Kaufmann, A. R., Pan, S. T., and Clark, J. R., 1945, *Rev. Mod. Phys.*, **17**, 87.
Keesom, W. H., and Kurrelmeyer, B., 1940, *Physica*, **7**, 1003.
Köster, W., and Schmidt, W., 1934, *Arch. Eisenhuttenwesen*, **8**, 25.
Krupkowski, A., 1929, *Rév. Metall.*, **26**, 131, 193.
Lowery, H., Bor, J., and Wilkinson, H., 1935, *Phil. Mag.*, **20**, 390.
Marian, V., 1937, *Ann. Phys., Paris*, **7**, 459.
Mott, N. F., 1935, *Proc. Phys. Soc.*, **47**, 571 ; 1936a, *Proc. Roy. Soc.* A, **156**, 368 ; 1936b, *Phil. Mag.*, **22**, 287.
Mott, N. F., and Jones, H., 1936, *The Theory of the Properties of Metals and Alloys* (Oxford : University Press.)
Néel, L., 1940, *Le Magnétisme* (Paris: Institut International de Coopération Intellectuelle), p. 2.
Owen, E. A., and Pickup, L., 1934, *Z. Krystallogr.*, **88**, 116.
Schmidt, W., 1933, *Ergebn. tech. Röntgenk.*, **3**, 194.
Shull, C. G., quoted by J. H. Van Vleck, 1951, (Report of Grenoble Conference) *J. Phys. Radium*, **12**, 269.
Stenzel, W., and Weerts, J., 1931, *Festschrift zum 50 jahrigen Bestehen der Platinschmelze G. Siebert* (Hanau : Alberti), p. 288.
Stoner, E. C., 1939, *Proc. Roy. Soc.* A, **169**, 339.
Svensson, B., 1932, *Ann. Phys., Lpz.*, **14**, 669.
Wheeler, M. A., 1939, *Phys. Rev.*, **56**, 1137.
Wohlfarth, W. P., 1949a, *Proc. Roy. Soc.* A, **195**, 434 ; 1949b, *Proc. Leeds Phil. Soc.*, **15**, 89.

B
5
2

Torque Curves and other Properties of Permanent Magnet Alloys

By K. HOSELITZ and M. McCAIG
Permanent Magnet Association, Central Research Laboratory, Sheffield

MS. received 1st *October* 1951

ABSTRACT. Further investigations of Alcomax III and related alloys have been made using a torque magnetometer. Samples with both columnar and random crystals have been used. Torque curves have been obtained after various sequences of heat treatment designed to throw light on the changes that occur in these alloys, and the magnitude and direction of the magnetic field applied during cooling has been varied. A method of deriving three independent constants of crystal anisotropy without using single crystals has been devised.

§ 1. INTRODUCTION

Torque measurements on columnar Alcomax III have been described by Hoselitz and McCaig (1951, to be referred to as I). This paper is also chiefly concerned with torque measurements on Alcomax III, although a few observations on other alloys are included. The torque curves have been obtained after a new series of heat treatments, the influence of the magnitude of the field applied during cooling has been investigated, and measurements have been made on samples with random crystals. Such samples do not give a torque curve unless they are cooled in a magnetic field.

In I it was shown that the magneto-crystalline anisotropy energy can be formally expressed as that for a tetragonal crystal having three independent anisotropy constants, but the problem of obtaining the individual values of all three constants was only partially solved. Values for all three constants have now been obtained by examining samples in which the field applied during cooling was at different angles to the columnar axis.

§ 2. EXPERIMENTAL METHOD

The torque magnetometer was the same as described in I. In order to obtain more accurate torque curves, the torque on each sample was measured over a range of 360° although the curve should repeat itself after 180°. The whole torque magnetometer was then turned through 120° relative to the magnet and the curve obtained again. A further curve was obtained with the magnetometer turned through another 120°. Each point on the final curve, which shows the torque for different angles between the specimen axis and magnetic field covering a range of 180°, was thus obtained as the mean of six readings, and any slight mechanical tendency of the magnetometer bearings to set preferentially in certain directions was eliminated.

The experiments were carried out on samples from three different casts of Alcomax III and one cast each of the other alloys investigated. The analyses are given in table 1; Alcomax IIIa was the alloy used in the previous work.

Table 1. Chemical Analysis of Specimens (wt. %)

	Ni	Co	Cu	Al	Nb	Fe
Alcomax IIIa	13·45	25·3	2·99	7·4	0·87	Balance
Alcomax IIIb	13·49	25·05	3·01	8·47	0·79	,,
Alcomax IIIc	13·40	25·00	2·99	8·22	0·70	,,
Alnico	19·0	12·75	5·99	9·36	—	,,
Hycomax	20·6	20·55	1·52	8·80	—	,,
Ticonal	13·8	24·75	3·01	8·20	—	,,
Alcomax IV	13·4	24·9	2·97	7·58	2·52	,,

§ 3. THEORY

Hoselitz and McCaig (1951) derived an expression for the torque on a disc of columnar alloy cut with the columnar axis parallel to a diameter of the disc, and cooled in a magnetic field parallel to this diameter. In the present work the field during cooling was not always applied along the columnar axis and it is assumed that, provided the field applied during cooling is sufficiently high, each crystallite acquires the same tetragonal anisotropy characterized by the expression for the energy density:

$$F = C + K_2'(1-\alpha_1^2) + K_4'(1-\alpha_1^2)^2 + K_4(\alpha_1^2\alpha_2^2 + \alpha_2^2\alpha_3^2 + \alpha_3^2\alpha_1^2)$$

in which α_1 is the direction cosine measured from the tetragonal axis, i.e. the cube edge nearest to the field applied during cooling, and α_2, α_3 are the direction cosines measured from the other cube edges. The actual magnitudes of K_2', K_4' and K_4 depend on the cooling speed and subsequent tempering treatment, but not, it is assumed, on the orientation of the crystal axes relative to the field applied during cooling. Thus K_2', K_4' and K_4 are the same for all crystallites in a given specimen, although α_1, α_2 and α_3 vary. The validity of these assumptions will be examined later. If no field is applied during cooling, K_2'

and K_4' are zero and a pure cubic anisotropy characterized by K_4 remains. To calculate the torque for a given specimen held in a given position, the energy F is first summed for all the crystallites in the specimen, and the resulting expression is differentiated with respect to the angle through which the specimen is free to turn in the torque magnetometer.

The theoretical analysis has now been extended to include a number of cooling arrangements in which the field was not applied parallel to the columnar axis but in some other direction. The calculations differ only in detail from those used to derive the torque curves in the previous paper. The configurations considered are described and numbered below, and are followed by the equations deduced for the torque T, numbered correspondingly. The field means in all cases the field applied during cooling.

Field parallel to columnar axis and a disc diameter:

$$T=(K_2'+K_4'+0{\cdot}125K_4)\sin 2\psi+(0{\cdot}438\ K_4-0{\cdot}5\ K_4')\sin 4\psi \qquad \ldots\ldots(1)$$

Field perpendicular to columnar axis, but both parallel to disc diameters:

$$T=(0{\cdot}819\ K_2'+0{\cdot}944\ K_4'-0{\cdot}125\ K_4)\sin 2\psi+(0{\cdot}438\ K_4-0{\cdot}347\ K_4')\sin 4\psi \qquad \ldots\ldots(2)$$

Columnar axis a disc diameter, but field parallel to disc axis:

$$T=(-0{\cdot}183\ K_2'-0{\cdot}306\ K_4'+0{\cdot}125\ K_4)\sin 2\psi+(0{\cdot}438\ K_4-0{\cdot}029\ K_4')\sin 4\psi \qquad \ldots\ldots(3)$$

Columnar axis parallel to disc axis, but field along a diameter:

$$T=(0{\cdot}637\ K_2'+0{\cdot}637\ K_4')\sin 2\psi \qquad \ldots\ldots(4)$$

Columnar axis parallel to a diameter but no field applied during cooling:

$$T=0{\cdot}125\ K_4\sin 2\psi+0{\cdot}438\ K_4\sin 4\psi \qquad \ldots\ldots(5)$$

Specimen with random crystals cooled in field parallel to a diameter:

$$T=(0{\cdot}55\ K_2'+0{\cdot}63\ K_4')\sin 2\psi-0{\cdot}013\ K_4'\sin 4\psi. \qquad \ldots\ldots(6)$$

The experimental torque curves were analysed by reading off the torque at a few convenient angles such as 45°, 135°, 22·5°, 157·5°. From these values the torque coefficients A and B in the equation $T=A\sin 2\psi+B\sin 4\psi$ were deduced. These coefficients were then equated to the corresponding coefficient in the appropriate equation above.

§ 4. RESULTS

(*a*) *Influence of Magnitude of Hardening Field*

Some investigations of the influence of the magnitude of the field applied during cooling are given first, because the results have a bearing on the probable validity of our basic assumptions. Fig. 1 shows the value of the coefficient A, which is a measure of the uniaxial anisotropy, plotted against the field. The specimens were random samples from Alcomax IIIb, the lower curve is for specimens hardened only and the upper curve for specimens that have also been tempered for 48 hours at 590° c and 48 hours at 560° c. The value of A has practically reached its maximum when the hardening field is 2000 oersted. A further increase in field does not increase A even for those crystallites which are far from parallel to the field. It follows that with the even higher field of 3000–4000 oersted used in all other experiments, all crystallites should reach their maximum anisotropy even when tehy are not parallel to the field but include any angle up to the maximum possible of $\cos^{-1}(1/\sqrt{3})$ with it. The real test of the theory will, of course, lie in the consistency of the results obtained for the various anisotropy constants using different combinations of eqns. (1) to (6).

(*b*) *Derivation of Individual Values of* K_2', K_4', *and* K_4

The values of *A* for the random crystal samples using different cooling speeds are conveniently shown in fig. 2 where *A* is plotted against cooling speed; there are three curves—the lowest is for samples tested after being cooled in a field, the middle curve is for samples that have also been tempered for 48 hours at 590° c and the highest for samples that have had a further period of 48 hours at 560° c.

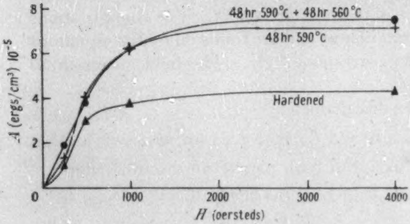

Fig. 1. Torque coefficient A of Alcomax III as a function of the field applied during cooling.

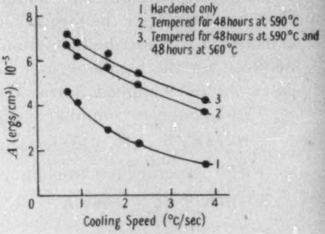

Fig. 2. Torque coefficient A of Alcomax III as a function of the cooling speed.

For the columnar samples the values of *A* and *B* for the variously treated specimens are shown in table 2. Equating the experimentally found numerical values of *A* and *B* to the corresponding theoretical values of the coefficients of sin 2ψ and sin 4ψ in eqns. (1) to (6) we obtain a possible ten equations from which the three constants K_2', K_4' and K_4 may be deduced. The results of these calculations are shown in table 3.

Table 2. Anisotropy Coefficients after different Heat Treatments

Cooling* (°c/sec) : 0·5. Tempering : nil.

Configuration	1	2	3	4	5
$A\times10^{-5}$	6·53	6·5	−1·39	4·62	
$B\times10^{-5}$	−0·71	−0·64	−0·58	−0·31	−0·37

Cooling* (°c/sec) : 0·5. Tempering : 48 hr. 590° c.

Configuration	1	2	3	4	5
$A\times10^{-5}$	10·15	9·0	−2·41	6·65	
$B\times10^{-5}$	−1·3	−1·06	−1·16	−0·31	−0·55

Cooling* (°c/sec) : 0·5. Tempering : 48 hr. 590° + 48 hr. 560° c.

Configuration	1	2	3	4	5
$A\times10^{-5}$	10·2	10·1	−1·78	7·4	
$B\times10^{-5}$	−1·17	−0·99	−0·65	−0·5	−0·78

Cooling* (°c/sec) : 4·0. Tempering : nil.

Configuration	1	2	3	4	5
$A\times10^{-5}$	2·38	1·44	−0·64	1·77	
$B\times10^{-5}$	+0·08	+0·03	−0·08	−0·05	+0·09

Cooling* (°c/sec) : 4·0. Tempering : 48 hr. 590° + 48 hr. 560° c.

Configuration	1	2	3	4	5
$A\times10^{-5}$	5·4	4·15	−0·68	4·44	
$B\times10^{-5}$	−0·24	−0·17	+0·1	−0·24	−0·09

* Cooling speed 900°–600° c.

Table 3. Crystalline Anisotropy Constants

Column		1	2	3	4	5	6	7	8	9
Data used				Columns 1 and 2			Columns 1 and 2 and 3 and 4			
Equation used		5b	3b	1b	2b	1a	2a	3a	4a	6a
Cooling* (° c/sec)	Tempering	K_4	K_4	K_4'	K_4'	K_2'	K_2'	K_2'	K_2'	K_2'
0·5	Nil	−0·85	−1·32	0·44	0·30	6·3	7·7	6·2	6·9	8·8
0·5	48 hr. 590° c	−1·26	−2·65	0·90	0·42	9·7	10·5	10·8	9·8	11·8
0·5	48 hr. 590°+ 48 hr. 560° c	−1·78	−1·49	0·90	0·54	9·7	11·7	7·4	10·9	12·4
4·0	Nil	+0·21	−0·18	−0·14	−0·04	2·5	1·9	3·6	2·7	2·5
4·0	48 hr. 590°+ 48 hr. 560° c	−0·21	+0·23	+0·50	0·36	5·0	4·6	3·0	6·5	6·6

All values of K are in units of 10^5 erg cm^{-3}.

* Cooling speed 900°–600° c.

Two equations for coefficients were derived from (1), (2), (3) and (5) and one each from (4) and (6). They are referred to by the numbers of the original equations with the letter a or b to distinguish whether the coefficients of sin 2ψ or sin 4ψ have been equated.

The agreement between values of the anisotropy constant derived from different cooling arrangements is remarkably good. From the results it appears that K_4 has about the same value for a specimen cooled at the same speed with and without a field, while K_4' is seen to be significant after certain heat treatments.

(*c*) *Crystal Anisotropy of Specimens quenched from various Temperatures*

For the purpose of this investigation two discs of Alcomax IIIa as used in I were used. The sequence of heat treatments and tests is indicated in table 4. In one set of experiments the sample was first placed in a furnace at about 930° c for 20 minutes, a treatment which had been shown to eliminate most of the effect of previous treatments, and then transferred directly to a second furnace at a lower temperature between 815° and 880° c. The sample was finally quenched in oil after 20 minutes at the lower temperature. In another series of experiments the sample was first placed in a furnace at the lowest temperature, 815° c, oil quenched after 20 minutes and tested; the process was then repeated at the next higher temperature and so on.

Table 4. K_4 after quenching from various Temperatures (all temperatures in °c)

Sample 1			Sample 2		
Heat treatment		$K_4 \times 10^{-5}$ (erg cm^{-3})	Heat treatment		$K_4 \times 10^{-5}$ (erg cm^{-3})
940	815 Q	−1·03	Cooled 930-600 1·1°c/sec		−0·6
925	835 Q	−0·3	815 Q		−1·68
925	855 Q	−0·64	835 Q		+0·4
930 Q		+0·85	855 Q		+0·71
940	880 Q	+0·13	880 Q		+0·26
920	850 Q	+0·8	920	850 Q	+0·51

Due to variability in the efficiency of quenching, or the speed of removal from one furnace to the other, it would be unwise to form too detailed conclusions on the basis of the above figures. The experiment, however, shows clearly that specimens quenched from above a certain critical temperature have positive cubic anisotropy, and specimens quenched from below this temperature have negative cubic anisotropy. The value of this critical temperature is established as lying between 835° and 855° c.

This conclusion is in harmony with the previous finding that K_4 becomes more negative as the rate of cooling decreases. The temperature range between 800° and 850° c in which the uniaxial anisotropy is produced in a magnetic field is also that in which the constant K_4 of the cubic part of the anisotropy changes rapidly from positive to negative in the absence of a field. It is possible that the presence of a magnetic field modifies a reaction already proceeding.

(*d*) *Spoiling Experiments*

The next set of experiments was on the rate of spoiling a fully treated sample by heating it above the tempering temperature. The coercive force and constant *A* were measured on samples from different casts but of about the same composition, after various heat treatments, and results are shown in fig. 3.

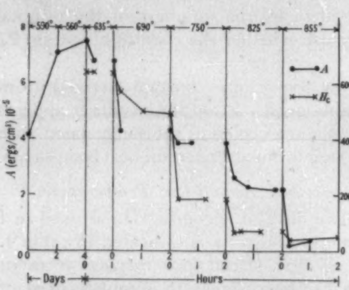

Fig. 3. Torque coefficient A and coercive force after heat treatment at successively higher temperatures.

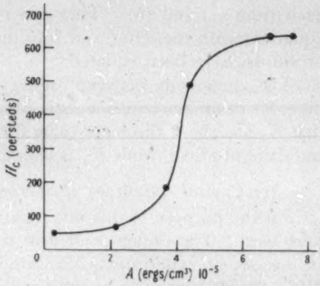

Fig. 4. Relation between coercive force and torque coefficient A of Alcomax III.

Both *A* and H_c decrease with time held at the spoiling temperature, but approach constant values. The constant values of both *A* and H_c are lower the higher the spoiling temperature, but there is not a linear relation between them (fig. 4). These results seem to indicate that there exists some kind of equilibrium or quasi-equilibrium state which can be reached in a comparatively short time at temperatures above 700° c, and very slowly indeed at temperatures below 600° c. This equilibrium state is associated with a higher coercive force the lower the temperature. Moreover the coercive force of a spoilt specimen can be partially restored by retempering at temperatures below 600° c. This observation does not conform with the more common process of magnetic hardening by precipitation where high coercive forces are usually connected with the very early stages of the reaction.

(*e*) *Crystal Anisotropy of various Alloys*

Although the most comprehensive study has been confined to one alloy, Alcomax III, some measurements have been made on four other alloys. The results are summarized in table 5. In this table Q refers to oil quenching from the temperature stated, C to cooling from 1250° c at the speed stated, the speed being mean rate between 900° c and 600° c, and H denotes that a magnetic field was applied parallel to the columnar axis during cooling. The values of *A* and *B*

Table 5. Measurements on various Alloys

Alloy	Heat treatment	$A \times 10^{-5}$	$B \times 10^{-5}$	$K_2' \times 10^{-6}$	$K_4' \times 10^{-6}$	$K_4 \times 10^{-6}$	$k_\perp$	$J_s^2/2K'_2$
Alnico	Q 930	−0·08	−0·3			−0·7		
	C 0·55 no H	−0·25	−0·35			−0·8		
	C 0·55 H	1·98	−1·68	−0·5	2·6	−0·8		
	C 3·8 no H	−0·06	−0·5			−1·1		
	C 3·8 H	0·49	0·3	0·8	−0·4	−1·1		
	„ +2 hr. 600°	0·56	0·4					
Ticonal	Q 930	0·23	0·3			0·69		
	C 0·5 no H	0·5	−0·27			−0·62		
	C 0·5 H	6·9	−0·64	6·2	+0·74	−0·62	0·9	0·98
	C 1·06 no H	0·07	−0·02			−0·05		
	C 1·06 H	8·03	0·0	8·03			0·98	0·76
	„ +48 hr. 590° 48 hr. 560°	9·7	−0·6				0·56	0·71
Alcomax IV	Q 930	−0·12	−0·1			−0·23		
	C 0·55 no H	−0·33	−0·52			−1·2		
	C 0·55 H	7·1	−0·95	6·4	0·86	−1·2	0·96	0·95
	C 1·1 no H	−0·22	−0·46			−1·05		
	„ +48 hr. 590° 48 hr. 560°	−0·21	−0·61			−1·4		
	C 1·1 H	6·3	−0·6	6·15	0·28	−1·05	1·4	0·98
	„ +48 hr. 590° 48 hr. 560°	10·8	−1·0	10·2	0·78	−1·4	0·64	0·59
Hycomax	Q 930	0·05	0·24			0·55		
	C 0·55 no H	−0·01	−0·02			−0·06		
	C 0·55 H	5·0	−0·5	4·0	0·96	−0·06	1·0	1·5
	C 1·0 no H	0·0	0·0			0·0		
	„ +16 hr. 650° 16 hr. 570°	0·04	−0·124			−0·28		
	C 1·0 H	3·7	−0·1	3·5	0·2	0·0	4·0	1·6
	„ +16 hr. 650° 16 hr. 570°	6·4	0·0	6·1	0·3	−0·28	0·4	0·8

A, *B* and *K* in erg cm^{-3}, Q=oil quenching from temperature stated (° c); C=cooling at speed stated (° c/sec).

should be reasonably trustworthy, but in the absence of checks obtained by cooling with the magnetic field in different directions relative to the columnar axis, the individual values of K_2', K_4' and K_4 are somewhat speculative.

Only a small K_2' term can be produced in Alnico. This result conforms to the fact that this alloy can be made only slightly anisotropic by magnetic hardening. For the remaining alloys the results resemble those for Alcomax III, although the range of variation of K_4 is rather less; no positive values of K_4 were found for Alcomax IV.

Various properties such as initial susceptibility and coercive force were also measured but the only quantity from which it has been possible to draw any significant conclusions is $k_\perp$ the initial susceptibility perpendicular to the preferred direction. If the initial magnetization process consists of rotation of the domain magnetization, the restoring force being provided by the crystal anisotropy, it has been calculated that $k_\perp$ should be given by $J_s^2/2K_2'$. Where appropriate, $k_\perp$ and $J_s^2/2K_2'$ are compared in table 5. In a number of cases the agreement is good, suggesting that rotation against the anisotropy energy is indeed the process of initial magnetization.

ACKNOWLEDGMENTS

The authors thank the Permanent Magnet Association for permission to publish this paper. Most of the torque measurements have been carried out by Miss Eileen Bentley.

REFERENCE

HOSELITZ, K., and MCCAIG, M., 1951, *Proc. Phys. Soc.* B, **64**, 549.

LETTERS TO THE EDITOR

Double Surface Lead Sulphide Transistor

An important step in the establishment of a theory of transistor action in germanium was the experimental proof that the effect is not solely a surface phenomenon. This was demonstrated by the wedge type and coaxial transistors which depend on the transmission of injected carriers through the bulk of the semiconductor.

It has been found that lead sulphide transistors show the same behaviour in this respect. The specimen mounting used for the experimental test is shown in fig. 1. The thickness *d* of the specimen was successively reduced by grinding until the crystal disintegrated. Very small values of *d* could be obtained only on specimens which contained crystallites of size greater than the dimension *a* (0·05 cm), a condition which was considered desirable also for a simple interpretation of the results. Each stage of grinding had to be followed by an acid etch to restore the transistor action. (Warm perchloric acid followed by a mixture of hydrofluoric acid, nitric acid and copper nitrate was found successful for this purpose.) Figure 2 shows the variation of optimum voltage gain with point spacing for the above configuration and, for purposes of comparison, for a type A transistor on the same specimen. As expected, the voltage gain decreases with increasing point spacing in both cases. The effective ranges of injected electrons are similar, and are approximately 5×10^{-3} cm in this specimen.

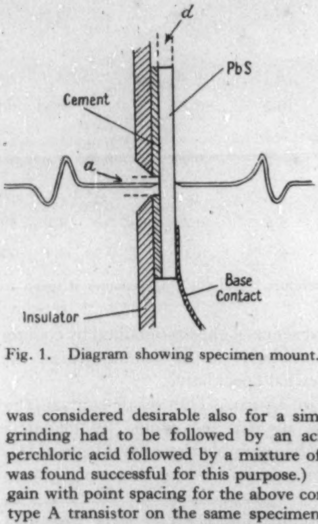

Fig. 1. Diagram showing specimen mount.

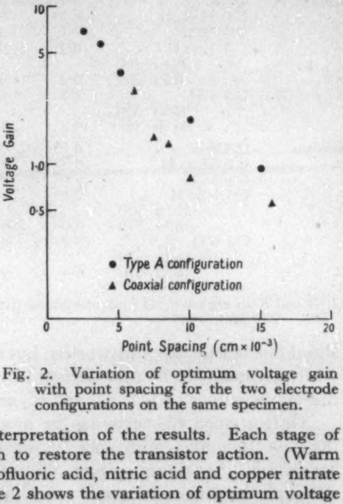

Fig. 2. Variation of optimum voltage gain with point spacing for the two electrode configurations on the same specimen.

Thanks are due to Professor R. W. Ditchburn for the support of this research.

Department of Physics,
University of Reading.
20th December 1951.

P. C. Banbury.

Photosensitive Neon-Argon Discharge Tubes in Photometry

The lowering of the striking or sparking potential in a discharge tube by irradiation is well known, and the effect in various gases has been investigated by Joshi (1940), Joshi and Deshmukh (1941), Arniker (1950), Prasad (1948) and others. In a recent paper Harries and von Engel (1951) explain the effects of the influence of irradiation on an electrodeless discharge in chlorine. It was also shown by Penning (1931) that if argon is introduced into a discharge tube containing neon the normal striking potential is considerably reduced and that the current through the tube is influenced by irradiation. Although these facts are established there is no evidence that the lowering of the striking potential by irradiation on a tube in a relaxation-oscillation circuit has been made use of. On the contrary, it was suggested by Om Prakash (1949) and others that neon discharge tubes should not be used in some types of experimental work when the illumination was not constant on account of their light-sensitive properties. Yeater (1945) coated discharge tubes to shield them from the effects of light, while Strassner (1951) illuminated discharge tubes to ensure stability when they were oscillating at low frequencies.

Experiments have been carried out in this laboratory, using tubes of the neon indicator valve type in relaxation-oscillation circuits, on the relationship between the period of oscillation and the striking potential when the tube is irradiateed. It is well known that in a circuit of this type the period $t = RC \ln (E-V_A)/(E-V_B)$, where V_A and V_B are the extinction and striking potentials of the tube respectively, E is the circuit battery voltage and RC the time constant. Hence changes in the striking potential should affect the frequency of the oscillations and, if the time constant is unaltered and if it can be assumed to a first approximation that the extinction potential remains the same, t should be proportional to $k - \ln(E-V_B)$, where k is a constant. The tubes which exhibited the effect to the greatest extent had a concentric arrangement of electrodes with a central disc anode mounted above an annular cathode. On account of the traces of argon, the striking potential was less than 100 volts. The glow was irradiated through the top of the tube by tungsten filament lamps and a calibrated cathode-ray oscillograph used to measure the difference between the striking potential V_B and the extinction potential V_A. The value of the striking potential when the tube was not irradiated was found by independent methods, and hence the extinction potential was estimated. A lowering of the striking potential on irradiation could be observed and measured by the decrease in amplitude of the trace on the oscillograph. Typical oscillograph traces of the charge–discharge cycles for one of the tubes are shown in fig. 1, (*a*) without and (*b*) with irradiation from a 100-watt lamp placed 3 inches from the tube. The time-base of the oscillograph was unaltered and the traces show the decrease in voltage and the corresponding increase in frequency. With telephones in the circuit the frequency was found by tuning to an oscillator, and values of t and V_B were determined for irradiations for lamps placed at various distances. Figure 2 shows t plotted against $\log(E-V_B)$. The linear relationship is in agreement with the theory, and when $t=0$, $\ln(E-V_B) = \ln(E-V_A)$.

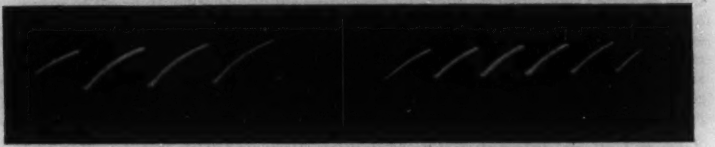

(*a*) (*b*)

Fig. 1.

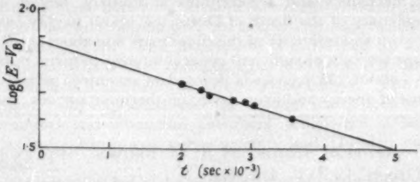

Fig. 2.

Further investigations were made to see if the tubes could be used satisfactorily as light-sensitive devices for quantitative photometric work. As changes of frequency are accompanied by proportional changes in the mean current through the tube, the response to illumination can be measured in terms of either of these quantities. The photometric arrangements were as recently described by Andrewes and Dillon (1951), the tube replacing the photovoltaic cell. Tungsten filament lamps of 15 to 150 watts of known luminous output provided the irradiation. Audio-frequencies between 300 and 400 c/s were selected for the fundamental note in the oscillating circuit. It was found that an illumination of 100 foot-candles increased the frequency up to 10%, with a corresponding increase of mean current depending on the characteristics of the tube and the circuit constants. If the tube can be regarded as a photoelectric cell, the sensitivity in μ A/foot-candle is of the order of one-tenth that of a photovoltaic cell of comparable area. Since the tubes showed fatigue effects and were sensitive to heat, illuminations greater than 300 foot-candles were avoided for routine work.

Satisfactory photometric results have been obtained and a full account will be given at a later date.

Work is also being carried out on the response of the tubes to light from oscillatory sources and on the spectral sensitivity of the tubes.

Department of Physics,
King's College of Household and Social Science,
London W.8.
21st December 1951.

T. J. Dillon.

Andrewes, U., and Dillon, T. J., 1951, *Amer. J. Phys.*, **19**, 514.
Arnikar, H. J., 1950, *Curr. Sci.*, **19**, 47.
Harries, W. L., and von Engel, A., 1951, *Proc. Phys. Soc.* B, **64**, 916.
Joshi, S. S., 1940, *Curr. Sci.*, **9**, 535.
Joshi, S. S., and Deshmukh, G. S., 1941, *Nature, Lond.*, **147**, 806.
Om Prakash, 1949, *Curr. Sci.*, **18**, 400.
Penning, F. M., 1931, *Phil. Mag.*, **11**, 961.
Prasad, B. N., 1948, *Curr. Sci.*, **17**, 235.
Strassner, R. M., 1951, *Electronics*, **24**, 70.
Yeater, M., 1945, *Phys. Rev.*, **67**, 74.

REVIEWS OF BOOKS

Actes du Colloque International de Mécanique (Poitiers 1950), Vol. I. (Publications Scientifique et Techniques du Ministère de l'Air, 248.) Pp. 298. (Paris : Service de Documentation et d'Information Technique de l'Aéronautique, 1951.) 1800 fr.

This volume, No. 248 in the series of scientific and technical publications issued by the French Air Ministry, is mostly of interest to the aero-engineer rather than to the physicist. It contains part of the proceedings of a colloquium organized to mark the opening of new buildings for mechanics and aerotechnics at Poitiers, linked with celebrations in honour of the tercentenary of the death of Descartes; about twenty-two pages are devoted to addresses on the work and influence of this great man, and about thirty to formal speeches, felicitous but perhaps scarcely of sufficient general interest to merit publication. The main part of the volume—about 235 pages—is devoted to seventeen articles, by sixteen French authors, on problems of energy and propulsion, on thermodynamics, and on heat exchange.

Mechanics and Properties of Matter, by R. C. Brown. Pp. ix + 276. (London : Longmans Green, 1950.) 10*s*. 6*d*.

This book forms only the first of four volumes covering the whole field of Physics so that obvious omissions from this volume may be accounted for in the others. For example, the kinetic theory of matter is used in the chapter on diffusion but no systematic account is given of kinetic theory nor is it listed in the Index. Explicit reference to kinematics is similarly omitted. The vague concept ' body ' is over-used; in many cases it would be better to develop such well-defined concepts as the 'particle', for the latter has to be used occasionally as on p. 57. It seems artificial to exclude the behaviour of vapours when Boyle's law is under discussion, but presumably this will also come in volume 2.

The diagrams are clear and generally illustrate the text well. Exception may be made to fig. 25 on p. 27 which shows an impossible curvature at the top of a vertical trajectory. The Newtonian constant of gravitation is too cursorily dismissed and no mention is made of the interesting problem of 'weighing the earth'. However, the book justifies its claim to be a straightforward presentation of the principles of Physics up to approximately the standard required by the Higher School Certificate and Intermediate Examinations.

F. C. CHAMPION.

Advanced Practical Physics for Students, by B. L. WORSNOP and H. T. FLINT. Pp. vii + 754. 9th Edition. (London: Methuen, 1951.) 30*s*.

.B
5
2

A course in practical physics has many aims. It should provide what Maxwell called 'experiments of illustration' to give the student direct experience of the more important phenomena of physics. It must exemplify standard experimental methods. It must teach the student to isolate the phenomenon that he wishes to examine. It must train him in the technique of measurement: to perform some experiments with high accuracy, and to devise others of perhaps more modest accuracy but which can be done within the resources of a given situation. The student must learn to make his apparatus good only where it needs to be, and yet to handle—if he proves worthy—a few examples of the highest grade of physical instrument. He must come to use 'the keenness of his eye, the quickness of his ear, the delicacy of his touch and the adroitness of his fingers', and to appreciate the wisdom of Pasteur: 'Chance favours the trained observer.'

The emphasis to be placed on each aim could well be debated. Moreover, the attainment of the ideal is limited by the equipment and time available, and by the abilities of both student and teacher. Nevertheless, it would have added to the value of Professor Worsnop's and Dr. Flint's *Advanced Practical Physics* if the experienced authors had discussed their objectives and the ways of approaching them. Their well-known book now appears in its ninth edition and, as before, it describes a great many of the experiments to be found in University teaching laboratories. The emphasis seems to be placed on experiments which do not take too long to carry out, using apparatus on which the student has little constructional work to do, and where the aim is almost entirely measurement, without making serious demands on the student's power of observation. The other aims of a practical course receive only indirect notice.

The text sometimes suffers from an inadequate exposition: for example, on page 276 the spectrometer is introduced by the statement that it 'consists essentially of a telescope and collimator', and the prism is first mentioned a page later as an adjunct necessary for carrying through Schuster's method of focusing. There is also an impression of a lack of 'feel' for the details of practical physics, indicated, for example, by the implication on page 382 that diffraction grating replicas are usually made photographically.

The book would have been better for a more thorough revision; tenses and phrases which still survive from the first edition give the reader the impression that he is reading a text written in the early 1920's. This impression is confirmed by the failure to revise sundry points of technique which have changed since the book was first written, such as the use of Nernst filaments as illuminants in galvanometer lamps. The section on Nuclear Physics could well have been expanded and the student introduced to such instruments as Geiger–Müller counters and ionization chambers, which are at least as common in laboratories to-day as were Einthoven galvanometers and Duddell oscillographs at the time of the first edition.

These comments are not intended to decry the physics of thirty years ago. They merely express disappointment that when it was deemed worth while to prepare a new edition of a well-known book, for which a "complete revision" is claimed in the preface, the opportunity was not taken for a more thorough overhaul. This would have enhanced the value of the book, which still provides much basic material for anyone who has to devise a course in practical physics.

R. V. JONES.

Survey of Modern Electronics, by P. G. ANDRES. Pp. + 522. (New York: Wiley and Sons; London: Chapman and Hall, 1950.) 46*s*.

This book is intended as a textbook for a short course in electronics, and chapters are included on basic concepts and current conduction, the hot cathode diode, the vacuum triode, multigrid and special vacuum tubes, gas-filled tubes, photosensitive tubes and devices, electronics in instrumentation, electronics in communications, electronic control and electronics in heating systems.

A knowledge is assumed of elementary electrical engineering, and the subject is treated with the minimum of mathematics, the emphasis being on descriptive physical explanations of the phenomena. The practical aspects are treated in a thorough manner, and the book contains much detail about specific applications of electronics, which should both arouse and maintain the interest of the reader as well as indicate the wide scope of electronic techniques.

Judged by British standards it is an unusual book because of the emphasis on the applications of electronics, but this should increase the value of the book for the practical engineer.

The book contains numerous and very good illustrations and diagrams, and each chapter ends with a list of problems and references. Unfortunately, the references are not very recent, and the present writer failed to note one of more recent date than 1946 : apparently American authors, like British authors, are subjected to considerable delays between the completion of the manuscript and the publication of the book.

The book is well printed and bound and can be recommended to students taking an electronic course who are specially interested in the practical aspects of the subject.

D. T.

An Introduction to the Theory of Control in Mechanical Engineering, by R. H. MACMILLAN. Pp. xiii + 195. (Cambridge: University Press, 1951.) 30*s*.

The increasing importance of automatic process control, of self-regulating systems and ' servo-mechanisms ' needs no emphasis; the published researches are extensive, and applications in the laboratory and industry increase every day. But although a great deal of the basic theory and of the principles of design has been executed in this country, no books on the subject have hitherto appeared here to this reviewer's knowledge.

Apart from its obvious practical importance, the academic value of the theory of control is considerable. As has been stressed in the Introduction to this book, the subject exerts a unifying influence on the student's specialized studies, bringing into one coherent set of ideas the behaviour of widely diverse dynamical systems : mechanical, electrical, chemical and biological. The future practical result of such studies, in enhancing the efficiency of our industries, depends upon these students. Both points of view are taken in this book. The first chapter presents the ideas and purposes of control and describes a number of automatic control systems, of very different kinds, already in common use, and should stimulate the beginner to visualizing the many possibilities; the great complexity and wide range of techniques involved are stressed in a way which should convince the reader of the essential need for studying the general mathematical theory before embarking upon design of any but the simplest system. Chapters 2 and 3 give details and practical illustrations of the various units employed in modern control systems, motors, pumps, hydraulic accumulators, data transmission links, and so on. The connection of such units into characteristic types of system is illustrated thoroughly. The misleading nature of the book title is evident here, there being no restriction to mechanical engineering; the electrical engineer and physicist will equally be at home. This first half of the book will be found quite digestible by the non-mathematical specialist, and will also be of interest to the forward-looking industrialist anxious to learn something of the possibilities of automatic control and of what techniques and equipment are involved.

From Chapter 4 onwards the book changes in tone and the mathematical theory is developed. A knowledge of simple linear differential equations with constant coefficients is essential and, as the material is extended, of functions of a complex variable and Laplace transforms also. The development of the subject matter, from the descriptive to the mathematical, proceeds at an accelerated pace, and the need for compression, due to the wide scope adopted, has forced a somewhat inadequate and occasionally naïve treatment of certain aspects of the subject. For example, the theory of data transmission by synchros is too brief and, as a result, the beginner may have difficulty in understanding a later section on static and dynamic errors; again, the notion of 'interaction' between cascade-connected units is quite a difficult one, and is here given very cursory treatment. Heaviside's Expansion Theorem is used with too little introduction, and the whole question of the determination of complex roots of a polynomial is made to appear too simple.

The author is clearly aware of such shortcomings and has included two Appendices, relating to functions of a complex variable and to Laplace transforms. As summaries they are brief and excellent, but rather inadequate for the reader who has no prior knowledge of these subjects. However, very great assistance is provided in the main text by the large number of worked practical examples.

The subject matter is restricted almost entirely to linear systems, though an excellent descriptive treatment is presented of the effects of non-linearity, backlash and friction. The book is intended as an introduction to the subject, and the mathematical treatment of non-linearity, of discontinuous or pulsed servos is wisely omitted. An excellent historical summary is appended, and both worked and unworked examples are included, together with a good bibliography.

E. COLIN CHERRY.

Fundamentals of Automatic Control, by G. H. FARRINGTON. Pp. xii + 285. (London: Chapman and Hall.) 30*s*.

In view of the number of original papers which have appeared in this country, relating to automatic control and servo systems, the dearth of books on these subjects has been regrettable. Recently, two books have appeared simultaneously, from different houses. One, from Cambridge University Press, has already been reviewed in this journal; the one considered here, from Chapman and Hall, is quite distinct in character and content.

By reason of historical accident, the subject of automatic control has evolved along two parallel paths, each with its own nomenclature, notation and approach to design. The newer of these has opened up the field of control mechanisms, electrical and mechanical, the development of which has proceeded apace by virtue of the application of the mathematical theory of feedback. It happens that modern electrical and mechanical engineers must, because of the nature of their business, possess knowledge of the relevant mathematics—mainly linear differential equations and function theory—and control ('servo') mechanism theory has been rapidly assimilated. Its practical application to the analysis and synthesis of a wide range of automatic systems has been one of the wonders of modern engineering. On the other hand, the far older science of process control—control of temperature, humidity, pH, etc.—has been slow in development, though striking practical results have been achieved. It may not be unfair to say that many of the engineers and chemists concerned are less mathematically inclined and that the mathematical theory of stable feedback systems has therefore not yet been widely applied by them. A great deal of process control has proceeded on a trial and error basis, albeit based on sound experience; but there is considerable scope in industry for the introduction of more precise methods of process control, and more attention to the application of the theory of servo mechanisms would undoubtedly be of advantage.

From this point of view the present book can perform useful service. It is concerned essentially with process control and aims at relating this to the theory and practice of control mechanisms. The method employed is principally that of analogy. In the first chapters various typical process control plants are examined and the basis of deriving the equivalent electric circuits is presented, relating to the component parts of the plant—thermal, hydraulic or pneumatic elements. This introductory material is rather illogical in order; for example, it is by no means clear whether the reader is expected to be familiar with a.c. vectors and simple circuit theory. However, this fault is compensated by an excellent later section which deals with the use of complex numbers, emphasis being laid on the use of the conjugate a.c. vector system, using the exponential notation.

Some of the nomenclature used will be unfamiliar to many engineers trained in servo mechanisms, being more suited to process control. The ideas of *desired value*, *controlled value*, *deviation*, and so on, are used rather than input signal θ_i, output response θ_0 or error. But the electric circuit analogies are developed clearly, in a way which shows a full understanding of the bases of such analogies. The behaviour of many systems is analysed and represented by loci on complex planes in the manner familiar to servo engineers. These analogies are given particular attention where they concern distributed systems; this is a wise emphasis, since many thermal, hydraulic or pneumatic elements are inherently distributed in character.

It is unfortunate that so few references have been included; the reader is constantly referred to " the published literature " for fuller details of cursorily treated material, but is given little assistance in finding it. Although no examination or other questions have been appended the book is rich in worked numerical examples, covering a wide range of process control systems. It is to be hoped that such systems will benefit in flexibility, simplicity and precision by the extended application to them of mathematical methods. To this end the book makes a valuable contribution. E. COLIN CHERRY.

Der Kreisel—Seine Theorie und seine Anwendungen. Zweiter Band; Die Anwendungen des Kreisels, by R. GRAMMEL. Pp. vi + 268. 2nd Edition. (Berlin : Springer-Verlag, 1950.) DM 30.0.

Satisfactory textbooks on the practical applications of gyroscopic principles are few and far between. Dr. Grammel's book can be welcomed, therefore, because it gives the essential mathematics in addition to the descriptive matter. The reader will find sufficient information on general principles to stimulate his thoughts and to guide him in the solution of his own problems.

The author has divided the book into three sections. In the first section of eighty pages he discusses gyroscopic effects, some desired and some unwanted, which arise in many diverse pieces of rotating machinery. A fairly detailed account of the critical speeds of rotors and shafts occupies about one-quarter of the section. Most readers will find this treatment adequate and will not need to refer to that monumental work, *Technische Dynamik*, by Biezeno and the present author. Other topics include the theory of pulverizing mills, the stability of vehicles moving in curved tracks, gyroscopic problems in rolling, pitching and yawing motions of ships and aircraft and the dynamics of the bicycle.

The second and largest section, of 130 pages, deals with true gyroscopic instruments, of which the gyro-compass is the outstanding example and receives a correspondingly detailed treatment. However, although it is natural that the products and aspirations of the firm of Anschütz should be given pride of place, it is a little surprising to find, on page 104, a diagram of the earliest Sperry compass but no mention anywhere of present-day Sperry and Sperry-type compasses with the Harrison–Rawlings modification. Again, the Brown compass is dismissed with a brief description of its damping system, but the control system is not mentioned.

The speed and course error of the gyro-compass receives conventional treatment. It is satisfactory for most conditions, but needs modification for high speeds and latitudes.

The discussion of the rolling error of the gyro-compass on pages 126–129 is not altogether satisfactory. The trouble starts with equation (64) on page 128, for the purposes of which the author has assumed that the error will be small. Had he not made this assumption he would not have reached the conclusion that the rolling error attains maximum values on the *true* courses N.E., S.E., S.W. and N.W., a miscalculation which others have also made and published. The truth is that the maxima occur on these *compass* courses, i.e. when the ship's head is directed at 45 degrees to the disturbed position of the gyro spin axis. In practice this distinction may not be very important, since methods must be and are adopted to reduce rolling error. However, when discussing the possible methods of achieving this result the author deals mainly with Anschütz practice. He appears to consider that the Harrison–Rawlings method used on Sperry-type compasses is not very satisfactory, but the fact remains that there are probably more compasses of the Sperry type in actual use in ships than there are of the other types he mentions.

Artificial horizons, attitude indicators, rate of turn meters, gyro direction indicators and other instruments used in ships and aircraft are dealt with in some detail in this same section of the book. The discussion of their reactions under various conditions of movement should help the reader to evaluate their errors.

The final section of the book is devoted to stabilization by direct gyroscopic action. Some astronomical matters and such devices as the boomerang and the discus first receive attention. These are followed by engineering applications, which include various types of monorail and anti-rolling apparatus for use in ships.

The book can be recommended as an introduction to the subject for the potential designer and as a useful addition to the library shelf. It is, of course, biased somewhat towards the products of the author's own country, but there are adequate references to other sources of information. It is not a 'popular' exposition. As usual, nowadays, the student will find the price rather high.

H. C. WASSELL.

Aerodynamics of Supersonic Flight: an Introduction, by ALAN POPE. Pp. xi + 185. (New York, Toronto and London: Pitman, 1950.) 25*s*.

One consequence of the vast defence programme in the United States of America, not generally appreciated outside that country, has been the considerable and rapid expansion of university and industrial research staff and facilities in subjects related to the requirements of the defence effort. Probably two-thirds of the institutions teaching technical subjects have Government contracts to work on fundamental aspects of defence. The scientific results are nearly all being published as soon as they are obtained.

The defence budget cannot remain at its present level for more than a few years. When the period of transition to more normal conditions arrives, wisdom and courage will be needed to obtain money for those technical institutions which are at present running on an income far in excess of their earlier expectations, due to defence contracts. The general recognition in the United States that an ever-increasing national standard of living requires, among many other things, an ever-increasing supply of scientists will probably ensure that these technical institutions will not have to endure more than a modest retrenchment.

A technical field of great importance in defence is the aerodynamics of supersonic flight. The book now being reviewed has been written for the training of the supporting staff in a research supersonics laboratory. It is well worth careful study as a type of technical book for teaching the supporting staff. The philosophy is that if a particular idea is of great practical value then, however recondite and subtle the idea is, a way must be found of explaining it on the elementary scale. Photographs and diagrams must be used and prepared with the greatest care in order to enable the student to appreciate the essential points, even if the mathematics is too difficult and the fundamental physical background is somewhat beyond his training and capacity.

The claim is made in the preface that the book can be made the basis of an elementary one-term course for undergraduate students in supersonics, to follow when the students have studied the differential and integral calculus and have had one term of elementary aerodynamics. The book covers the standard shock wave relations, including oblique shocks, flow in ducts, two-dimensional flow from nozzles and the Prandtl–Meyer corner expansion, flat-plate and lenticular aerofoils, the elements of supersonic tunnels and an elementary discussion of three-dimensional flow, including sweepback, rectangular trapezoidal and delta wings, and flow past cones. Each chapter has a few instructive examples, often numerical application of formulae. The diagrams are extremely good and the plates are fascinating. The style is good on the whole, but there are some lapses into frightful hyphenated jargon. 'Engineering units' are used, including that atrocity for density, 'slugs per cubic foot'. Reynolds number is written *RN*. However great are the difficulties of discovering a satisfactory set of symbols for this subject, the use of a pair of letters for a single parameter is a bad principle.

In spite of these blemishes the book is of great interest. The claim of the author that many of the most important features of the dynamics of supersonic flight can be explained in an elementary way has been proved, to some extent at least, while the practical engineering outlook which is so forcefully presented will be refreshing to readers who like to see a subject developed for the student in such a way that the present frontier of knowledge in a great industry is continuously borne in mind.

The book is recommended because it treats its subject in a novel way and because the diagrams and plates practically explain the subject on their own.

W. G. PENNEY.

Some Aspects of Fluid Flow (Report of a Conference organized by the Institute of Physics, October 1950, at Leamington Spa). Pp. viii + 292. (London: Edward Arnold, 1951.) 50*s*.

This book contains the minutes of what must have been a most successful and stimulating conference in which engineers and physicists were comparing notes in common fields. Fifteen papers were presented on topics ranging from the combined flow of solids and fluids to the use of ship models. The papers were divided into four groups: Group I. Industrial problems; Group II. Fundamental problems; Group III. Techniques for the study of fluid flow; Group IV. Instances of application of present knowledge.

The field which received the most attention—four papers—was the combined flow of fluids and solids, ranging from the flow of fluids through packed beds of solid to the settling of suspensions. In an intermediate position come subjects such as the 'fluidization' of solid particles and methods of separation of dust from a stream of gas. All these subjects are of very great industrial importance, and yet are still handled almost entirely by empirical methods, and one member complained that different workers report their results in ways that make comparison difficult. In most of the other subjects dealt with, such as the design of jets and the use of models, the basic principles are well understood.

A very valuable feature of the papers is the large number of references to journals so diverse that no one person is likely to be familiar with them all. For example, in the subject of combined flow of fluids and solids there are a large number of references which it would have been very hard indeed for either a physicist or an engineer to hunt out for himself.

The papers were followed by summaries, made by the chairman, of the discussions of five groups. These summaries, in which many topics receive only a sentence apiece, could well have been omitted. In the opinion of the reviewer, such discussions should either be reported verbatim or not at all.

The reviewer feels bound to complain loudly about the price of this excellent book, which will put it out of the reach of young workers in allied fields. It does indeed seem a waste to bind the book (much of which will be out of date in a few years) in such a lavish style, and to print it on art paper. The accuracy of printing and the technical execution of the diagrams and illustrations are all excellent—better than is really needed!

H. N. V. TEMPERLEY.

Colour Cinematography, by A. CORNWELL-CLYNE. Pp. xvi + 780. 3rd Edition. (London: Chapman and Hall, 1950). 84*s*.

It is now twelve years since the 2nd edition of Cornwell-Clyne's well-known book on colour cinematography appeared and while that period could perhaps hardly be described as a halcyon period for colour photography, a considerable body of scientists and technicians have been busy improving and developing the complex processes on which colour photography depends. In addition, much progress in the related subjects of colorimetry and colour vision has taken place. This activity is well reflected in this new edition, in which much new material appears, so that the book forms an extensive compendium of information.

Colour cinematography is an awkward subject on which to write a book, since so much vital information never finds its way into the usual channels of publication, and if it appears in print at all, it is in the form of patent specifications which are hardly the highest form of literature. Cornwell-Clyne has therefore had the unenviable task of summarizing a large number of such specifications, and an important part of the book consists of a digest of the patent literature.

Although the book is divided into three parts and a series of appendices, the real meat of the book is found in Part I, which consists of 580 pages, and in particular in Chapter 2 (225 pages) on the Theoretical Basis, in Chapter 3 (62 pages) on Additive Processes and in Chapter 4 (184 pages) on Subtractive Processes. Whether the mass of material included here could have been pruned with advantage, is perhaps a matter of opinion, but a more critical approach might have led to a clearer presentation of a very complicated matter. As an example, greater discrimination in the selection of the visual data described in the book might have led to a useful condensation of this section without the sacrifice of any essential information.

In the preface, the author has some rather harsh things to say about the aesthetic content of colour films and, no doubt, many people would agree with him. One cannot, however, help feeling some sympathy for those responsible for the artistic side of film production, since they can hardly make a really satisfying use of their medium until they have acquired a sound understanding of the processes of colour photography and they must at times find the subject pretty forbidding. Cornwell-Clyne's book is not, I think, intended as a textbook for the art director, but it is to be hoped that this contribution to the literature will lead to further technical improvements and thus indirectly contribute to our greater aesthetic entertainment.

W. D. WRIGHT.

Semi-Conducting Materials—Proceedings of the Reading Conference, 10–15th July 1950. Ed. H. K. HENISCH. (London: Butterworth, 1951.) 40*s*.

The sub-title and the foreword of 14 lines are the only indication that this collection of twenty-eight papers on semiconducting materials is, in fact, the Proceedings of an International Conference on the subject and, of the foreword, only four lines specifically refer to the Proceedings here presented:

> "The Reading Conference 10–15th July 1950, of which this volume constitutes the Proceedings, provided research workers from this country and abroad with an opportunity for discussion of the most recent progress. Over 200 physicists and engineers took part, among whom it was a pleasure to welcome 80 visitors from other countries."

As no discussions of the papers are reproduced, the book appears at first sight as an issue of a scientific periodical in which, by some chance, all papers deal with semiconductors. Its real significance, however, consists in its representing the nearest thing to what used to be called a treatise on a scientific subject, i.e. a complete, up-to-date, concise but understandable review. It is to the credit of the organisers that by the selection of the speakers this book provides, in fact, a reasonably complete cross section of contemporary semiconductor physics, and to the credit of the authors that they have given well-readable accounts with a satisfactory selection of references.

It is obviously impossible to refer here to each of the 28 papers, and it would be an invidious task to refer to a few in particular. The reader will get a good idea of the theoretical problems involved, of the classification of materials, of measuring techniques, absorption spectra, of some recent ideas and experiments concerning carrier injection, transistors and surface phenomena, of the effect of nucleon bombardment, of motion of electrons in single crystals and in polycrystalline materials, of the influence of lattice defects and, of course, of the results obtained in measurements on a large number of particular materials. Further, there are papers on a particular class of semiconductors which have recently been called oxidic semiconductors and on some properties of thin metallic films.

The most serious omission (not the organisers' fault) is the lack of reference to recent Russian attempts to revise the theoretical basis of conduction in solids, for instance, by the introduction of polarons, electron pairs, etc.

The fact remains that this book will be studied and consulted again and again by everybody working on semiconductors or on allied fields, and it should be on the shelves of any physics library keeping a representative collection of periodicals. W. E.

Practical Electron Microscopy, by V. E. Cosslett. Pp. xiii + 299. (London: Butterworths Scientific Publications, 1951.) 35*s.*

This book should be welcomed as filling a definite and pressing need for a comprehensive manual written for the user of the electron microscope. It deals in detail with all aspects of the instrument and its operation. In addition, a general description is given of most of the techniques for specimen preparation in current use. The text is written on a level clearly meant to be capable of being understood by the non-physicists who may undertake work with the electron microscope. The book starts with the simple principles of the optical microscope, and these are extended to the electronic instrument using magnetic lenses. The general principles and theory of the various components of the instrument are explained, with special reference to their importance in the operation of the instrument.

After reading the chapters on specimen techniques the reader should be in a good position to practise the manipulations described. The descriptions include the important details so often omitted but in practice essential. From the preparation of supporting films the reader is taken through the processes of mounting particles, thin films, micro-organisms and biological tissue. Surface replicas are described in a second chapter on technique.

The penultimate chapter discusses briefly the limitations of electron microscopy and the future prospects of improvement. The book is concluded by a discussion of the electrostatic electron microscope and other modified forms of the instrument which have been developed for specific purposes.

It is a little unfortunate that an appreciable number of technical errors appear in the first part of the book, and some of the explanations are not as clear as they might be. The chapter on the electron gun is most seriously in error, but this is partly because it was written before certain recent results were made public which considerably modify previous ideas on the electron gun operation. The explanation of the physical optics of resolving power perpetuates the regrettable custom of dealing with regular lattice objects for coherent conditions of illumination and point objects for incoherent conditions. One fundamental mistake is made in this explanation with reference to Figure 49.

M. E. H.

CONTENTS FOR SECTION A

PAGE
Dr. Suraj N. Gupta. Quantization of Einstein's Gravitational Field: Linear Approximation . . . 161
Mr. J. H. Haywood. The Equations of Motion and Coordinate Condition in General Relativity . . . 170
Dr. R. H. Dalitz. On Polarized Particle Beams . . . 175
Prof. Eiichi Ishiguro, Mr. Tadashi Arai, Dr. Masataka Mizushima and Prof. Masao Kotani. On the Polarizability of the Hydrogen Molecule . . . 178
Dr. A. B. Bhatia. On the Theory of Electrical Conductivities of Monovalent Metals . . . 188
Mr. G. C. Fletcher. Density of States Curve for the 3d Electrons in Nickel . 192
Mr. D. J. Littler. A Determination of the Rate of Emission of Spontaneous Fission Neutrons by Natural Uranium . . . 203
Dr. K. W. H. Stevens. Matrix Elements and Operator Equivalents connected with the Magnetic Properties of Rare Earth Ions . . . 209
Dr. S. Hayakawa. The Possible Effects of κ-Mesons in the Cosmic Radiation . 215
Miss N. D. Sayers and Prof. K. G. Emeléus. Experiments on Production of Auroral Radiation . . . 219
Letters to the Editor:
  Mr. B. S. Chandrasekhar and Dr. K. Mendelssohn. Helium II Transfer on Metal Surfaces . . . 226
  Dr. J. K. Hulm. Anomalous Thermal Conductivity of Pure Metals at Low Temperatures . . . 227
  Mr. D. D. Desai, Mr. K. S. Korgaokar and Dr. B. B. Laud. Transition Probabilities of some Band Systems of Nitrogen . . . 228
Contents for Section B . . . 230
Abstracts for Section B . . . 231

ABSTRACTS FOR SECTION A

Quantization of Einstein's Gravitational Field: Linear Approximation, by SURAJ N. GUPTA.

ABSTRACT. The approximate linear form of Einstein's gravitational field is quantized by using an indefinite metric. It is shown that only two types of gravitons can be observed, though many more can exist in virtual states in the presence of interaction. The observable gravitons are shown to be particles of spin 2. Using the interaction representation, the interaction of the gravitational field with the matter field is briefly discussed.

The Equations of Motion and Coordinate Condition in General Relativity, by J. H. HAYWOOD.

ABSTRACT. A new coordinate condition has been considered and the equations of motion of two bodies in their weak and quasistatic gravitational field have been derived to the second approximation. A number of additional second order terms appear in the new equations which, however, have no influence on either the secular motion of the centre of mass or the rotation of periastron of the two-body system.

On Polarized Particle Beams, by R. H. DALITZ.

ABSTRACT. A partially polarized beam of particles is represented by a statistical operator in spin space. For nucleon–nucleon scattering a theorem stated by Wolfenstein in 1949 connecting the two simplest experiments involving polarized nucleons is shown to depend on the invariance of the interaction potential under time-reflection.

On the Polarizability of the Hydrogen Molecule, by EIICHI ISHIGURO, TADASHI ARAI, MASATAKA MIZUSHIMA and MASAO KOTANI.

ABSTRACT. The polarizability of the hydrogen molecule is calculated theoretically. The energy of the molecule, under an external electrostatic field, is calculated by the variation method, using 11+10 terms and 11+9 terms James–Coolidge type wave functions, for the polarizability parallel to and perpendicular to the molecular axis respectively. By expanding the energy in powers of the field strength, the polarizability is determined. By using a Morse function for the adiabatic potential of the molecule, the 0–0 and 0–1 matrix elements of the polarizability between vibrational states are calculated, with the result: $\alpha_{00}=7{\cdot}89$, $\gamma_{00}=2{\cdot}78$, $\alpha_{01}=1{\cdot}39$, $\gamma_{01}=0{\cdot}90$ for ordinary hydrogen H_2, and $\alpha_{00}=7{\cdot}75$, $\gamma_{00}=2{\cdot}68$, $\alpha_{01}=1{\cdot}13$, $\gamma_{01}=0{\cdot}71$ for heavy hydrogen D_2 (in units of 10^{-25} cm^3), where α is the mean polarizability and γ the anisotropy.

On the Theory of Electrical Conductivities of Monovalent Metals, by A. B. BHATIA.

ABSTRACT. It is shown that on the basis of the Bloch–Peierls–Bardeen theory of conductivity, the use of $\theta_R \simeq \theta_D$ in the Bloch–Grüneisen formula is a reasonable approximation in the temperature range $T \gtrsim \theta_D$. At very low temperatures $T \ll \theta_D$, however, $\theta_R = \theta_L$. This, it is shown, disagrees with experimental data much more than the *ad hoc* use of $\theta_R \simeq \theta_D$ in the Bloch–Grüneisen formula.

Density of States Curve for the 3d Electrons in Nickel, by G. C. FLETCHER.

ABSTRACT. A calculation is made of the energy density of electronic states for the 3d electrons in metallic nickel, using the approximation of tight binding. The early stages of the calculations and preliminary results have been previously summarized by Fletcher and Wohlfarth in 1951. The theoretical basis of the approximation is outlined and the validity of the underlying assumptions examined. The required overlap integrals are evaluated and the secular equation for the energy as a function of wave vector is solved exactly over the energy range of interest for nickel. The density of states curve is computed graphically. Among results of physical interest obtained are : bandwidth $2{\cdot}7_0$ev, degeneracy temperature $1{\cdot}4_5 \times 10^3$ deg K, low temperature electronic heat coefficient γ $1{\cdot}6_9 \times 10^{-3}$ cal. mol^{-1} deg^{-2} (compared with the experimental value of $1{\cdot}74 \times 10^{-3}$). The results are compared with those obtained by the cellular method of approximation used by Krutter in 1935, and Slater in 1936.

A Determination of the Rate of Emission of Spontaneous Fission Neutrons by Natural Uranium, by D. J. LITTLER.

ABSTRACT. By comparison with a calibrated neutron source, the total rate of emission of primary neutrons in the Graphite Low Energy Experimental Pile has been found. The rate of emission of spontaneous fission neutrons from natural uranium is computed to be $59{\cdot}5 \pm 3{\cdot}3$ neutrons/g/hr of uranium.

Matrix Elements and Operator Equivalents Connected with the Magnetic Properties of Rare Earth Ions, by K. W. H. STEVENS.

ABSTRACT. An account is given of the methods used to determine the matrix elements of crystal field potentials with particular reference to rare earth ions. Emphasis is laid on the importance of Wigner coefficients in such problems and the idea of using equivalent angular momentum operators is developed. For convenience in applying the results a table of matrix elements are included.

The Possible Effects of κ-Mesons in the Cosmic Radiation, by S. HAYAKAWA.

ABSTRACT. The decay and nuclear interaction schemes of κ-mesons are discussed. A tentative interpretation is made of some anomalous interactions of penetrating particles observed recently below ground. Further possible experiments testing the hypotheses made are suggested.

Experiments on Production of Auroral Radiation, by N. D. SAYERS and K. G. EMELÉUS.

ABSTRACT. Further experiments have been made on the production in the laboratory of the 'forbidden' red and green auroral lines, and the ultra-violet transauroral line of OI. The mean concentration of oxygen atoms in the $1\,^1S_0$ and $5\,^5D$ states in the columns has been found from absolute intensity measurements. The decay of the green radiation produced by a Tesla discharge through a high-pressure source has been investigated with a photo-multiplier tube. It occurs at approximately the rate to be expected if the atoms in the ^1S state are undergoing spontaneous transitions to lower atomic levels, but complicating factors make it difficult to deduce transition probabilities from the experiment.

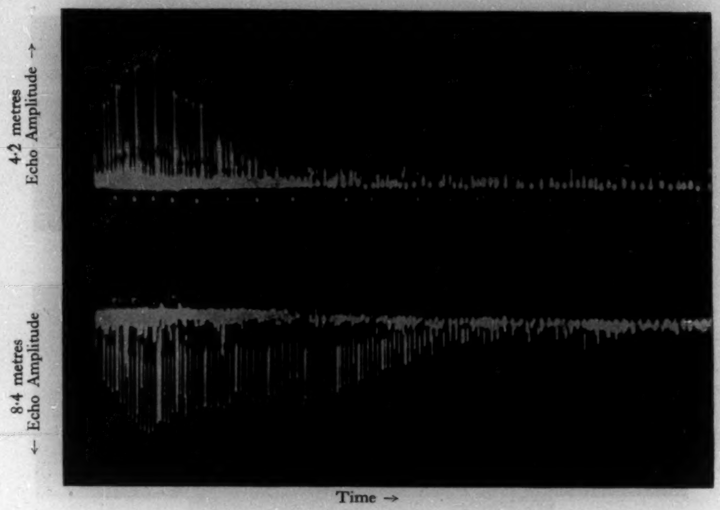

(*a*) Short duration radio echo from a meteor trail at wavelengths of 4·2 and 8·4 m, showing the λ^2 relation between the amplitude decay times. Pulse repetition frequency 750 c/s.

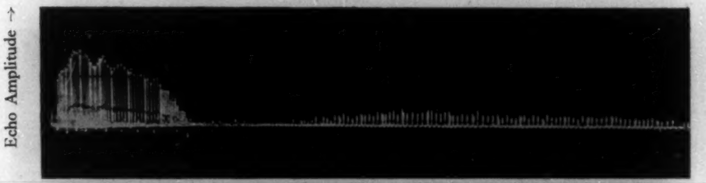

(*b*) (i) Fresnel type echo in which the uniform decay of amplitude is interrupted, giving place to a slow amplitude fluctuation. Pulse repetition frequency 750 c/s.

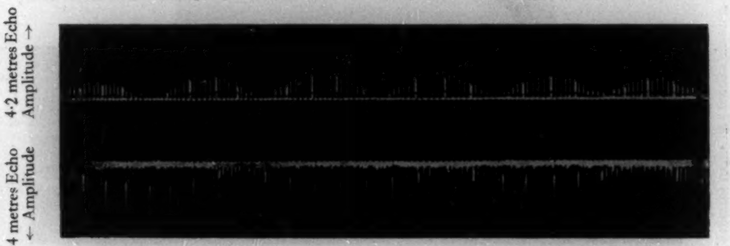

(ii) Simple amplitude fluctuations in a radio echo from a meteor trail, showing the $(\cos^2)^{1/2}$ variation in amplitude associated with two reflected waves of varying phase beating together. Pulse repetition frequency 750 c/s.

PLATE I.

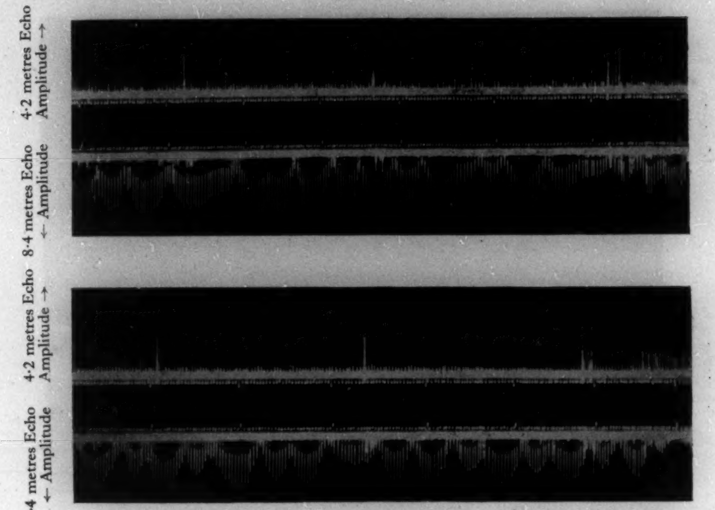

(*a*) Section of a long duration meteor echo at wavelengths of 4·2 m and 8·4 m, showing the period of fluctuation to be proportional to the wavelength. Pulse repetition frequency 150 c/s. (Calibration marks are 0·2 sec apart.)

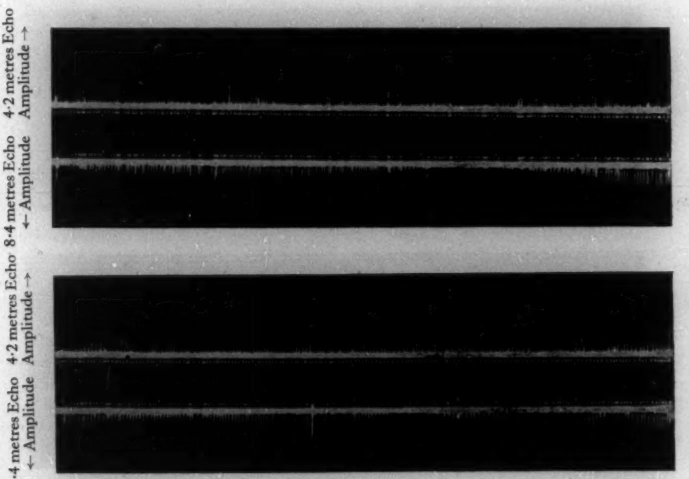

(*b*) An example of the more confused fluctuations in amplitude normally occurring in the radio echo from a long duration meteor trail. Pulse repetition frequency 150 c/s.

PLATE II.

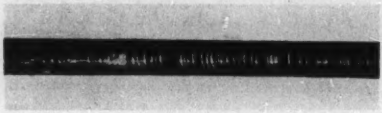

Fig. 2. Photograph of part of crystal ($\chi=52°$) which did not show strain ageing. (×5½)

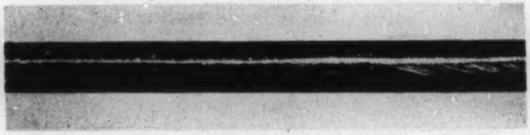

Fig. 3. Photograph of region of heavy glide in crystal which shows strain ageing ($\chi=11°$). (×8)

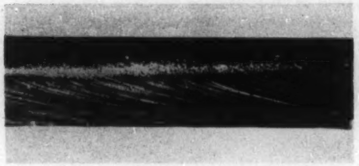

Fig. 4. Photograph at higher magnification of centre of region of heavy glide, showing dense packing of glide bands ($\chi=11°$). (×16)

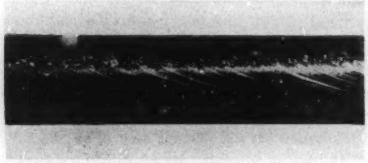

Fig. 5. Photograph at higher magnification of edge of region of heavy glide, showing gradual decrease in density of bands to right of photograph ($\chi=11°$). (×16)

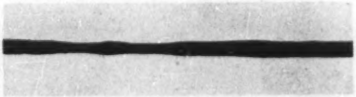

Fig. 6. Silhouette of crystal containing regions of heavy glide.